PROGRESS IN RESEARCH

January 1, 1979 - December 31, 1979

By the

Theoretical Nuclear Physics Group

January 1980

Department of Physics
University of Texas
Austin, Texas

DISCLAIMER

PROGRESS IN RESEARCH

January 1, 1979 - December 31, 1979

By the

Theoretical Nuclear Physics Group

January 1980

Department of Physics
University of Texas
Austin, Texas

TABLE OF CONTENTS

I. INTRODUCTION

This is a progress report, describing the accomplishments in basic research in nuclear physics carried out by the theoretical nuclear physics group of the Department of Physics of The University of Texas at Austin, during the period of January 1, 1979 to December 31, 1979.

The major part of the report is contained within subsections A, B, C, and D of Section II. The subsection A is a complete presentation of our research achievements and their significance. Both work completed and work in progress are covered, the coverage of the latter being given in somewhat more detail than that of the former. In subsection B, title pages of papers published during the year are reproduced, while in subsection C, first pages of papers submitted but not yet in print are reproduced. These papers are numbered as B-1 through B-18 and C-1 through C-9, according to the order in which they appear in these two subsections. In subsection D there are copied abstracts of talks presented at APS and other meetings.

The subsection A was written in such a way as to give an overview of our work, its interrelations, and its relation to work done by other groups. As is seen, a large variety of subjects are included as part of our work, and thus they are presented in five separate parts; (i) through (v). The overall subject in each part can be found in the list of contents given at the beginning of this report. In the presentations of subsection A, frequent reference is made to papers in subsections B and C and also to many other papers. These papers are summarized in the list of references given at the end of subsection A.

II. THEORETICAL RESEARCH

II. A. OVERVIEW OF THE WORK PERFORMED

i. REACTIONS INDUCED BY LOW ENERGY LIGHT IONS

a). Exact finite range DWBA calculations of two-nucleon transfer reactions (Takemasa, Tamura and Udagawa)

For the heavy-ion induced reactions, transferring one- or more nucleons, it is customary to perform calculations based on the exact-finite-range (EFR) method. This is not yet, however, the case with the light-ion induced reactions, including two-nucleon transfer reactions (TNTR). This is partly because one rather naively believes that the zero-range (ZR) approximation works there. The other reason is that the EFR calculations for light-ion induced reactions are surprisingly time consuming.

We noticed, however, that the interpolation technique, introduced by Low and Tamura[1] and used in a computer program SATURN-MARS[2] for heavy-ion reactions can be applied to the light-ion reactions as well. Takemasa, Tamura and Udagawa thus modified the previous heavy-ion TNTR program,[3] and completed a new program to be used for light-ion induced TNTR. With this new program, detailed analysis were made of $^{92}Zr(t,p)^{94}Zr$ reaction with $E_t = 20$ MeV, leading to the 0^+, 2_1^+, 2_2^+, and 4_1^+ states, and also of the $^{208}Pb(p,t)^{206}Pb$ reactions with $E_p = 32$ and 40 MeV, leading to the 0_1^+, 2_1^+, 4_1^+, 6_1^+ and 7_1^- states. These calculations were made by using realistic triton wave functions and a multi-configuration space for two-neutrons. Such calculations have become possible for the first time, because of the fast method we employ.

The results[4] of the calculations were compared with those of the ZR calculations, as well as with experimental data. It was found that, as far as angular distributions are concerned, the EFR and ZR calculations gave results

which are almost identical and agree well with experiment. This feature was found for all the ℓ values and the incident energies considered, and some of the examples that demonstrate this fact are shown in Fig. 1.

It was further found that finite-range effects were not important even in predicting relative magnitudes of the cross sections leading to different final states, if the incident energy was rather low. However, this ceases to be the case for reactions with higher incident energies. We in fact found, for instance, that the 7 cross sections in the ^{209}Pb(p,t) reaction, relative to the 0^+ cross section, differed by 50% in the ZR and EFR calculations.

The absolute magnitude of the cross sections was found to agree with experiment within a factor of several, when the EFR method is used. On the other hand the ZR calculations underestimated the magnitudes by more than a factor of 10 to 50. The absolute magnitude depends rather sensitively on the potential parameters used in the calculations. Therefore, the agreement with experiment within a factor of several may allow us to conclude that the EFR calculations can explain even the absolute magnitude of the cross sections.

The computer program used for the EFR-DWBA calculation discussed above was then extended so that EFR-CCBA (coupled-channels Born approximation) calculations can also be performed. An application of this new program has then been made to analyze data for the ^{118}Sn(p,t)^{116}Sn reaction at $E_p = 52$ MeV,[5] and this work was published very recently.[6] A very important aspect of using the EFR rather than the ZR method is seen conspicuously in Fig. 2, in that the dip at about 10° in the angular distribution of the ground state transition is very nicely fit with EFR calculations (either DWBA or CCBA), but not with the ZR calculations. Note that the theoretical reproduction of this dip has been a long standing problem among those working in the TNTR problems.[7]

The fitting of the ground state angular distribution alone cannot discriminate between the EFR-DWBA and EFR-CCBA methods. However, with the former, the magnitude of the 2^+ cross section relative to the ground state cross section is predicted too small by about a factor of 3, while with the latter, it is too large by only a factor of 1.3. It would thus be obvious that EFR-CCBA calculation is needed, albeit the need of a fairly computational time, in order to fit the data with satisfaction.

b). Analysis of a (d,p) reaction to unbound states (Coker et al.)

We have made a large number of studies in the past of (d,p), (d,n) and (^{3}He,d) reactions populating unbound states (see for example Ref. 8). Recently, Coker in collaboration with experimentalists at Michigan State, carried out an analysis of the ^{10}Be(d,p)^{11}Be reaction at 25 MeV incident deuteron energy. The $1/2^+$ ground, $1/2^-$ 0.32 MeV and $5/2^+$ 1.78 MeV states were strongly populated and were described using DWBA and CCBA approaches. DWBA and CCBA were found to agree almost perfectly, despite the strong deformation of ^{10}Be. The Gamow-state approach of Coker[8] was used to extract spectroscopic factors and neutron decay widths of the levels, which were compared to other experiments and to the theoretical predictions of Cohen and Kurath. It is on the basis of our new experimental data, and our calculations, that an assignment of $5/2^+$ is made for the 1.78 MeV state with high confidence. This work has been published.[9]

c). Pick-up-like contributions to the (p,p') cross sections in the continuum (Tamura, Udagawa and Amakawa)

Previously, we showed that the use of the multi-step direct reaction (MSDR) theory was rather powerful in fitting cross sections of various reactions in

the continuum.[10] A somewhat more careful analysis made later particularly for the (p,p') process revealed, however, that our approach needed a further improvement. The calculated cross sections turned out to be too small at very small angles, and at almost all the angles for the transitions corresponding to large values of E_x, the excitation energy of the residual nucleus. We shall discuss the second point in the next subsection d). In the present subsection we shall discuss the first point.

In Fig. 3, we show data of the ^{209}Bi(p,p') reaction taken at $E_p = 62$ MeV.[11] This figure also gives the earlier MSDR results; the dotted lines were obtained when only the one-step processes were considered, while the dashed lines were obtained when the two-step contributions were added.[10] Fig. 3 shows that, even with the latter, there remains a large discrepancy at smaller angles, the discrepancy increasing as E_x increases. With the belief that this discrepancy could be removed by adding contributions of (p,2p) and (p,np) type processes, we undertook the following calculations.

The calculation was made assuming that the above processes can be described as pick-up type reactions leading to an unbound but mutually attracting di-proton or proton-neutron system. For simplicity, a zero-range (ZR) approximation was made, allowing us to perform the calculations in almost the same way as what is well known for a (p,d) calculation; the only difference was that we had to reevaluate the so-called D_o factors. The cross sections thus obtained were added to the previously calculated MSDR cross sections (dashed lines in Fig. 3), and the total cross sections thus resulted are plotted in Fig. 3 by solid lines. It is seen that the solid lines agree very well with experiment. This result was reported at a conference.[12]

To be more precise, however, the newly obtained pick-up type cross sections were multiplied by an arbitrary factor of 2.5, in obtaining the solid lines in Fig. 3. In other words, the calculated cross sections were too small by a factor of 2.5, although their angle and E_x dependence is in good accord with experiment. It is quite possible that this underestimate resulted from our use of the ZR approximation. Had we used the EFR method instead, this problem might not have been encountered. This possibility is under investigation in cooperation with Amakawa.

d). Microscopic versus collective form factors in calculating the (p,p') cross sections in continuum (Lenske and Tamura)

In the preceding subsection, we noted that the MSDR results[10] tended to underestimate somewhat the cross sections at very large E_x. A conceivable way to remove this difficulty is to add the contributions of steps higher than the one and two which have been considered so far. Before undertaking such an elaboration, however, it would be worthwhile to reinvestigate the validity of one of the approximations made in Ref. 10, and elsewhere, in order to make the calculations feasible. It is the use of the so-called collective form factors.

In Ref. 10, it was argued that the use of the collective form factor can be justified, in view of the fact that we are interested in fitting only the summed (or averaged) cross sections, and this may indeed be the case to a large extent. When the discrepancy in the magnitude we are faced with is only by a factor which is much less than two, however, it becomes meaningful to make a more subtle investigation of this point. A possible approach is to compare the predictions of the cross sections made by using the collective form factor, on the one hand, and the microscopic form factor on the other.

We (Lenski and Tamura) thus took up again the $^{208}Pb(p,p')$ reaction,[11] and performed calculations to obtain microscipic cross sections to excite a variety of one-particle-one-hole (1p1h) states. In order to describe the radial parts of the wave functions for nucleons occupying the particle and/or hold orbits, the harmonic oscillator wave functions were used throughout. The effective interaction between the projectile proton and the target nucleon was taken as Gaussian with $V_o = -15$ MeV and the range parameter $\mu = 1.8$ fm. The knockout exchange contributions were included by using the LEA method of Petrovich, et al.,[13] which was later confirmed[14] to be a good approximation for the $^{208}(p,p')$ reaction (for comparatively low E_x). An imaginary form factor was also taken into account in the sense of Satchler's hybrid model.

The choice of a specific pair of particle and hole orbits decides a Q-value, and for such a Q-value the cross sections were also calculated by using a (Q-independent) collective form factor. A conclusion drawn from these calculations was that the angular distributions obtained with the collective model (CM) and the microscopic model (MM) are essentially the same irrespective of the choice of a 1p1h pair, and thus of the Q-value, and also of the transferred angular momentum L. This result is very reassruing in that it justifies the use of CM in Ref. 10, at least in predicting correctly the L-dependence of the angular distributions.

The L-dependence of the predicted magnitudes of the cross sections do differ, however, between CM and MM, and this is the result we expected to have. Take, e.g., the excitation of a $(1h_{9/2}^{-1}, 2g_{9/2})$ state with $Q = -6.91$ MeV which allows $L = 3$, 5, 7 and 9. Let us denote by R the ratio of the angle integrated CM and MM cross sections, normalized in such a way that $R = 1$ for the lowest

possible L, i.e., L = 3. Our calculation showed that R = 1, 0.57, 0.46 and 0.32 for L = 1, 3, 5 and 7, respectively. This means that CM underestimated (relatively) the cross sections corresponding to larger L. As another example, we took the $(1g^{-1}_{9/2}, 1i_{11/2})$ state at Q = -18.2 MeV. We found that R = 1, 0.63, 0.61, 0.70 and 0.58, respectively, for L = 2, 4, 6, 8 and 10, repeating the same trend as shown above.

We noted above that the MSDR cross section was slightly too small.[10] The above result, which shows that we had somewhat underestimated the cross sections corresponding to larger L, may be taken to provide a way to remove this difficulty. Since we had evaluated the cross sections coming from lower L values more accurately,[10] in that the sume-rule limits[15] were carefully watched and spectroscopic strengths derived microscopically[16] were used, we may retain their values as they are. The above result then shows, that we may multiply the old MSDR values with large L by a factor of R^{-1}, which is in the range of two, as far as the above examples are concerned. We already have obtained the R factors for a number of other 1plh pairs, and found that R < 1 in a large fraction of cases. However, there are cases which give R > 1 for larger L. A notable example is the $(1f^{-1}_{7/2}; 1k_{17/2})$ state at Q = -30.5 MeV. Here we have R = 1, 4.28, 14.23 and 52.25, respectively, for L = 5, 7, 9 and 11. Since our experience[10] shows, however, that the two-step contributions begin to supercede the one-step contributions, the above counter-example may not be too serious a problem. Up to now, the residual interaction within the nucleus was neglected in the MM calculations. Presently, calculations are in preparation in which configuration mixing effects will be studied. The averaged first step contribution of the continuum cross section is then given by a sum of elementary 1plh-cross sections. We expect that the averaging will wash out the above

stated differences between the MM and the CM cross sections. At this stage it seems to us that the CM and the MM will give within a constant factor essentially the same results for the continuum cross section.

e.) Analyzing power in the continuum (p,p') reaction (Chang, Tamura and Udagawa)

Recently, Sakai et al.[17] measured the analyzing power A in reactions leading to the continuum, induced by polarized proton beam with $E_p = 65$ MeV. Targets used were ^{28}Si, ^{58}Ni and ^{209}Bi, and it was found that A was surprisingly large even at large angles and at comparatively large E_x.

It should be noted, however, that the statement that A was "surprisingly" large was based to a large extent on intuition. One may expect that the cross sections at large angle and large E_x are sums of various complicated contributions, and thus that any particular signature like A would simply be washed out.

We have shown, however, that the (p,p') continuum cross sections can be fit to a rather satisfactory degree by the MSDR method.[10] We (Chang, Tamura and Udagawa) thus thought it would be worthwhile to see to what extent essentially the same method would apply in reproducing the observed A, and thus undertook the following calculation.

In Ref. 10, protons were treated as spinless particles. In obtaining nonvanishing A, however, this simplifying treatment has to be abandoned. Thus a fairly large modification had to be made in the computer program ORION-1. This also resulted in an increase of the computational time (by a factor of three or so). In order to avoid being faced with a too large number of partial waves, and also with too light a target, we chose $^{58}Ni(p,p')$ as an example. In

the new calculation the optical potential of Menet et al.[18] was used, as in Ref. 10, except, of course, we now set $V_{so} \neq 0$.

The result of calculation is compared with experiment in Fig. 4. The dashed lines represent the predicted A, without making any artificial modification. It is seen that they fit data nicely for all E_p', i.e., for all E_x considered, in the angular range of 30°-60°. They overshoot, however, the experimental A at angles larger than 60°. We show in Fig. 4 also the calculated A times 1/3, by solid lines, and it is seen that they give a much better overall fit to data. It should be noted that the experimental A in the $\theta \geq 60°$ region is only very weakly dependent on the angle, having values of about 15%, 10% and 7%, respectively, for $E_x = 12 - 16$, $20 - 24$ and $28 - 32$ MeV. Since the calculated A was multiplied by the same factor of 1/3, irrespective of E_x, the above fit means that our calculation has succeeded in predicting the E_x dependence of A correctly.

From what we discussed in the beginning of the present subsection, it is rather surprising that the theoretical A was itself too large compared with experiment. Such a result came about, because the individual cross sections, which are to be summed to give the continuum cross section and thus the A in the continuum, all had very similar and large A values, particularly at large angles. This was true for both the one- and two-step cross sections, and thus the expected washing out of A did not take place. We have not yet understood clearly why A stays so large even for two-step processes. Probably there exists a rather simple geometrical explanation.

It may be possible to obtain[9] better fit to data, even without an artificial factor like 1/3, by modifying slightly the spin-orbit interaction in the Menet et al. potential. It appears that a similar need was noticed in a work[19] in

which A was measured in a (p,p') process, leading, however, not to the continuum but to (almost) discrete states.

The discrepancy we have in Fig. 4 at $\theta = 20°$, might also be removed in this process as well. However, it is more likely that the discrepancy is due to the neglect of the pick-up type process we discussed in the above subsection c). Note again that this process dominates the small angle cross sections.

f.) Breakup of ^{3}He into d and p (Udagawa and Tamura)

The break up orocesses in nuclear collisions have attracted a greatly revived interest recently. Earlier studies of this subject almost exclusively concentrated on deuterons.[20,21] More recently, however, it was found that not only deuterons, but also more strongly bound projectiles, like α, are broken up rather easily.[22] Very detailed coincidence data were taken for the so-called elastic and inelastic break up of ^{3}He.[23] We have analyzed this data,[24] and a brief summary of this work will be given here.

We start with the EFR-DWBA theory, as formulated by Rybicki and Austern.[25] We view the process as an inelastic excitation of the projectile which may be called a into a continuum. This nucleus a will eventually be broken up into two constituents, x and b, say. The DWBA amplitude is then written as a six dimensional integral, familiar in the EFR-DWBA theory, containing the coordinate $\underline{r}_a$, describing the position of a with respect to the target, and the coordinate $\underline{r}_{xb}$, describing the relative position of x and b. For the latter degree of freedom, the upper limit permitted to the orbital angular momentum ℓ is very severely limited, because if $\ell > 2$, the above transition amplitude becomes extremely small. We can thus construct easily the explicit form of

the wave function of $\underline{r}_{xb}$ degree of freedom, and thus perform the three dimensional integral over $\underline{r}_{xb}$, obtaining a form factor to be used to describe the inelastic excitation of the projectile $\underline{a}$. To be more precise, this form factor depends on ℓ, r_a and E'_x, the last quantity describing the kinetic energy (in the asymptotic region) of the relative motion between $\underline{x}$ and $\underline{b}$. We may thus write the form factor as $F_\ell(E'_x, r_a)$.

A great deal of simplification was then made by noting that the inelastic process concerned is highly peripheral, and thus that it is a good approximation to replace the above F_ℓ in the following factorized form; $F_\ell(E'_x, r_a) = A_\ell(E'_x) f_\ell(r_a)$. Once the functional form of the factors A_ℓ and f_ℓ are obtained, the calculation of the breakup process is reduced to a fairly small number of sets of inelastic scattering calculations, which is performed rather easily.

We show in Fig. 5 part of the results obtained. Shown is the triple differential cross section, where θ_d is fixed at 15°, while θ_p and E_d are varied. (Since this is the case of an elastic breakup, E_p is fixed once E_d is given.) It should be noted that a constant normalization factor of $N = 2.9$ was multiplied to the theoretical cross sections in presenting them by solid lines in this figure.

The agreement with experiment achieved in Fig. 5 is very good. The gradual shift of the peak value of E_d, as $|\theta_p|$ is increased, is well reproduced. Also the relative magnitudes of the triple cross sections agree very well with experiment for each value of θ_p. This means that, since the above factor $N = 2.9$ was used independent of θ_p, our theory also fits the angular distribution of the cross section with respect to θ_p (for a fixed θ_d).

In the study made so far, we confined our interest to the elastic breakup process. However, the data of Ref. 23 include those of inelastic breakup, and

its analysis would also be very interesting. The technique developed in the present work can be extended fairly easily to this new analysis. We first describe the inelastic scattering to an excited state in the target, and then continue the calculation to describe the breakup that follows. The new calculation is thus certainly more involved, but it is feasible.

g.) Adiabatic treatment of the deuteron break-up -- a possible examination of its validity (Amakawa et al.)

The adiabatic treatment of the break-up effect on stripping[26] and elastic scattering[26,27] of deuterons has been shown to lead to a good fit to some of the data of reactions induced by deuterons. It seems to us, however, that somewhat more general investigations are needed concerning the validity of this approximate treatment. This may be made by comparing results of calculations made with and without the adiabatic treatment. We shall make such a comparison by taking a simple three-body model, because results with this model and with more accurate three-body treatment and/or coupled-channel calculations are available.[28,29]

The model consists of a proton and a neutron, with a relative coordinate $\vec{r}$, moving around an infinitely heavy nucleus, the center of mass of p and n from the nucleus being measured by $\vec{R}$. The Hamiltonian of this system may be written as $H = K_R + V(\vec{r},\vec{R}) + H_r$. Here $V(\vec{r},\vec{R})$ simply denotes sum of interactions V_p, between p and the nucleus, and V_n, between n and the nucleus.

The adiabatic approximation is to simply replace H_r, the Hamiltonian to describe the relative motion between p and n, by $-\varepsilon_d$, the binding energy of deuteron. Then the Hamiltonian depends on $\vec{r}$ only through the potential $V(\vec{r},\vec{R})$, and thus the corresponding Schrödinger equation can be considered as that of $\vec{R}$,

the coordinate $\vec{r}$ being treated only as a parameter. We can thus solve this equation for each value of $\vec{r}$, obtaining the scattering amplitudes $T(\vec{r})$. Once $T(\vec{r})$ is obtained, the deuteron elastic and break-up amplitudes can be obtained and $T_{dd} = \int |\phi_d(r)|^2 T(\vec{r}) d\vec{r}$ and $T_{\vec{k}d} = \int \phi_k^*(\vec{r}) T(\vec{r}) \phi_d(r) d\vec{r}$ where ϕ_d and $\phi_{\vec{k}}$ are, respectively, the wave functions of the deuteron and the p - n continuum states with momentum $\vec{k}$.

The three-body calculation by Austern, Vincent and Farrell[28] is available at E_d $(=E+\varepsilon_d)$ = 22.9 MeV with the Gaussian potential for V_p and V_n. Fig. 6 shows the elastic partial-wave S-matrix elements of Austern et al., illustrated by open circles, those calculated by the adiabatic approximation (——•——) and those by the Watanabe model (--•--). One sees that the adiabatic treatment removes the trouble which the Watanabe model had for lower partial waves. The break-up cross sections $\sigma_b(k)$ to p - n continuum states with momentum k are calculated in the adiabatic approximation and are compared in Fig. 7 with those calculated from the tabulated amplitudes of Ref. 28. Closeness of the two results is rather assuring albeit is somewhat surprising. The average excitation energy, ε_{av}, defined by $\varepsilon_{av} = \int dk \varepsilon_k \sigma_b(k) / \int dk \sigma_b(k)$ is found to be about 4.3 MeV. The inverse of the collision time (v/R) in this case is about 8 MeV, and the ratio ($4.3/8 \approx 0.5$) gives a crude idea of the validity of the adiabatic treatment.

Coupled-channel calculations applied to essentially the same three-body model as in Ref. 28 were performed at $E_d = 40$, 60 and 80 MeV, by the method of Nishioka et al.[29] The calculated partial-wave S-matrix elements at $E_d = 40$ MeV are compared in Fig. 8 with those obtained based on the adiabatic treatment and on the Watanabe model. The agreement between the results of the coupled-

channel and the adiabatic calculations is quite good, indicating that the adiabatic treatment becomes more reliable at this high energy, as expected. We also found that better agreement was obtained at still higher energies; $E_d = 60$ and 80 MeV. It thus seems that the adiabatic treatment has a rather wide range of validity. This work has been done in collaboration with A. Mori, H. Nishioka, S. Yamaji and K. Yazaki.

ii. HEAVY ION INDUCED REACTIONS

a.) Parametrization of overlap integrals (Udagawa, Tamura and Price)

During the past year, as in two preceding years, we were rather heavily involved in MSDR (multi-step direct reaction) analyses of a variety of continuum spectra in reactions induced by relatively-light heavy ions. As we have remarked in a number of earlier occasions, our MSDR calculation became practicable because we were able to express, among other things, the overlap integrals of DWBA by an analytic function with a few parameters. In our earlier publications, however, we did not have opportunity to explain in detail how this parametrization was done, and how faithfully the parametrized overlap integrals reproduced their original DWBA values. In order to fill this gap, we worked out in great detail the parametrization for the case of a $^{100}Mo(^{14}N, ^{12}B)$ reaction,[30,31] and explained it in a recent paper.[32] Here we shall summarize briefly what was done in this paper.

The one-step DWBA overlap integral, $I^{(1)}$, depends, among other things, on the orbital angular momenta ℓ_a and ℓ_b of the partial waves in the incident and exit channels, on the reaction Q-value and on the transferred orbital angular momentum, ℓ. For transfer reactions, they further depend on ℓ_1 and ℓ_2, the orbital angular momenta which the transferred particle has with respect to the rest of the donor and recipient nucleus, respectively. Our procedure is to express $I^{(1)}$ as accurately as possible by an analytic function which has the Q-value and the above angular momentum quantum numbers as variables.

In Ref. 32, we found that $I^{(1)}$ can be expressed as a product of 4 factors. Two of them have gaussian forms, representing the well known ℓ-window effects. The third factor, which is also well known, is a phase factor originating from

the two-distorted waves involved, and expresses the optics of the beam. The fourth factor, which we called N_0, had not been investigated very carefully in any earlier publication. We thus concentrate on this factor.

First of all, we found that N_0 is almost Q-independent. This implies that the Q-dependence of the magnitude of $I^{(1)}$ is entirely taken care of by the two window factors. The N_0 factor was found, however, to have a rather subtle dependence on the angular momenta involved. Its dependence on ℓ is the most important, particularly because it describes effects such as recoil.

The N_0 with the non-normal parity ℓ, often referred to as the recoil term, is very small for small ℓ_a. However, its magnitude relative to N_0 of the no-recoil term (i.e. the term with a normal parity ℓ) increases with the increasing ℓ_a, becoming comparable at a certain value of ℓ_a. This ℓ_a-dependence of the relative magnitudes of the recoil to no-recoil terms describes, of course, the well known energy dependence of the recoil effects. N_0 depends also on other angular momenta involved, particularly on $\ell_d = \ell_b - \ell_a$. It was found that the details of this ℓ_d dependence varied according to the value of ℓ, particularly whether it was of normal of non-normal parity. It was shown in Ref. 32, that we were able to trace the origin of such subtle behavior, by looking very closely at the way the EFR form factors are constructed for different ℓ values.

Once the parametrized form of the overlap integrals is thus obtained, it becomes possible to express in analytic forms also the cross sections and other quantities, such as polarizations of the reaction products. This was already discussed in last year's progress report; see also Ref. 31. In our recent publications, similarly simple expressions were also derived to describe the cross sections and angular correlations of the breakup processes; see below. These expressions are very useful, not only in facilitating the numerical

calculations, but also in obtaining good physical insight into the mechanisms of the reaction.

We also confirmed that these simplified expressions do reproduce very well the exact results. In Fig. 9, we compare the cross sections obtained by using the approximate formula (full line) and the exact expressions (circles). The good agreement obtained amply justifies our use of this simplified formulas.

b.) Transfer reactions leading to polarized ^{12}B (Udagawa and Tamura)

Earlier,[31] we succeeded in explaining the polarization[30] of ^{12}B produced in the $^{100}Mo(^{14}N,^{12}B)^{102}Ru$ reaction with incident energy $E_{lab} = 90$ MeV. More recently, similar data were taken by Ishihara et al. at Texas A&M for the $^{232}Th(^{13}C,^{12}B)^{233}Pa$ and $^{197}Au(^{19}F,^{12}B)^{204}Bi$ reactions.[33] Calculations were thus made for these reactions, following the same method as Ref. 31. In these calculations, we treated both reactions as one-step processes, transferring one and seven nucleons, respectively, and then used the spectroscopic densities, $\rho_s^{(1)}$, obtained based on the shell model. In Fig. 10, we summarize results of such calculations,[31,33] together with data. The figure includes both the cross sections σ and the polarizations P.

We first note in Fig. 10 that the measured P has a common characteristic feature as a function of the outgoing energy E_b of ^{12}B. It has comparatively large positive values for the highest E_b, and then decreases monotonically as E_b decreases, until it becomes zero at an E_b, where the σ reaches its peak value. For still smaller E_b, P becomes slightly negative and stays almost constant. Our calculations reproduce very well this observed feature, particularly in the higher E_b part of the spectra.

As was discussed in Ref. 31, our theoretical P can be written as a sum of two terms, P_1 and P_2, where P_2 specifically describes contributions from the interference between transition amplitudes of successive ℓ values. Thus, clearly, P_2 is entirely due to the recoil effect, and in this sense has a genuinely quantum mechanical origin. Corresponding interference effects never take place in the cross section, and thus the information concerning the polarization provides us with a unique test of our theory.

We plot in Fig. 11 contributions from P_1 and P_2 separately. As seen, P_1 is negative definite, while P_2 is positive definite. The value of P_2 is particularly large at the higher E_b. It is thus seen that P_2 dominates at higher E_b, making P positive there.

It is also interesting to examine the dependence of P on the incident energy E_a. As is well known, the recoil effect, because of which P_2 is non-vanishing, becomes more important with increasing E_a. Therefore, it is expected that the observed P will increase with increasing E_a. An examination of this energy dependence was made, and the results are shown in Fig. 12, where the P at the highest E_b of the (^{14}N,^{12}B) reaction is plotted as a function of E_{eff} ($=E_a-V_c$, V_c being the height of the Coulomb barrier).[30,34] So far there are available only three (^{14}N,^{12}B) data with different E_a and/or different targets. Yet, one sees clearly that the observed P indeed increases (approximately linearly) with increased E_{eff}, as was expected.

The above success in explaining the behavior of the observed P seems to convince us that the higher E_b part of the spectra are indeed due to the one-step direct reactions. This conclusion may not be too surprising as regards reactions like (^{13}C,^{12}B) and (^{14}N,^{12}B), in which a very small number of nucleons are transferred. It is however, somewhat surprising to find that the same is

true, as seen in Fig. 10, even in reactions like (^{19}F, ^{12}B), in which seven nucleons are transferred. In this regard, it may be worthwhile to point out that there are other types of measurements which indicate the presence of (one-step like) direct reactions, yet transferring more than ten nucleons. A notable example of such processes is what is called "massive transfer."[35] Thus, after all, a transfer of a large number of nucleons in direct reaction processes appears to take place rather commonly, and not exceptionally.

The theoretical prediction presented by solid lines in Fig. 10 begins to disagree with experiment as we move to lower E_b regions. To be noted in particular is the fact that the E_b, at which the calculated and experimental σ starts to disagree, shifts toward higher values, as the number of the transferred nucleons increases. This is not inconsistent with our picture that the multistep contributions, which we have totally ignored so far, will become important at the higher E_b the larger is the number of nucleons transferred.

Finally, we point out that the higher E_b part of the spectra, which remains unexplained by the one-step calculation, seems to be related to the so-called deep inelastic events. We feel it is the case because the spectrum observed for the above (^{19}F, ^{12}B) reaction at a larger angle ($\theta > 50°$), where the deep inelastic events are believed to dominate, has a shape very similar to what was left unexplained at $\theta = 25°$ (being represented by a dashed curve in Fig. 10).

c.) Alpha-transfer reactions and their competition with breakup processes (Udagawa and Tamura)

It has long been considered that the breakup of a projectile is one of the typical examples of peripheral processes, and may contribute importantly to the continuum spectra of reactions induced both by light and heavy ions. This is

indeed the case, and very recently many experimental evidence has been accumulated. In order to analyze such data, we developed a very simple, yet rather accurate method, and it was outlined in subsection i - d.

As was discussed there already, we view the breakup as an inelastic excitation of a projectile a, consisting of b and x which are initially bound together, into a continuum state which may be written as $a' = b + x$. The resultant transition amplitude is then written as a coherent sum of products of two factors, the spectroscopic amplitude, A_ℓ, and the DWBA transition amplitude, $\beta_{\ell m}$. The A_ℓ factor describes the strength of the transition $a \to a' = b + x$ while $\beta_{\ell m}$ does the transfer of the energy from the relative motion between a and the target to that b and x, ℓ being the transferred angular momentum. The above mentioned sum is taken coherently over ℓ. It is the A_ℓ-factor that decides the ways with which different projectiles are broken up.

The A_ℓ depends on many physical quantities that the projectile is described by. They are, e.g., the binding energy B (the kinetic energy E_x) and the orbital angular momentum $\ell_2(\ell_x)$ of the initial bound (final continuum) state other than ℓ. It has been thought for a long time that the B-dependence is the most important and thus that projectiles with small B, like ^2H and ^6Li would most easily break up. We found, however, that the dependence on ℓ-, ℓ_2- and E_x was also very important.

First of all we emphasize that A_ℓ decreases quite rapidly with increased ℓ. This was discussed in detail in our previous studies.[24,36] Because of this fact, it is quite safe to ignore contributions from ℓ beyond 2. (Usually the $\ell = 0$ contribution dominates.) When considered as a function of E_x, A_ℓ has a strong peak at E_x around the energy equal to the height of the Coulomb barrier between b and x. This height is in the 2 to 4 MeV range for light heavy-ion

projectiles. This means that the breakup proceeds with very small E_x, i.e., by transferring a very small amount of energy into the relative motion between x and b. One important consequence of this fact is that the value of ℓ_x must also remain small. Indeed, we have found that the process is usually dominated by the $\ell_x = 0$ component, i.e., by the s-wave.[24,36]

The above ℓ- and ℓ_x-dependence of A_ℓ leads to an interesting projectile dependence of the breakup. Let us compare the breakup of ^{20}Ne and ^{14}N into $\alpha + ^{16}$O and $\alpha + ^{10}$B, respectively. As is well known, the dominant component of α in the ^{20}Ne and ^{14}N ground states are, respectively, in the s and g states, i.e., $\ell_2 = 0$ and 4. In order to excite these α into the s state, i.e., $\ell_x = 0$ we must have $\ell = 0$ and $\ell = 4$, respectively. Since, as we remarked, $|A_4| \ll |A_0|$, it is evident that the breakup of ^{14}N is much more suppressed as compared with that of ^{20}Ne. We shall show soon that a very clear evidence for the breakup of ^{20}Ne was found, but not for ^{14}N. The B-dependence also works unfavorably to the breakup of ^{14}N. In ^{14}N, B = 11.6 MeV, while B = 4.7 MeV in ^{20}Ne.

So far we have discussed only the A_ℓ factor. The $\beta_{\ell m}$ factor gives rise to an important effect as well. It is reduced strongly when the Q-value is large. Recall that the breakup is dominated by the $\ell = 0$ contribution. The $\ell = 0$ process is, however, poorly Q-matched for large $|Q|$, reducing the cross section. However, the Q-mismatch decreases with increasing incident energy. Therefore, even if the breakup is too weak to be observed at low energies, it may be observed at higher energies. Some evidence of this energy dependence will be discussed shortly.

A very clear evidence of the ^{20}Ne breakup was found recently by an experiment by Nagatani et al.,[37-39] who observed inclusive spectra of reactions, ^{40}Ca(^{13}C,^{9}Be), ^{40}Ca(^{14}N,^{10}B) and ^{40}Ca(^{20}Ne,^{16}O) with the incident energies of

149 MeV, 153 MeV and 262 MeV, respectively. It was found that at very forward angles, say 5° - 8°, the observed cross sections for the (^{20}Ne,^{16}O) reaction are larger by an order of magnitude compared with those for the other two reactions. It should also be remarked that the cross sections of the (^{20}Ne,^{16}O) reaction decreases very rapidly as the angle is increased, making the (^{20}Ne,^{16}O) cross section about the same as those of the other two at larger angles.

It was also found that the theoretical cross sections obtained by assuming a one-step α-transfer process[37] explained very well the observed cross section of the (^{13}C,^{9}Be) and (^{14}N,^{10}B), but not of the (^{20}Ne,^{16}O) reactions. From this, it was concluded that there was in fact some other mechanism contributing to the (^{20}Ne,^{16}O) reaction, presumably the breakup of ^{20}Ne. This idea was further supported by the fact that the position of the peak in the spectra lie at about 4/5 of the incident energy.

Having this evidence in mind, we performed numerical calculations of the transfer and breakup processes[36] and the results are presented in Fig. 13. As seen, the calculation reproduces the observed data very well. Note that the experimental peak cross sections increase by about a factor of 2 to 3 as the incident energy increases from 149 to 262 MeV, and our calculation reproduces this as well. This is evidence of the energy dependence we discussed above.

A fact to be noted here is that we have introduced an arbitrary normalization factor of 1.6 in the breakup cross sections in obtaining the fit in Fig. 13. As will be shown below, the inclusive data seems to contain not only the elastic breakup, but also the inelastic breakup contributions. The above normalization factor may be interpreted to take into account the latter.

A further insight into the process may be obtained by measuring coincident data, and such an experiment was also done by Nagatani et al.[39] We present in

Fig. 14 the result of the measurement and the corresponding theoretical predictions, which are seen to fit the data very well. A remarkable feature seen in the measured angular correlation curve is that the width is extremely narrow; about 5°. Such a narrow width has never been observed in the angular correlation data taken in ^{14}N induced reactions,[40,41] the typical width observed being about 20°. This fact presents an indirect support of our previous conviction that ^{14}N is very unlikely to break up;at least for those energies (E<210MeV) studied so far.

Probably, ^{16}O is one of the best candidates for breakup other than ^{20}Ne. Indeed, the ^{16}O breakup yields have been observed by a Berkeley group[42] with $E(^{16}O) = 310$ MeV. Nagatani et al.[39] also performed a similar experiment finding that the breakup begins to take place at $E(^{16}O)$ around 200 MeV for a ^{58}Ni target. This is another evidence of the energy-dependence of the breakup.

Summarizing, we have seen the presence of the projectile- and energy-dependencies of the breakup, and that they can be understood very well in terms of the present theory. The theory is found to describe very well also the angular correlation data. Our theoretical treatment has so far been confined to the elastic breakup. A coincident measurement,[39] however, revealed that there are sizable contributions form the inelastic breakup. To deal with inelastic breakup processes, we have to extend the present theory, but it will be done without much difficulty.

d.) Higher-step direct reaction analyses (Udagawa, Price and Tamura)

As was discussed in subsection a) the calculations that include only the one-step contributions fail to explain the so-called deep inelastic component of the spectrum. It would then be natural to investigate whether these deep

inelastic components can be attributed to the contributions from higher-step processes. We studied[43] as an example of the two-step process the $^{27}Al(^{20}Ne,^{12}C)$ reaction at $E_{lab} = 120$ MeV.[44] The calculation was made by first fitting the data of the $^{27}Al(^{20}Ne,^{16}O)$ reaction, assuming there a one-step α-transfer mechanism. This fitting fixed several parameters involved in the calculation. Then the two-step calculation for the $(^{20}Ne,^{12}C)$ reaction was made without introducing any additional parameter. The results of these calculations are shown in Fig. 15 and are compared with experiment.

It is seen that the overall qualitative agreement of the calculated results with experiments is good. However, quantitatively the calculated cross sections are too small by about a factor of 2, the discrepancy increasing as the energy of the outgoing ^{12}C increases. In Fig. 15 there are also plotted the difference (dotted line) between the calculated and experimental cross sections. One notable feature seen is that the position of the peak of the dotted line appears at a slightly higher $E(^{12}C)$ than that of the calculated two-step cross section. It might be possible to ascribe this unexplained part of the spectrum to the one-step direct ^{8}Be transfer. Such an investigation will be done in the future.

In order to study further the effects of the multi-step processes, we took up also the inelastic scattering of ^{16}O by ^{58}Ni at the incident energy of $E_{lab} = 100$ MeV.[45] The spectrum at 35° is shown in Fig. 16(a). It is seen that there are two humps at $E_x = 0 - 15$ and $15 - 40$ MeV regions, where E_x is the excitation energy of ^{58}Ni. These two humps are normally ascribed to the quasi-elastic and deep-inelastic processes, respectively.

In addition to cross sections, measurement was also made[45] of the circular polarization of γ-rays emitted from the residual nucleus, $^{58}Ni^*$. The γ-ray circular polarization allows one to extract the polarization P_N, of $^{58}Ni^*$, and

it was found that at the $^{16}O'$ energies correspond to the first and second humps, respectively, P_N was negative and positive. This implies that the quasi-elastic and deep-inelastic components are associated with the processes coming from the near side (positive deflection) and the far side (negative deflection) processes. The measured P_N are reproduced in Fig. 16(b).

In order to facilitate the estimation of contributions from the two-step, as well as the one-step processes to the cross section, σ, and to P_N, we first investigated the possibility of parametrizing the overlap integral, $I^{(2)}$, of the two-step processes. We found that $I^{(2)}$ was also characterized by windows similar to those of $I^{(1)}$. The windows in $I^{(2)}$ were found, however, to be somewhat less characteristic than they were in $I^{(1)}$ in that the shape of the windows were distorted rather strongly from the simple gaussian form, and also that the values of some of the window parameters dependend in a complicated fashion on the other parameters involved, making it very difficult to express analytically the former in terms of the latter. Also some parameters were very sensitive to the other parameters involved in the calculations, particularly to the imaginary part of the optical potential, which is not very well known for the channels involving highly excited nuclear states. Therefore, it was unavoidable that the parametrized amplitudes did not always reproduce faithfully the exact two-step DWBA amplitudes.

Nevertheless, we tried to fix the parameters in a way very similar to what we did for $I^{(1)}$. Important features of the results obtained may be summarized as follows: i) The values of the deflection angles $\Psi^{(i)}$ ($i = 1$ and 2, respectively, for the one- and two-step process) were definitely positive and negative for $i = 1$ and 2, respectively. The magnitudes of $\Psi^{(i)}$ depend only very slightly on the Q-values, making it acceptable to set $\Psi^{(1)} = 10°$ and $\Psi^{(2)} = -20°$ for all

the Q-values involved. ii) The Q-dependence of the centers of the windows of $I^{(2)}$ is nearly the same as that of $I^{(1)}$. Thus for both $I^{(1)}$ and $I^{(2)}$ we can use $\ell_d^{(o)} = 0.6Q$ and $\ell_b^{(o)} = 48 + 0.6Q$. iii) The most poorly determined parameters are the widths of the centers for $I^{(2)}$, which are somewhere between 5 and 10. Those for $I^{(1)}$ are, however, rather well determined to be about 5. The widths of the two-step process is thus larger than those of the one-step.

The calculations of σ and P_N were then performed by using the spectroscopic densities (i.e., the densities of the deformation strengths, or the response functions) calculated by Liu-Brown.[16] The orbital angular momentum transfer of $\ell = 0 - 8$ were considered in the calculations. In Ref. 16, such calculations were made for only up to $\ell = 4$. Those for $\ell = 5 - 8$ were thus calculated by using a simple model of the multipole forces.[46] Slight modifications were introduced to thus obtain spectroscopic densities so as to improve the fit to experimental σ.

The theoretical one- and two-step cross sections are plotted in Fig. 17(a), separately by dotted lines. As seen, the one-step contributions explain very well the observed first hump at the lower excitation energy, $E_x \simeq 0 - 15$ MeV. As will be discussed shortly, the one-step contribution also explains very well the observed P_N at this region of E_x. The two-step contribution, however, is not sufficient to explain the rest of the spectrum, in particular the spectrum under the second hump. This discrepancy may indicate that the contributions of still higher order processes have to be taken into account. In order to make a crude estimate of such higher order contributions, calculations of the third order processes were made by assuming that $I^{(3)} = aI^{(2)}$, where the constant a was fixed so that the resultant total spectrum agreed with the data at 20°. The calculated total cross sections at 35° are then plotted in Fig. 16(a) by a full line. As seen, the overall agreement with the data is now very good. The

assumed value of $\underline{a}$, however, is somewhat too large as compared with that expected from a simple extrapolation of the overlap integral. Probably, this effiectively includes the fourth and higher order processes. In Fig.16(b), we also include the final calculated P_N by a full line. The agreement is seen to be very good.

There are a few other papers either published or submitted during the past year. They include the summary talk[47a] at the International Conference on "Dynamical Properties of Heavy-Ion Reactions", held at Johannesburg, August, 1978, a lecture note at the Post-Conference School also at Johannesburg[47b], an invited paper presented[47c] at the International Workshop on "Reaction Models for Continuous Spectra of Light Particles", Bad Honnef, November, 1978, and finally an invited paper[47d] presented at the International Symposium on Continuum Spectra of Heavy Ion Reactions, San Antonio, December, 1979. We organized this last Symposium ourselves, in collabotation with the experimental group at the Cyclotron Institute, Texas A&M University.

Two papers were published in Computer Physics Communications, the one[48a] dealing with Coulomb wave functions with complex angular momenta, the other[48b] with a new method of constructing form factors for EFR-DWBA calculations. Another paper dealing with the calculation of the Regge poles will be published shortly[48c]. Finally, a paper which dealed with a problem of dissipation in the time-dependent Hartree Fock calculations was also published recently[49].

iii. MEDIUM ENERGY PHYSICS

(W.R. Coker*)

a.) Preliminary

Since 1976 we have been very actively engaged in a collaborative program of experimental and theoretical research in medium energy nuclear physics, principally the study of scattering and reactions of 800 MeV protons on nuclei. Our theoretical efforts actually began about a year before our experimental program, making use of 1 GeV proton elastic scattering data for a variety of target nuclei, obtained at Saclay and Gatchina.

From the very beginning of our research program, we have held very firmly to the pragmatic philosophy that hard results are of primary importance, and can only evolve from precise, reliable experimental data and sophisticated, state-of-the-art theoretical analyses. As will be apparent from what follows, in our studies to date experiment and theory have merged to play complementary and very closely linked roles. Our program has provided the nuclear physics community with a large quantity of accurate data on elastic scattering of 0.8 GeV protons on a wide range of target nuclei, as well as the results of theoretical analyses aimed at learning as much as possible concerning the matter density distributions of the various target nuclei. To date about a dozen papers have appeared in print presenting the data and the results of the analyses.[50-63]

---

*Most of the research described here was carried out in collaboration with Assoc. Prof. G. W. Hoffmann and Dr. L. Ray, whose research is currently supported by DOE contract EY-76-S-05-5224, Task B. This collaboration is expected to continue.

The original motivation given in the 1960's for doing proton elastic and inelastic scattering experiments at intermediate energies was that the theoretical approaches which could be employed to deduce nuclear structure information from the data were thought to be free from various ambiguities which plague studies at incident proton energies of 300 MeV or less. The standard argument went that at medium energies the impulse approximation is expected to work well. As a result, one could begin from the free nucleon-nucleon scattering phenomenology and derive microscopic optical potentials or distorted wave impulse approximation (DWIA) transition matrix elements that would very directly describe proton elastic and inelastic scattering in terms of nucleon densities and moments of the target nuclei. Furthermore, the incident momentum at proton kinetic energies of about 1 GeV is large enough that the spatial resolution afforded by the available momentum transfer range would be sufficient to extract fairly detailed information concerning the radial shape of the nuclear matter density distributions involved in the scattering and reactions. It was even asserted frequently in the literature that information could be obtained regarding the positional or momentum correlations of pairs of nucleons in nuclei, and a vast amount of theoretical effort was devoted to deriving formal expressions for contributions of various kinematic and dynamic nucleon-nucleon correlations to the predicted cross sections.

It is not too great an exaggeration to say that up until new data from Saclay and Gatchina appeared medium energy physics was essentially a dataless field, and many of the problems in related theoretical work could be traced back to this disconnection from reality. As we began to analyze these new data theoretically, however, we saw that the problems of the field were far from over. First, the nucleon-nucleon phenomenology itself is in a sad state

at these energies. Second, it became apparent that serious reliability problems still existed even with the new 1 GeV proton-nucleus elastic scattering data. This experience provided valuable guidance to our experimental effort, since it demonstrated clearly how certain errors in scattering angle determination or absolute cross section calibration could completely erase the subtle nuclear structure effects which one is interested in learning more about through analysis of such data.

In many ways, the results of existing theoretical analyses of such data documented in the literature were almost as disturbing as the apparent unreliability of the data itself. Tremendous efforts were focussed on the relatively minor contributions to the scattering process from nucleon-nucleon correlations, but the overwhelmingly important first-order, density-related contributions were handled in ways that were absurdly crude and which we found in our own calculations to be quite incapable of describing the experimental data more than qualitatively.

We hoped to avoid both the experimental and theoretical errors we had encountered in earlier work. A fairly massive experimental effort was mounted at the High Resolution Spectrometer facility of the Clinton P. Anderson Meson Physics facility in Los Alamos, to provide medium energy proton elastic scattering cross sections of unprecedented reliability and range of momentum transfer. Elastic angular distributions and analyzing powers were obtained at LAMPF for 800 MeV polarized proton elastic scattering from the target nuclei ^{12}C, $^{40,42,44,48}Ca$, $^{46,48,50}Ti$, ^{54}Fe, $^{58,64}Ni$, ^{90}Zr, $^{116,124}Sn$ and ^{208}Pb.[50-64] All of these data have now been reduced to final form and made available to the nuclear physics community in tabulations.

As was explained in detail in last year's annual report and elsewhere, we intended to have from the beginning a reasonably unified treatment of elastic

and inelastic scattering and analyzing power, in terms of a microscopic description of the nucleon-nucleon interaction potential.[65] Because of the reasons also given in last year's annual report, we avoided the use of a multiple-scattering diffraction theory[66] in obtaining cross sections, relying instead insofar as was possible on the equation-of-motion techniques developed by Feshbach and his collaborators.[65,67] A notable advantage of the use of the latter is that it can be reduced directly to corresponding low-energy forms, permitting one to make use of various established nuclear phenomenologies at intermediate energies.[68] We also note that we took special care in deriving spin and charge dependent part of the nucleon-nucleus optical potential[69,70] based on the KMT approach.[65]

When our preliminary analyses[50-52] were found to be very primising, and to give densities in surprisingly close agreement with Hartree-Fock predictions, we completely redid the analyses, constructing an approximately model-independent neutron density, and making a very careful and thorough study of experimental and theoretical sources of error and uncertainty in the analysis.[56] The resulting uncertainties amounted to ± 0.07 fm in the root mean square neutron radius; as far as the radial neutron densities were concerned, the error envelopes became significant in width only well within the nuclear interior. This encouraged us to increase the sophistication of our analyses still further.[62] We included the (very tiny) effects of center-of-mass, Pauli and dynamical nucleon-nucleon correlations within the nucleus, and electromagnetic corrections to the proton density arising from the electric and magnetic form factors of the neutron and the magnetic form factor of the proton -- which tended nearly to completely cancel the correlation effects. These corrections reduced the error ultimately to about ± 0.05 fm in the rms neutron radii, of which about ± 0.03 fm arises from

uncertainties in the free nucleon-nucleon amplitudes.[62] Further significant reduction in the uncertainties is not practical until the experimental situation in medium energy nucleon-nucleon physics changes drastically. With all sources of error taken into account, the agreement between the deduced neutron matter densities and the corresponding densities predicted by Hartree-Fock formalisms is extremely impressive, and has provided much of the motivation for our further work in this area, both experimental and theoretical. See Figs. 17-21.

Our inelastic scattering studies, both experimental and theoretical, have concentrated so far on low-lying collective states of even-even nuclei. As a result, we have used the DWBA (as opposed to the so-called DWIA) and the coupled channels approach -- for the first time at medium energies, so far as we know.[68] In the theoretical analyses, the inelastic analyzing power data which have become available from the LAMPF HRS proton elastic and inelastic scattering survey with polarized proton beams have played an important role.[58,64] In our collective DWBA form factors, if one begins with the microscopic KMT proton-nucleus optical potential, one automatically generates a so-called "Full Thomas form" for the spin-orbit contribution to the inelastic transition matrix element.[64] This additional term, usually neglected in low energy inelastic proton scattering analyses, is important at medium energy in giving the inelastic angular distributions the proper slope, and the inelastic analyzing powers the proper shapes. In two recent papers, we have emphasized both the experimental and theoretical importance of this "deformed spin-orbit" term in the inelastic form factor.[58,64]

In the coupled channels framework we have studied inelastic transitions to various highly collective states of ^{12}C and ^{24}Mg, and shown that the various paths by which the reactions can occur have distinct partial angular distributions, allowing one to determine the deformation parameters for the various collective

nuclear shapes far more accurately than has hitherto been possible in proton and ^{4}He scattering studies at 25 to 100 MeV.[55,63] Axially non-symmetric nuclear shapes were particularly important in accounring for the shapes and magnitudes of the inelastic angular distributions for population of various members of the gamma-vibrational band in ^{24}Mg.[63] See Fig. 22.

Some other experimental user groups at LAMPF have focussed much effort on obtaining data for proton inelastic scattering to particle-hole states, and some usable data now exist for several nuclei. However, the microscopic DWBA approach used for such transitions at low energy is notoriously unsatisfactory, and there is no reason to expect that its DWIA form will work any better at 800 MeV -- in fact some preliminary studies indicate that if anything it works worse than at low energies. Therefore we don't see a great deal of hope that these data for weak inelastic transitions will be able to provide the sort of relatively clean nuclear structure information we have been able to extract from the elastic scattering and from the inelastic scattering to strongly collective states.

We now turn to a discussion of the work published during 1979, and a brief description of work in progres..

b.) Uncertainties in neutron densities determined from an approximately model-independent analysis of 0.8 GeV polarized proton scattering from nuclei

This work was discussed in some detail in last year's progress report and will be mentioned only briefly here.[56,62] The first order, spin-dependent microscopic KMT optical potential was used to study 800 MeV polarized proton elastic differential cross section and analyzing power data for target nuclei

^{58}Ni, ^{90}Zr, $^{116,124}Sn$ and ^{208}Pb. Approximately model-independent target neutron density distributions were constructed in order to investigate the uncertainties in the deduced neutron densities resulting from the statistical error of the experimental data and the finite range of momentum transfer in the experimental angular distributions. Numerous other experimental and theoretical sources of error and uncertainty were considered in obtaining a realistic estimate of the total error in the deduced neutron density distributions and their root mean square radii. The typical error from the first order analysis was found to be ± 0.07 fm. Impressive agreement was found between the deduced model-independent neutron matter density distributions and the corresponding densities predicted by Hartree-Fock approaches, as seen in Figs. 17-2.. (In further work,[62] an extension of that just described, the few important second-order terms were included as well as equally small electromagnetic corrections to the proton form factor, reducing the error to ± 0.05 fm. Coker was not directly involved in this later work.)

c). Effects of spin-orbit deformation in inelastic proton scattering at 0.8 GeV (in collaboration with experimental groups from Rutgers, UCLA, Minnesota, Oregon and Northwestern).

New differential cross section and analyzing power data for 0.8 GeV polarized protons incident on ^{12}C, $^{116,124}Sn$, populating the first 2^+ excited state, were obtained by the University of Texas experimental group in collaboration with those listed above. These data were analyzed theoretically in terms of the DWBA using collective form factors which included spin-orbit contributions. It was found that a reasonable description of the analyzing power data could be obtained in this way, although of course the breakdown of the DWBA at backward

angles (greater than 15° in the c.m.) for ^{12}C was notable (and well understood). Without the deformed spin orbit term it was not possible to describe the inelastic analyzing power data, even qualitatively.[58,64]

d.) Elastic differential cross sections and analyzing powers for polarized protons incident on $^{40,42,44,48}Ca$ at 0.8 GeV (in collaboration with experimental groups from UCLA, LAMPF, Rutgers, Minnesota, Northwestern, Oregon and Pennsylvania)

As an extension of our original elastic scattering survey, data for the calcium isotopes were analyzed using the first-order KMT approach.[61] Very good fits were obtained to the elastic cross sections and analyzing powers; neutron density distributions and neutron and proton rms radii were obtained from the analyses. See Fig. 23. The difference between the neutron and proton rms radii for each isotope could be compared to results of a large number of independent experiments, including other medium energy and low energy proton scattering data, ^{4}He scattering data, Coulomb excitation studies, pionic atom data, pion elastic scattering and pion total cross section data. Considering the rather different ranges of experimental and theoretical error in the various methods of determining the rms radius differences, generally good agreement was found between our values and those resulting from other approaches. There was also good agreement with Hartree-Fock predictions. See Fig. 17. However, whell-model predictions gave results much too large and attempts to estimate such differences using Coulomb energy systematics give results much too small, compared to all the other approaches, for these isotopes.

e.) A coupled-channels analysis of proton inelastic scattering to the gamma-vibrational band in ^{24}Mg

As this work was not discussed in last year's progress resport, it will be presented in more detail here than the previously discussed work.

In the even-even deformed nuclei, the first several excited states can be classified as belonging either to the ground state rotational band, or the the β- and γ-vibrational band sequences. For the specific case of ^{24}Mg, a number of analyses have been made of proton and ^{4}He inelastic scattering data, employing the collective rotational model and the coupled-channels formalism. While these analyses have met with considerable success, there have also been significant failures. Calculated angular distributions for the 2^+, 1.37 MeV and the 4^+, 4.12 MeV members of the ground state rotational band, as well as the 2_2^+, 4.24 MeV "band-head" of the γ-vibrational band in ^{24}Mg, agree quite well in shape and magnitude with the measured cross sections and confirm the applicability of the simple rotational model to this nucleus. On the other hand, very drastic disagreement between predictions and data is found for the 8.12 MeV 6^+ state, assumed a member of the ground state rotational band, as well as for the 5.2 MeV 3^+, the 6.01 MeV 4_2^+ and the 7.8 MeV 5^+ states, assumed to be members of the γ-vibrational band.[71]

However, if one has recourse to a apherically symmetric description of ^{24}Mg and the ordinary one-step distorted wave Born approximation (DWBA)[68] one can obtain a good fit to the inelastic scattering data for the 6.01 MeV 4_2^+ state. At 800 MeV, for instance, the DWBA fit to the 4_2^+ state is good at forward angles although it becomes out of phase with the data at the back angles. This fact supplies the clue to what may be wrong with the coupled-channels calculations. Previous descriptions of the intrinsic nuclear

vibrations about a deformed equilibrium shape have been restricted in such a way as to rule out a direct transition from the ground state to the 4_2^+ state, by allowing (in the notation of Bohr[72]) only $(Y'_{22}+Y'_{2-2})$ vibrations. Naqib and Blair[73] have previously argued that there exists a large $\Delta\ell=4$ as well as $\Delta\ell=2$ transition strength in ^{24}Mg, based on a particle-hole description of the 4_2^+ state. The simplest way to take into account direct $\Delta\ell=4$ paths is to include in the coupling potential such terms as $(Y'_{42}+Y'_{4-2})$. The coupled-channels formalism of Tamura[74] was thus extended to allow a direct coupling of the ground state and the 4_2^+ state in the γ-vibrational band.

In an investigation of the effect of the additional $\alpha_{42}(Y'_{42}+Y'_{4-2})$ vibrational mode, the values of α_{42} as well as other deformation parameters were varied freely to obtain the best description of the 800 MeV (p,p') cross sections for the states of the ground state rotational band and of the γ-vibrational band. These <u>same</u> intrinsic deformations and vibrational mode strengths were then used in corresponding coupled-channels calculations for the 20.3 and 40 MeV (p,p') data. Results at these three energies are summarized on Fig. 22.

The description of the γ-vibrational band, while vastly improved, is not perfect. The 800 MeV calculations with α_{42} nonzero slightly overestimate the magnitudes of the 2_2^+ and 4_2^+ states at the larger angles, predict too deep a minimum near 24° for the 3^+ state, and continue to fail to reproduce the angular distribution of the 5^+ state. As these discrepancies are rather small, compared to the original discrepancy removed by the inclusion of the $\alpha_{42}(Y'_{42}+Y'_{4-2})$ terms, they could well result from a complex interplay between several less important processes omitted in the present calculations. These include additional terms of the $\alpha_2(Y'_{\lambda 2}+Y'_{\lambda-2})$ form, spin-flip processes, couplings to

other bands, or even inadequacies of the simple macroscopic collective rotational model.

We finally note that tolerably good fits are also obtained at all energies for the 3^+, 5.2 MeV state, from which one can qualitatively estimate the importance of spin-flip contributions to the inelastic cross section for that state to be a diminishing function of incident proton energy, and quite small at 800 MeV.

f.) Elastic proton scattering at high momentum transfers

Recently, the 800 MeV $p + {}^{208}Pb$ proton elastic scattering data have been extended to a center of mass angle of 42.5° (cross section) [31° (analyzing power)]. In this interval, the cross section data decrease in magnitude by a factor of 10 billion. These new data are consistent with, but quantitatively superior to, the older data, possessing superior statistical accuracy in the region of overlap -- typically less than 1% for angles less than 20°, 2% from 22 to 30°, and adequate out to the largest angles. In the theoretical analysis we were mainly interested at first in seeing whether the larger range of momentum transfer would affect the error envelopes of the neutron density distributions, or the value obtained for the neutron rms radius. We found that within experimental error limits there is satisfactory agreement. See Fig. 21. However, in the microscopic KMT calculations, a curious artifact appeared: an accidental cancellation between the nuclear and Coulomb scattering amplitudes at about 35°. See Fig. 24. This called into question in our minds (not for the first time) the curious treatment of the Coulomb interaction in medium energy proton elastic scattering calculations. Up until a few years

ago it was generally neglected totally in calculations presented in the literature; in formal workouts of the KMT theory it is largely ignored. As described elsewhere, we have included a realistic Coulomb interaction from the beginning. (In investigating the origin of the cancellation, one has to study various subtle higher-order corrections to the Coulomb term that arise in a KMT formalism because the scattering problem solved is for a nucleus with one less nucleon than the actual target nucleus. This work has mainly been carried out by L. Ray, in collaboration with Prof. R. Thaler of Case Western University.)

However, there are other problems not directly related to the treatment of the Coulomb interaction, which show up at the larger momentum transfers. For instance, the predicted diffraction pattern gets increasingly out of phase with the experimental one past 30°. No change in nuclear densities, etc., can repair this discrepancy without destroying the agreement at smaller angles. In trying to guess the source of this discrepancy, one is faced with the problem that a large number of approximations are made in the conventional microscopic KMT calculation, which affect the optical potential in first order at high momentum transfer. Among these are the impulse approximation itself, since a much higher momentum can be transferred between the incoming nucleon and the target nucleus than between two free nucleons. Other approximations that should perhaps be corrected include neglect of Fermi motion of target nucleons, neglect of the total momentum dependence of the free nucleon-nucleon amplitudes, neglect of off-shell effects in the nucleon-nucelon amplutides, neglect of Pauli blocking in the target nucleus, neglect of coupling between the spin of the incoming nucleon and the angular momentum of nucleons in the nucleus, and so on.[70] All of these approximations are clearly fairly good at 800 MeV, and it is likely that removing each of them will require immense work and have essentially no

effect on the predicted angular distribution at large momentum transfers... or worse, that the various effects will tend to cancel. We are trying to think of ways that experiment can give theory a clue as to which directions are worth pursuing in the immediate future.

It is worth mentioning that an obvious first order correction that is rarely even thought of, much less mentioned in this context, is that the kinematic transformations used to relate the free nucleon-nucleon amplitudes to the proton-nucleus reference frame are valid only for zero momentum transfer![70] In short, in asking the question of how to make reliable KMT microscopic calculations for proton nucleus scattering at large momentum transfer, we are opening a Pandora's box and it would be rash to predict what will emerge.

g.) Total reaction cross sections for 0.8 GeV protons on nuclei

There are approved proposals for HRS at LAMPF to measure p + nucleus total reaction cross sections; the actual data should materialize within the coming year. In the microscopic reaction theories used to generate the optical potentials we have used at medium energy, the absorption is generated directly from the empirical total nucleon-nucleon cross sections, using the familiar optical theorem. If there are fairly important absorption mechanisms within the nucleus for 800 MeV incident protons that do not involve direct collision between the incident proton and a single target nucleon in the first step, it would be expected that the theories predict the absorption incorrectly, and therefore will predict the total proton-nucleus reaction cross sections incorrectly. We have therefore made theoretical predictions of these cross sections in advance of the experiments, in order to provide a stringent test of the commonly

used theoretical formalism of p+nucleus scattering at medium energies. We do not anticipate any serious discrepancies, because all our experience to date indicates that the absorption is very well predicted (perhaps to 95% confidence level) by the simple impulse approximation that is the basis of the conventional KMT approach. Therefore this effort is more a service to the experimentalists than a genuine theoretical investigation. Only if interesting discrepancies show up will these calculations be pursued any further. See Fig. 25.

(In a related project, L. Ray computed proton-nucleus total and reaction cross sections for ^{12}C, ^{16}O, ^{27}Al, ^{56}Fe, Cu, Ge, ^{127}I and ^{208}Pb from 100 to 2200 MeV. The calculations were based on the Kerman, McManus and Thaler formalism, the impulse approximation and local optical potentials with Pauli, short range dynamical and center-of-mass correlations included. The proton-nucleus scattering amplitudes were obtained from phase shift solutions or directly from the published N-N data. The proton and neutron densities were obtained from electron and proton scattering results or from Hartree-Fock predictions.)

h.) Isotopic differences in neutron matter densities due to single neutrons

In the most recent proton-nucleus elastic scattering data at 800 MeV from HRS, a statistical error of less than 1% has been achieved, while the relative normalization from run to run can be fixed to $\pm 1.5\%$. This makes possible an experiment, and accompanying theoretical analysis, with some novel features. Our experimental collaborators intend to propose, at our urging, an experiment to compare proton elastic scattering from ^{90}Zr and ^{91}Zr targets of very precisely known thickness. If the target thickness uncertainty is on the order of 1 to 2%, but not greater, it will still be the dominant source of error in the expression $[(d\sigma/d\Omega)_{^{91}Zr} - (d\sigma/d\Omega)_{^{90}Zr}]/(d\sigma/d\Omega)_{^{90}Zr}$.

A rough theoretical prediction of the differences between the ^{90}Zr and ^{91}Zr angular distributions, due to the extra neutron in ^{91}Zr, gives a very distinctive and rapidly oscillating (period about 5°) cross section difference function, which has an envelope with a slope of about a percent per degree, so that by 20° the differences are approaching 20%. It therefore appears to us that if we empirically adjust the neutron densities for ^{90}Zr and ^{91}Zr as they appear within the most sophisticated KMT microscopic analysis we are able to do by the time the data are available, we will be able to ascertain by fitting to the experimental data a fairly informative curve for the difference between ^{91}Zr and ^{90}Zr neutron densities. It will be interesting to see, for instance, how closely this difference resembles the prediction of the simple shell model for the valence neutron. If results are promising, it may be possible to push this sort of comparison further, along the lines already explored successfully for nuclear electromagnetic form factors via electron scattering.

1.) Diffraction model for medium energies?

One question which has been raised several times by our experimental collaborators is whether or not there is a simple optical diffraction model which one could apply to the 800 MeV proton-nucleus elastic scattering data in order to "read off" the nuclear matter radius. As a matter of fact, the simplest possible "black disk" approximation for the scattering amplitude, namely

$$d\sigma/d\Omega \sim (kR^2)^2 |J_1(x)/x|^2, \quad x = kR\theta ,$$

gives an excellent reproduction of the positions of the minima in the experimental angular distributions, although of course it does not provide even a

qualitative reproduction of the actual angular distribution. It is also not entirely clear how the strong absorption radius R is related to the actual nuclear matter radius, a priori. Generally one finds R is roughly $1.2\ A^{1/3}$ fm, making this an excellent simple homework problem for nuclear physics courses, but not terribly useful for quantitative work.

We therefore tried several other, more sophisticated diffraction models, which included Coulomb scattering and a complex index of refraction within nuclear matter. The most attractive of these was the model proposed by Ericson,[75] in which the S-matrix is parametrized directly as a Woods-Saxon form in angular momentum space, namely (for spinless particles)

$$S_\ell(E) = [1 + \exp((\ell_0 - \ell - i\rho)/\Delta)]^{-1}$$

where ℓ_0, ρ, and Δ are parameters. This approach can easily be generalized to include spin and to predict both cross sections and polarizations. However, while one finds that one can obtain an essentially perfect fit to the 800 MeV polarized proton elastic scattering angular distributions and analyzing powers using this approach, it does not appear possible to extract a strong absorption radius from the parameters in a consistent way. For spinless particles, $R \approx \ell_0/k$ agrees fairly well with the value obtained from the black disk model, but for the realistic spin-1/2 case it has not been possible so far to find a plausible, unambiguous or empirically justifiable way to relate the nuclear matter radius to the fitting parameters of any simple diffraction model that includes spin effects. We have, during the course of the investigation, learned a great deal about the unitarity of the S-matrices predicted by the KMT approach (see Section iii (f)), not all of it good news by any means.

iv. NUCLEAR COLLECTIVE MOTIONS

(Weeks and Tamura)

Using the boson expansion technique,[76] Tamura and Weeks, have been describing the low-lying positive parity states of even-even nuclei in the mass range A = 70 - 200. Results for Sm appeared recently[77] and the results for Ru-Pd[78] as well as for Os-Pt[79,80] isotopes have been completed.

The Ru-Pd isotopes are basically mildly deformed nuclei which are expected crudely to have a pure phonon nature. In other words, equal spacing between, zero phonon ground state, one phonon 2^+ state, two phonon triplet states (0^+,2^+, 4^+), three phonon quintet states (0^+,2^+,3^+,4^+,6^+) and so on. The calculations for $^{98-104}$Ru and $^{102-110}$Pd can be found in Figs. 26 and 27. We note the excellent prediction of the 3^+ state lowering out of the quintet as mass increases as well as the fit to the ground band and the ordering of the two phonon triplet states. Magnetic dipole, electric quadrupole moment and B(E2)'s were also calculated and very good agreement with the data was obtained.[78]

As we leave the rare earth region where the nuclei are well deformed prolate, and simultaneously approach the N = 126 and Z = 82 closed shells, the nuclear shape should become spherical. The Os-Pt isotopes afford an excellent opportunity to study the characteristics of this transition. Our microscopic calculations enable us to witness the competition between the oblate nature of the few proton holes and the varying nature of the different numbers of neutron holes.

In Fig. 28 the ground, and gamma band predictions for $^{186-194}$Os and $^{188-198}$Pt are presented.[80] The lowering of the gamma band and then its increase as mass increases is well described. The ground band states are also nicely predicted.

Our results for the Os-Pt region have a simple interpretation in terms of the gamma unstable model of Wilets and Jean.[81] This model requires no deformation and large anharmonicity. In boson notation such a requirement demands the largeness of terms which push up (N, v = N - 2) components of wavefunctions relative to (N, v = N), where N is the number of bosons and v is the number of bosons not coupled pairwise to zero angular momentum. The microscopic calculations bear this out and result in a decay scheme as shown in Fig. 29 which is a schematic illustration for a nucleus such as $^{192-196}$Pt. The major boson component for each wavefunction is listed. Since the E2 operator is linear (dominantly) in the number of bosons, one can easily understand the salient features of the decay pattern, which agrees with experiment for these nuclei. Note that the 4_γ prefers to decay to the 2_γ or more significantly to the 4_g much more strongly than to the 3_γ which is against what one would anticipate. Also the second excited 0^+ state (0_3^+) decays to the first 2^+ state as opposed to $^{188-190}$Os where 0_3^+ decays dominantly to the 2_γ state due to the larger deformation. The appearance of the $0' - 2_1' - 2_2'$ sequence which decay as shown is also a consequence of the gamma unstable like nature.

In Fig. 30 we present potential surfaces for this region and note the transition from prolate Os to oblate Pt with both $\gamma = 0°$ and $\gamma = 60°$ (the right and left hand sides of the potential plot respectively) having in most cases comparable well depths. The overall loss of anharmonicitiy is apparent for both isotopes as mass increases. This results in a potential for ^{198}Pt where the prolate well has disappeared. Thus ^{198}Pt should not be expected to have a tendency to execute oscillations which destroy axial symmetry (gamma vibrations) as readily as in ^{196}Pt. This is seen both experimentally[82] and theoretically in our calculations.[80]

All our energy spectra were obtained using two parameters (f_2 and g_2) which represent the strengths of our residual microscopic interactions (quadrupole particle-hole and quadrupole pairing). These dimensionless numbers are estimated to have the values $f_2 = 1.0$ and $g_2 = 0.8$ for all nuclei which are collective. In Fig. 31 a plot of f_2 (crosses) and g_2 (dots) versus A is given. We see that they are quite consistent over a mass range of 100 nucleons. This consistency occurs because of the microscopic nature of the calculations. One thing which we have noticed is that the g_2 parameter is fairly sensitive to the number of single particle orbits considered in the calculation. Thus for Os-Pt where many orbits were considered g_2 was reduced somewhat.

In Fig. 32, we summarize our quadrupole moment calculations for the first 2_1^+ states as well as for experiment. Smooth lines connect the theoretical points for the Ru-Pd, Sm, and Os-Pt isotopes. Experimental Q_2 and their error bars for these nuclei are represented by vertical dotted lines.

For Ru-Pd, we note that not a great deal of transition is taking place and the theoretical and experimental points are pretty well localized. These nuclei which are all mildly prolate are well described by our method.

The $^{148\ 154}$Sm isotopes are a different story. These isotopes have been known for a long time to span a transition from the spherical-like ^{148}Sm to the well deformed prolate ^{154}Sm with ^{150,152}Sm being typical examples of so-called transitional nuclei. Our energy levels and, as seen in Fig. 32, our quadrupole moments are predicted very well.

The Os-Pt region is even more interesting. As mass increases in Os, we find that deformation is lost, as the prolate nature of the many neutron holes is reduced. Nevertheless, all the Os isotopes are predicted to be prolate and for $^{186-192}$Os our results agree almost perfectly with experiment. For Pt,

however, the nuclear shape is predicted to change from prolate for $^{188-190}$Pt to oblate for $^{192-198}$Pt, and what's more surprising is the fact that the quadrupole moment is increasing as mass increases. This of course can be understood as being due to the gradually decreasing prolate nature of the neutron holes as mass increases. Only for $^{194-198}$Pt is experiment known and we agree very nicely although in ^{198}Pt we may have too small a prediction. Nevertheless, the experimental Os-Pt transition from prolate to oblate is clearly reproduced.

Having now a fairly good description of collective states we may consider the excitation and coupling of noncollective modes so as to extend the scope of our work. In this regard we are looking at the 0^+ states in the Ge region.[83] Here we plan to couple the pairing vibrational solution to the collective solutions to reproduce energies and two nucleon transfer data. We solve the RPA equations for the pairing interaction and find that the 0^+ states so obtained are orthogonal to the spurious state and that the collective pairing vibrations for $^{70-72}$Ge lie slightly below 2Δ. Choosing a constant G and single particle energies taken from Ref. 84, our agreement with the experimental 0^+ states is very good, as seen in Fig. 33. The coupling to the purely collective states is needed to push the 0^+ energy still lower in $^{70-72}$Ge. The experimental 0^+ in ^{74}Ge is probably a collective state and should come out of the regular boson expansion calculations.

Preliminary work attempting to describe the backbending phenomena[85] by coupling previously truncated higher energy quasiparticle pair modes to the collective spectrum has also been begun. In Fig. 34 we show the results of the coupling of $(i_{13/2})^2$ $_{I=2,4...12}$ to the collective quadrupole spectra and its comparison to experiment. We see that the microscopically derived coupling which used the same strength as in the collective calculation and hence

involved no parameters, is a little too strong. This result is somewhat encouraging and more detailed analyses will be forthcoming.

Finally a better understanding of the boson expansion procedure which enables the calculations to be done has been put forth.[86] In addition, the limitations and domain of validity of the calculation has been drawn out. In this work, the understanding of the Pauli principle preserving terms in the construction of the boson representation of the collective fermion operator has been given. The results are that the boson series converges with little violation of the Pauli principle when the fermion operator contains many quasi-particle pair components with individually small amplitudes. In that case and when the physical nature of the problem justifies the ansatz that the structure of many states may be thought of as arising from multiple excitations of this collective mode then the boson expansion can be expected to work quite nicely. Our success for a large number of nuclei shows that this assumption is valid for the low energy states, even in nuclei that lie fairly close to closed shells.

REFERENCES

1. K. S. Low and T. Tamura, Phys. Rev. C 11, 789 (1975).
   T. Tamura, Phys. Rep. 14C, 59 (1974).
2. T. Tamura and K. S. Low, Comp. Phys. Commun. 8, 349 (1974).
3. D. H. Feng, B. T. Kim, T. Udagawa and T. Tamura, Comp. Phys. Commun. 12, 293 (1976).
4. T. Takemasa, T. Tamura and T. Udagawa, Nucl. Phys. A321, 269 (1979). (See also B-1.)
5. K. Yagi et al., Phys. Lett. 44B, 447 (1973).
6. T. Takemasa, T. Tamura and T. Udagawa, Phys. Lett. 87B, 25 (1979). (See also B-2.)
7. T. Udagawa, T. Tamura and T. Izumoto (1973); unpublished.
8. L. Ray and W. R. Coker, Phys. Rev. C 13, 1367 (1976) and references therein.
9. B. Zqieglinski, W. Benenson, R. G. H. Robertson and W. R. Coker, Nucl. Phys. A315, 124 (1979). (See also B-3.)
10. T. Tamura, T. Udagawa, D. H. Feng and K.-K. Kan, Phys. Lett. 66B, 109 (1977). T. Tamura and T. Udagawa, ibid., 71B, 273 (1978); 78B, 189 (1978).
11. F. E. Bertrand and R. W. Peele, Oak Ridge National Laboratory Report, ORNL--469 (1970).
12. T. Udagawa and T. Tamura, contribution to the International Symposium on the Gian Multipole Resonances, Oak Ridge, Oct. 15-17 (1979).
13. F. Petrovich et al., Phys. Rev. Lett. 22, 895 (1969).
14. E. C. Halbert and C. R. Satchler, Nucl. Phys. A233, 265 (1974).
15. G. F. Bertsch and S. F. Tsai, Phys. Reports, 18C, 125 (1975).
16. K. F. Liu and G. E. Brown, Nucl. Phys. A265, 385 (1976).

17. H. Sakai et al., contribution to the International Symposium on Continuum Spectra of Heavy Ion Reactions, San Antonio, Dec. 1979.

18. J. J. H. Menet et al., Phys. Rev. C 4, 1114 (1971).

19. D. C. Kocher, F. E. Bertrand, E. E. Gross and E. Newman, Phys. Rev. C 14, 1392 (1976).

20. R. Serber, Phys. Rev. 72, 1008 (1947).

21. G. Baur and D. Trautman, Physics Reports 25C, 293 (1976).

22. J. R. Wu, C. C. Chang and H. D. Holmgren, Phys. Rev. Lett. 40, 1077 (1978).
J. R. Wu, C. C. Chang, H. D. Holmgren and R. W. Knootz, preprint.
A. Budzanowski, G. Baur, C. Alderliesten, J. Bojowald, C. Mayer-Bröricke, W. Oelert, P. Turek, F. Rösel and D. Trautman, Phys. Rev. Lett. 41, 635 (1978).

23. N. Matsuoka, A. Shimizu, K. Hosono, T. Saito, M. Kondo, H. Sakaguchi, Y. Toba, A. Goto, F. Ohtani, and N. Nakanishi, Proc. of INS intern. Symposium on Nuclear Direct Reaction Mechanism, ed. by M. Tanifuji and K. Yazaki. (1978) p. 574: See also Nucl. Phys. A311, 173 (1978).

24. T. Udagawa and T. Tamura, Phys. Rev. C 21, in press. (See also C- 1.)

25. F. Rybicki and N. Austern, Phys. Rev. C 6, 1525 (1972).

26. R. C. Johnson and P. J. R. Soper, Phys. Rev. C1, 976 (1970).
J. D. Harvey and R. C. Johnson, Phys. Rev. C3, 636 (1971).

27. H. Amakawa, A. Mori, S. Yamaji and K. Yazaki, Phys. Lett. 83B, 13 (1979).

28. N. Austern, C. M. Vincent and J. P. Farrell, Jr., Ann. of Phys. 114, 93 (1978).

29. H. Nishioka, S. Saito, H. Kanada and T. Kaneko, Prog. Theor. Phys., in press.

30. K. Sugimoto et al., Phys. Rev. Lett. 39, 323 (1977).

31. T. Udagawa and T. Tamura, Phys. Rev. Lett. 41, 1770 (1978) and 42, 1501 (1979).

32. T. Udagawa, T. Tamura and D. Price, Phys. Rev. (in press). (See also C-2.)

33. M. Ishihara, T. Shimoda, H. Frolich, H. Kamitsubo, K. Nagatani, T. Udagawa and T. Tamura, Phys. Rev. Lett. 43, 111 (1979). (See also B-4).

34. N. Takahashi, Y. Miyake, Y. Nojiri, T. Minamizono, A. Mizobuchi, M. Ishihara and K. Sugimoto, Phys. Lett. 78B, 397 (1978).

35. A. C. Kahler, D. R. Zolnowski, H. Yamada, S. E. Cale, J. Pierce, and T. T. Sugihara, contribution to International Symposium on Continuum Spectra of Heavy Ion Reactions, San Antonio, Texas (December, 1979), p. 23.

36. T. Udagawa, T. Tamura, T. Shimoda, H. Frolich, M. Ishihara and K. Nagatani, Phys. Rev. C20, 1949 (1979). (See also B-5).

37. H. Frolich, T. Shimoda, M. Ishihara, K. Nagatani, T. Udagawa and T. Tamura, Phys. Rev. Lett. 42, 1518 (1979). (See also B-6).

38. K. Nagatani, Proceeding on Symposium on Heavy Ion Physics From 10 to 200 MeV/AMU held at Brookhaven National Laboratory (July, 1979).

39. E. Takada, T. Shimoda, T. Yamaya, N. Takahashi, K. Nagatani, T. Udagawa and T. Tamura, contribution to International Symposijm on Continuum Spectra of Heavy Ion Reactions, San Antonio, Texas (December, 1979); p. 9 and p. 34.

40. J. W. Harris, T. M. Cormier, D. J. Geeseman, L. L. Lee, Jr., R. L. McGrath, and J. P. Würm, Phys. Ref. Lett. 88, 1460 (1977);
H. Ho, R. Albrecht, W. Dünnweber, G. Graw, S. G. Steadman, and J. P. Würm, Z. Physik A281, 235 (1977);
T. Shimoda, M. Ishihara, H. Kamitsubo, T. Motobayashi and T. Fukuda, Proc. of the IPCR (Institute of Physical and Chemical Research) Symposium, Hakone, Japan, ed. by H. Kamitsubo and M. Ishihara, p. 93 (Sept., 1977);
R. H. Siemssen, J. Wilcznski, and A. v.d. Woude, Proc. of the Intern. Symposium Workshop on Reaction Models for Continuum Spectra of Light Particles, Bad Honnef, W. Germany, ed. by J. Ernst, p. 47 (1978).

41. R. K. Bhowmik et al., Phys. Rev. Lett. 43, 619 (1979).

42. C. K. Gelbke et al., Physics Reports 42C, 311 (1978).

43. T. Udagawa, T. Tamura and B.T. Kim, Phys. Lett. 82B, 349 (1978). (See also B-7).

44. J.B. Natowitz et al., Nucl. Phys. A277, 477 (1977).

45. W. Trautmann et al, Phys. Rev. Lett. 39, 1062 (1977).

46. A. Bohr and B. R. Mottelson, Nuclear Structure, vol. ii (W.A. Benjamin Inc., London, 1975).

47. a. T. Tamura, South African Jour. Phys. 1, 244 (1978). (See also B-8).

b. T. Tamura and T. Udagawa, Proc. Post-Conf. School, (Johannesburg) p.88 (1978). (See also B-9).

c. T. Tamura, Proc. Int. Natl. Workshop, Bad Honnef, (Nov. 1978) p.1 (See B-10).

d. T. Udagawa and T. Tamura, Proc. Int. Natl. Symp., San Antonio, (Dec. 1979), to be published. (See also C-3).

48. a. T. Takemasa, T. Tamura and H.H. Wolter, Comp. Phys. Commun. 17, 351 (1979). (See also B-11).

b. T. Tamura, T. Udagawa, K.E. Wood and H. Amakawa, Comp. Phys. Commun. 18, 163 (1979). (See also B-12).

c. T. Takemasa, T. Tamura and H. H. Wolter, Comp. Phys. Commun. (in press). (See also C-4).

49. K. -K. Kan and T. Tamura, Phys. Rev. C 19, 2058 (1979). (See also B-13).

50. G. S. Blanpied, et al., Phys. Rev. Lett. 39, 1447 (1977).

51. G. W. Hoffmann, et al., Phys. Rev. Lett. 40, 1256 (1978).

52. L. Ray, et al., Phys. Rev. C18, 1756 (1978).

53. G. W. Hoffmann, et al., Phys. Lett. 76B, 383 (1978).

54. G. S. Blanpied, et al., Phys. Rev. C18, 1436 (1978).

55. L. Ray, et al., Phys. Rev. Lett. 40, 1547 (1978).

56. L. Ray, W. R. Coker and G. W. Hoffmann, Phys. Rev. C18, 2641 (1978). (See B-14).

57. G. W. Hoffmann, et al., Phys. Lett. 79B, 376 (1978).

58. R. P. Liljestrand, et al., Phys. Rev. Lett. 42, 363 (1979). (See also B-15).

59. G. Igo, et al. , Phys. Lett. 81B, 151 (1979). (See also B-16).

60. L. Ray, et al., Phys. Lett. 83B, 275 (1979).

61. G. S. Adams, et al., Phys. Rev. Lett. 43, 421 (1979).

62. L. Ray, Phys. Rev. C19, 1855 (1979).

63. L. Ray, et al., Phys. Rev. C20, 1236 (1979). (See also B-17).

64. L. Ray and W. R. Coker, Phys. Lett. 79B, 182 (1978).

65. A. K. Kerman, H. McManus and R. Thaler, Ann. Phys. (N.Y.) 8, 551 (1959).

66. For instance, R. J. Glauber, in Lectures in Theoretical Physics, ed. by W. E. Britten and L. G. Dunham (Interscience, 1959), pp. 315-413.

67. H. Feshbach, A. Gal and J. Hüfner, Ann. Phys. (N.Y.) 66, 20 (1971).

68. W. R. Coker, L. Ray and G. W. Hoffmann, Phys. Lett. 64B, 403 (1976).

69. E. Kujawski and J. P. Vary, Phys. Rev. C12, 1271 (1975).

70. L. Ray and W. R. Coker, Technical Report UTNT 3, University of Texas Department of Physics, 1977 (unpublished).

71. For complete reference, consult Ref. 63 above.

72. A. Bohr, Mat. Fys. Medd. Dan. Vid Selsk 26, #14 (1952).

73. I. Naqib and J. S. Balir, Phys. Rev. 165, 1250 (1968).

74. T. Tamura, Rev. Mod. Phys. 37, 679 (1965).

75. T. E. O. Ericson in Preludes in Theoretical Physics (North Holland, 1966), pp. 321-329.

76. T. Kishimoto and T. Tamura, Nucl. Phys. A192, 264 (1972); A270, 317 (1976).

77. T. Tamura, K. Weeks, and T. Kishimoto, Phys. Rev. C20, 307 (1979). (See also B-18).

78. K. Weeks and T. Tamura (to be published). (See also C-5).

79. K. Weeks and T. Tamura (to be published). (See also C-6).

80. K. Weeks and T. Tamura (to be published). (See also C-7).

81. L. Wilets and M. Jean, Phys. Rev. 102, 788 (1956).

82. H. Bolotin (private communication).

83. D. Ardouin et al., Phys. Rev. C 18, 2739 (1978).

84. G. Bertsch, in The Practitioner's Shell Model, (North Holland, Amsterdam, (1972)), p. 4.

85. F. S. Stephens, Rev. Mod. Phys. 47, 43 (1975).

86. F.J.W. Hahne and T. Tamura (to be published). (See also C-8).

K. Weeks and T. Tamura (to be published). (See also C-9).

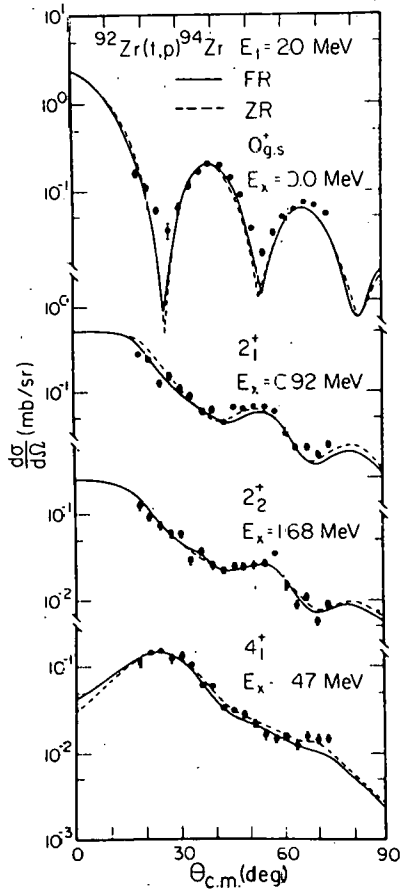
92Zr(t,p)94Zr E_t = 20 MeV
FR
ZR
0+g.s
E_x = 0.0 MeV
2+1
E_x = 0.92 MeV
2+2
E_x = 1.68 MeV
4+1
E_x = 1.47 MeV
dσ/dΩ (mb/sr)
θc.m.(deg)

Fig.1

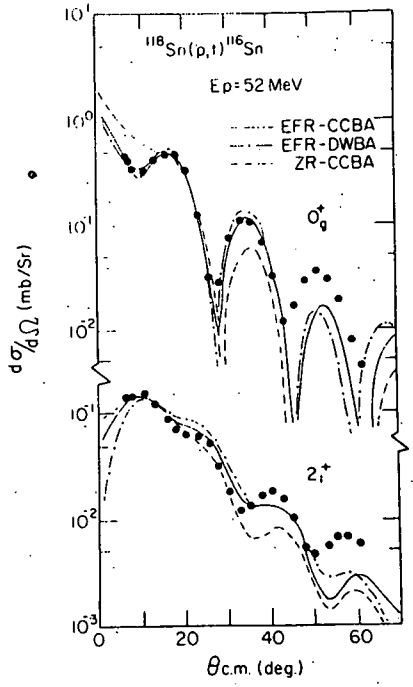
118Sn(p,t)116Sn
Ep = 52 MeV
EFR-CCBA
EFR-DWBA
ZR-CCBA
0+g
2+1
dσ/dΩ (mb/Sr)
θc.m. (deg.)

Fig. 2

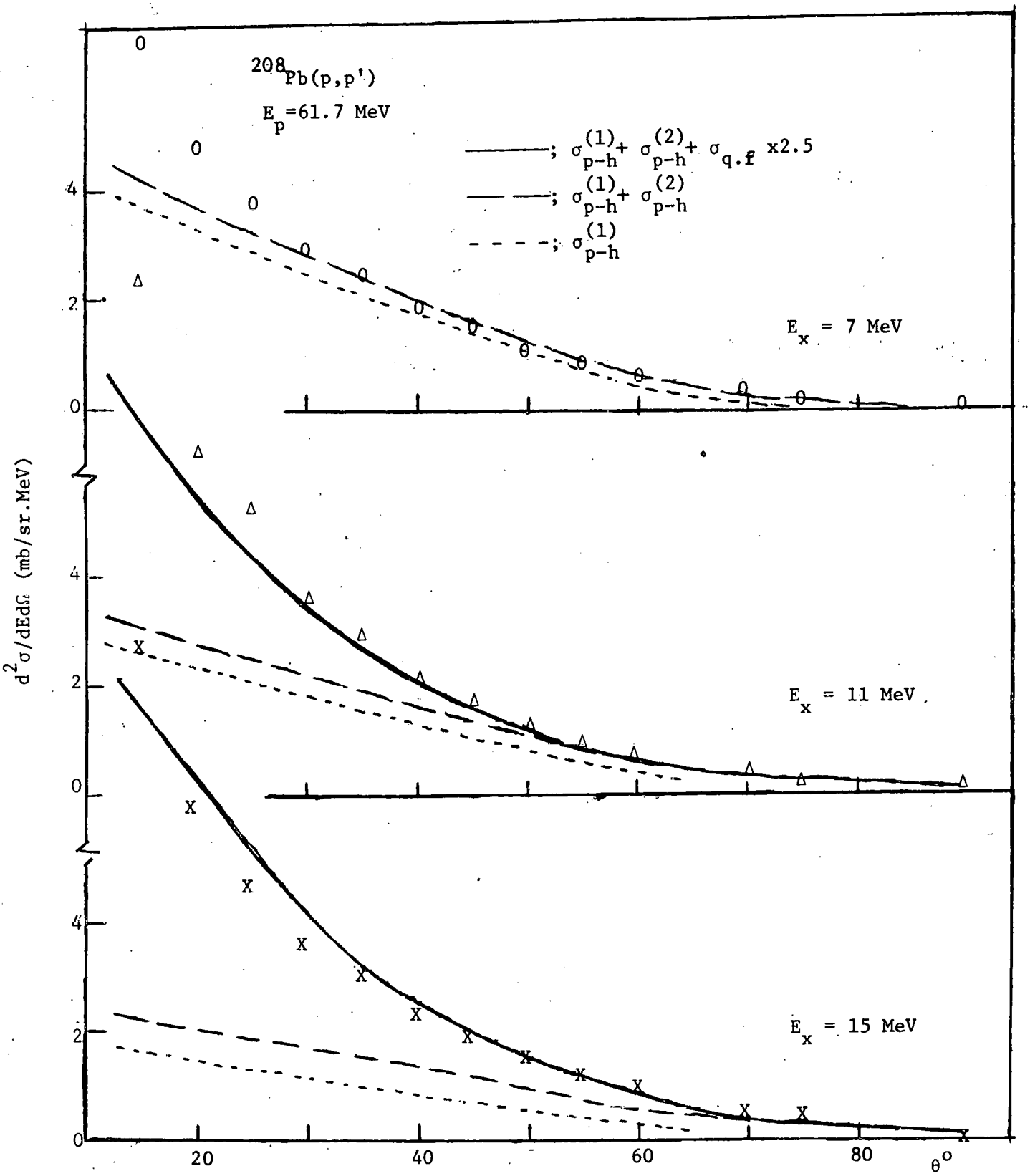
208Pb(p,p')
Ep=61.7 MeV
——; σ(1)p-h + σ(2)p-h + σq.f x2.5
— —; σ(1)p-h + σ(2)p-h
- - - -; σ(1)p-h
Ex = 7 MeV
Ex = 11 MeV
Ex = 15 MeV
d2σ/dEdΩ (mb/sr.MeV)
θo
0
2
4
20
40
60
80

Fig.3

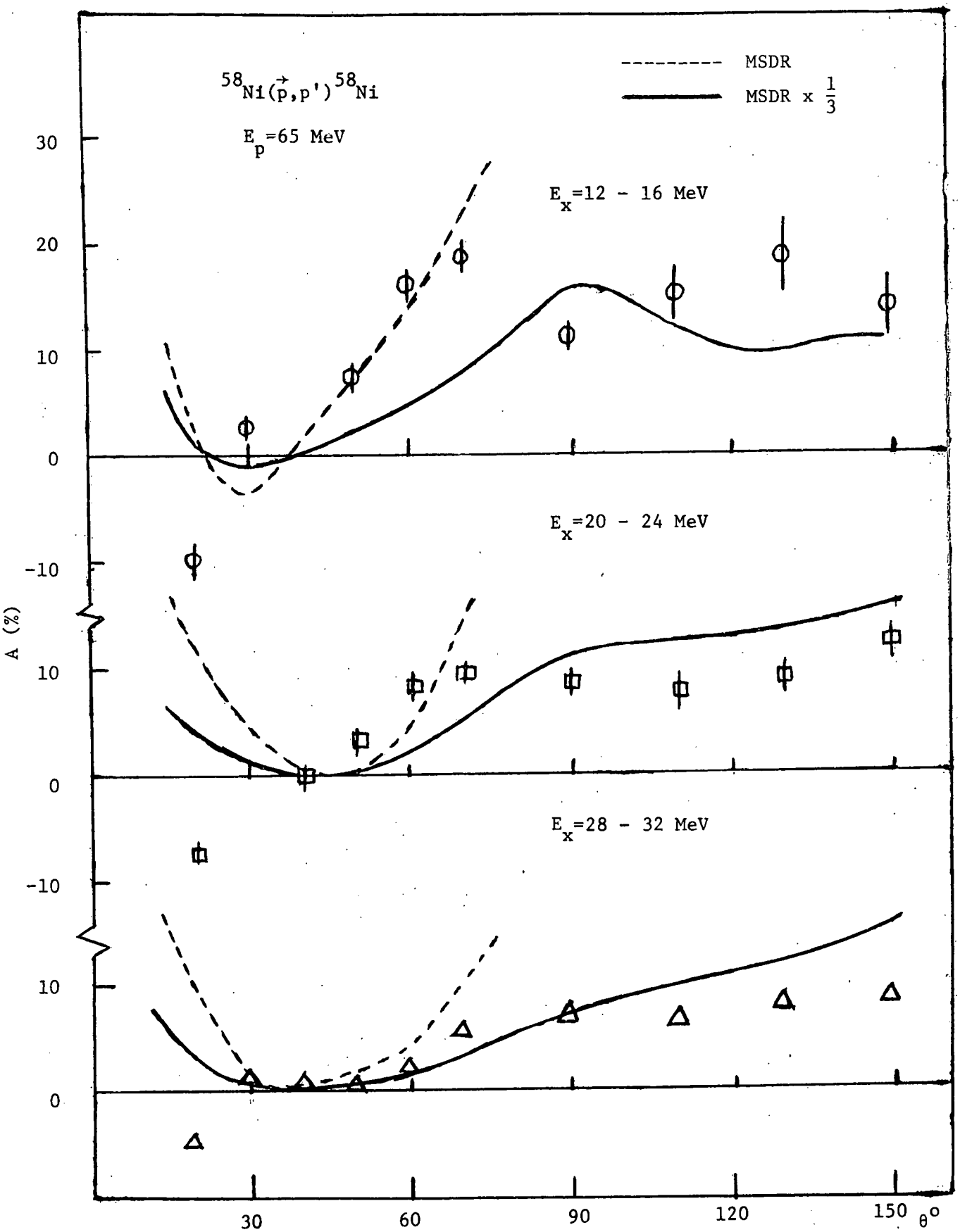
$^{58}Ni(\vec{p},p')^{58}Ni$
E_p=65 MeV
MSDR
MSDR x $\frac{1}{3}$
E_x=12 - 16 MeV
E_x=20 - 24 MeV
E_x=28 - 32 MeV
A (%)
30
20
10
0
-10
30
60
90
120
150
θ°

Fig.4

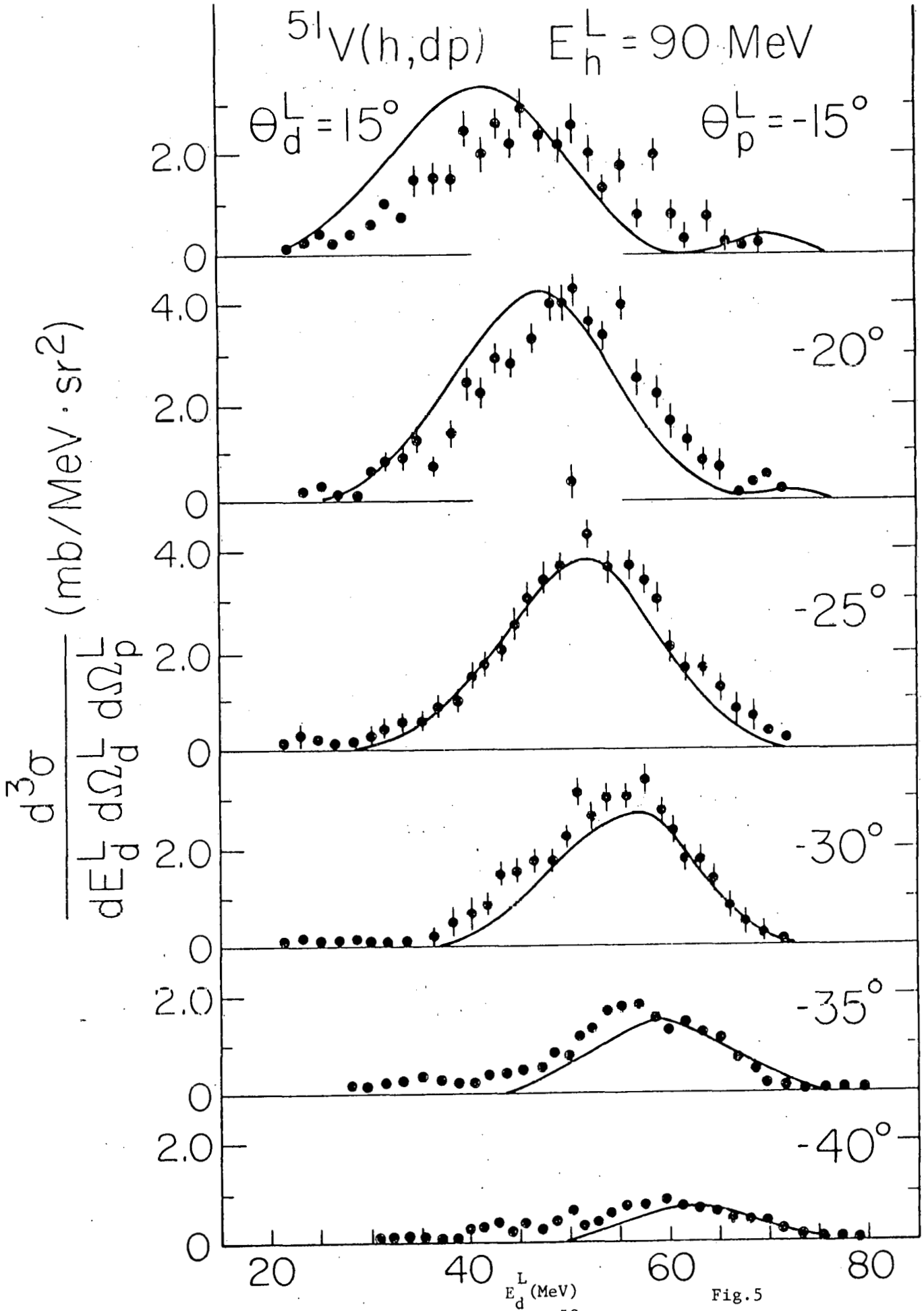
$^{51}V(h,dp)$ $E_h^L = 90$ MeV
$\theta_d^L = 15°$
$\theta_p^L = -15°$
-20°
-25°
-30°
-35°
-40°
$\frac{d^3\sigma}{dE_d^L\, d\Omega_d^L\, d\Omega_p^L}$ (mb/MeV · sr²)
E_d^L (MeV)

Fig.5

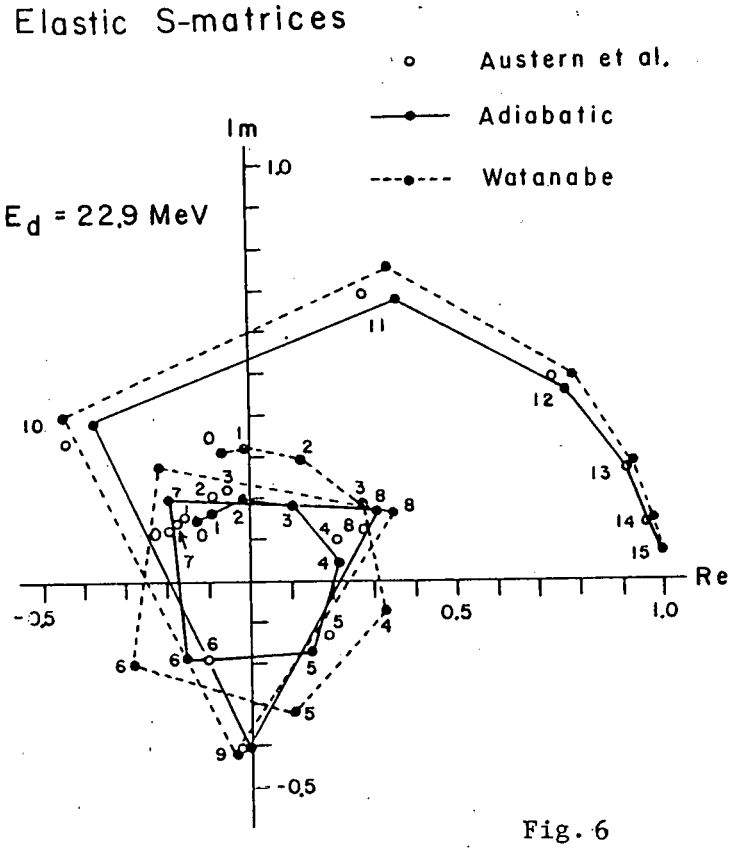

Fig. 6

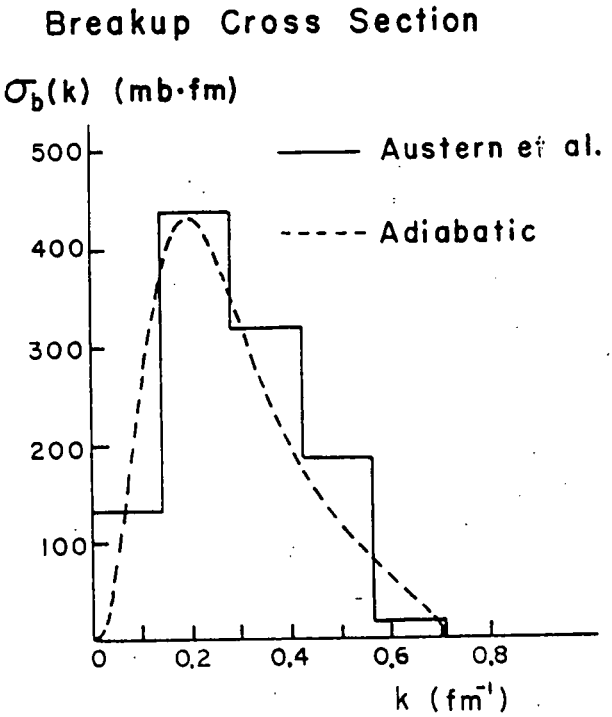

Fig. 7

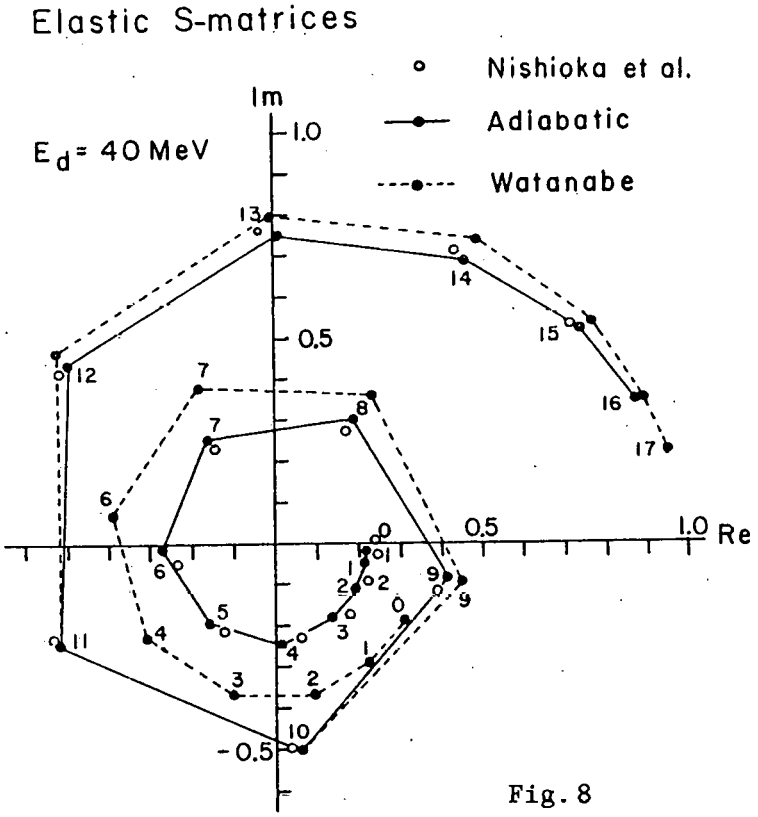

Fig. 8

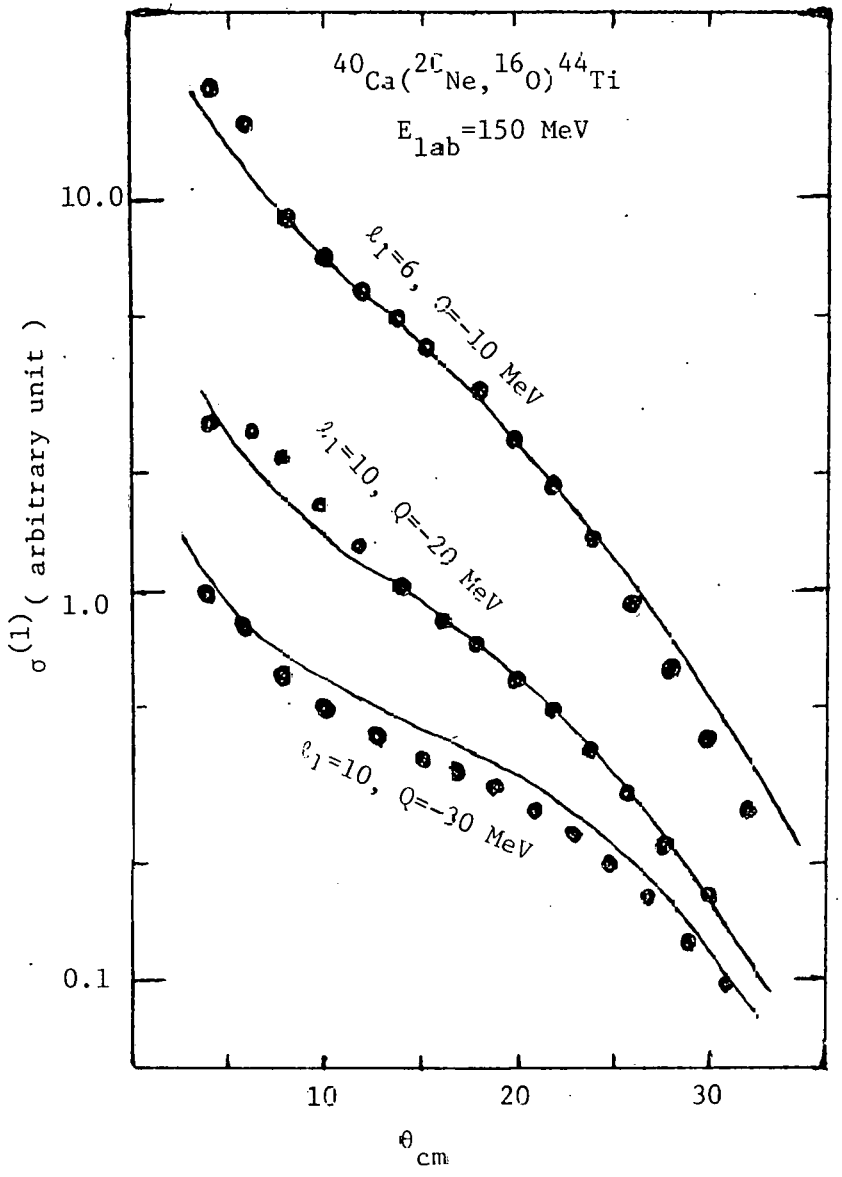
$^{40}Ca(^{20}Ne, ^{16}O)^{44}Ti$
E_{lab}=150 MeV
ℓ_1=6, Q=-10 MeV
ℓ_1=10, Q=-20 MeV
ℓ_1=10, Q=-30 MeV
10.0
1.0
0.1
$\sigma^{(1)}$(arbitrary unit)
10
20
30
θ_{cm}

Fig. 9

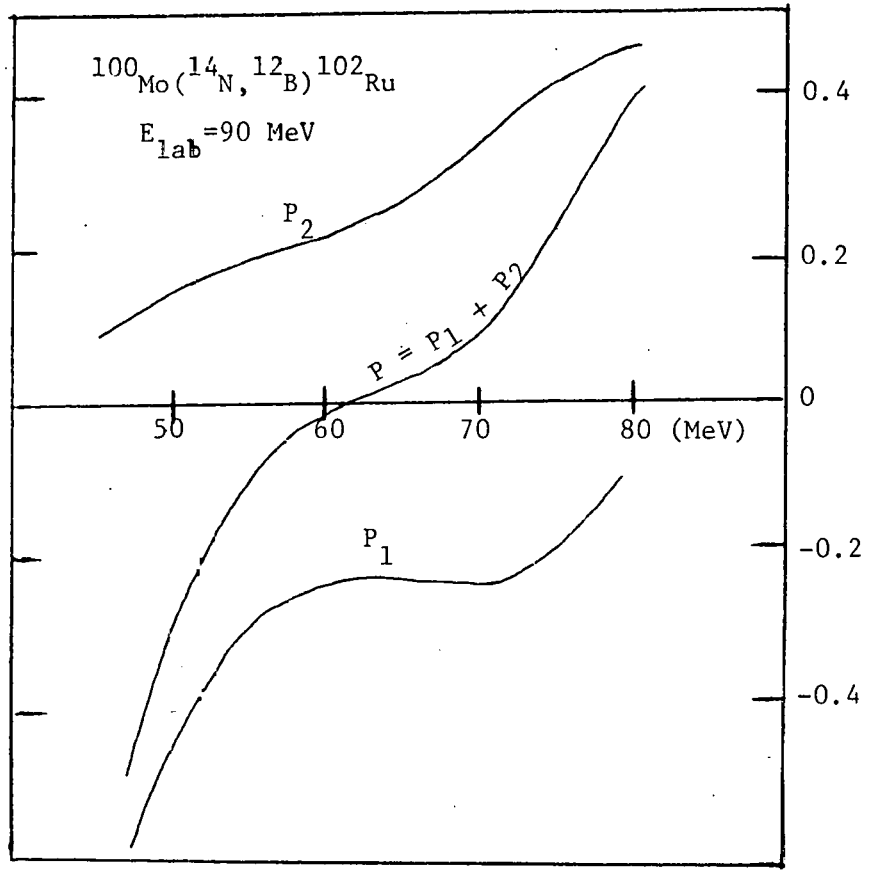
$^{100}Mo(^{14}N, ^{12}B)^{102}Ru$
E_{lab}=90 MeV
P_2
P = P1 + P2
P_1
50
60
70
80 (MeV)
0.4
0.2
0
-0.2
-0.4

Fig. 11

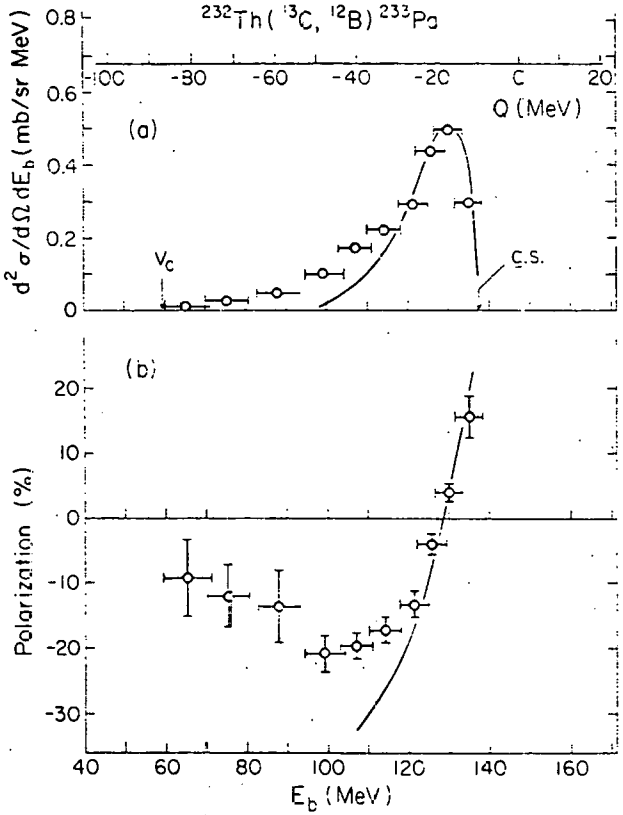
^{232}Th(^{13}C, ^{12}B)^{233}Pa
$d^2\sigma/d\Omega\, dE_b$ (mb/sr MeV)
Q (MeV)
(a)
V_c
g.s.
(b)
Polarization (%)
E_b (MeV)

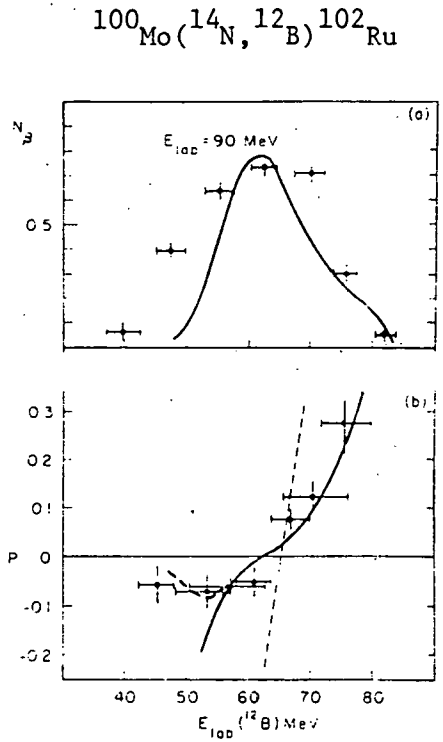
^{100}Mo(^{14}N, ^{12}B)^{102}Ru
E_{lab} = 90 MeV
(a)
(b)
P
E_{lab} (^{12}B) MeV

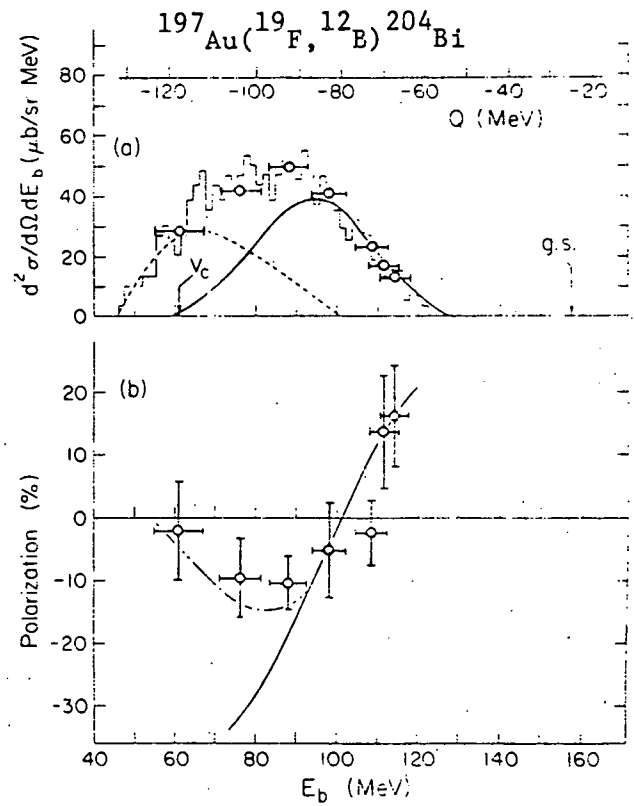
^{197}Au(^{19}F, ^{12}B)^{204}Bi
$d^2\sigma/d\Omega\, dE_b$ (μb/sr MeV)
Q (MeV)
(a)
V_c
g.s.
(b)
Polarization (%)
E_b (MeV)

Fig. 10

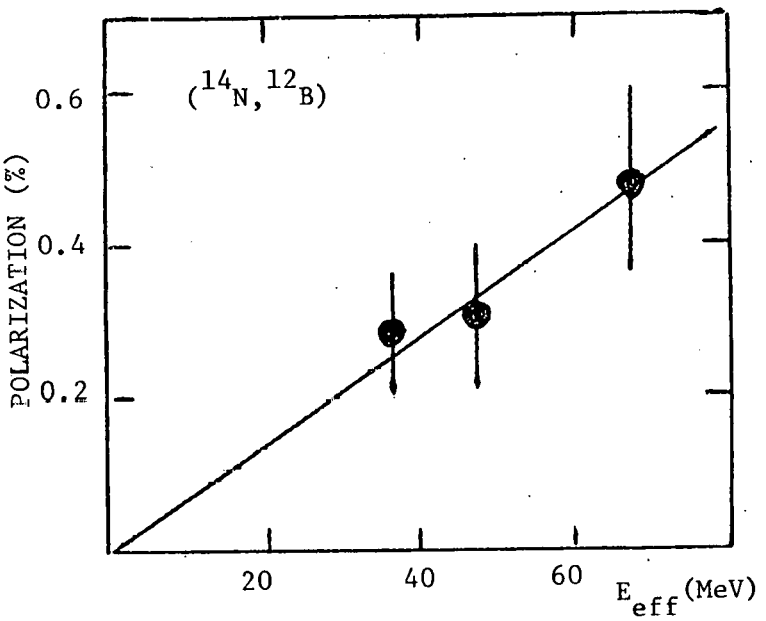
(14N, 12B)
POLARIZATION (%)
0.6
0.4
0.2
20
40
60
Eeff (MeV)

Fig. 12

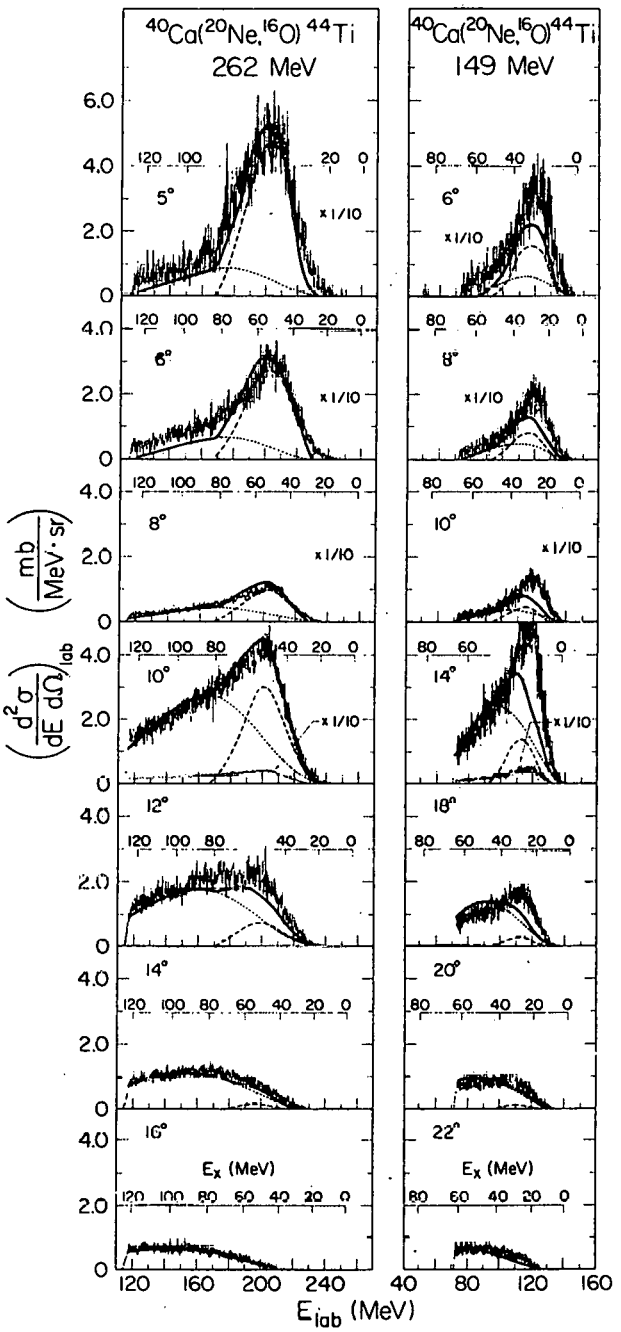
40Ca(20Ne,16O)44Ti
262 MeV
40Ca(20Ne,16O)44Ti
149 MeV
(d2σ/dE dΩ)lab (mb/MeV·sr)
Elab (MeV)
Ex (MeV)

Fig. 13

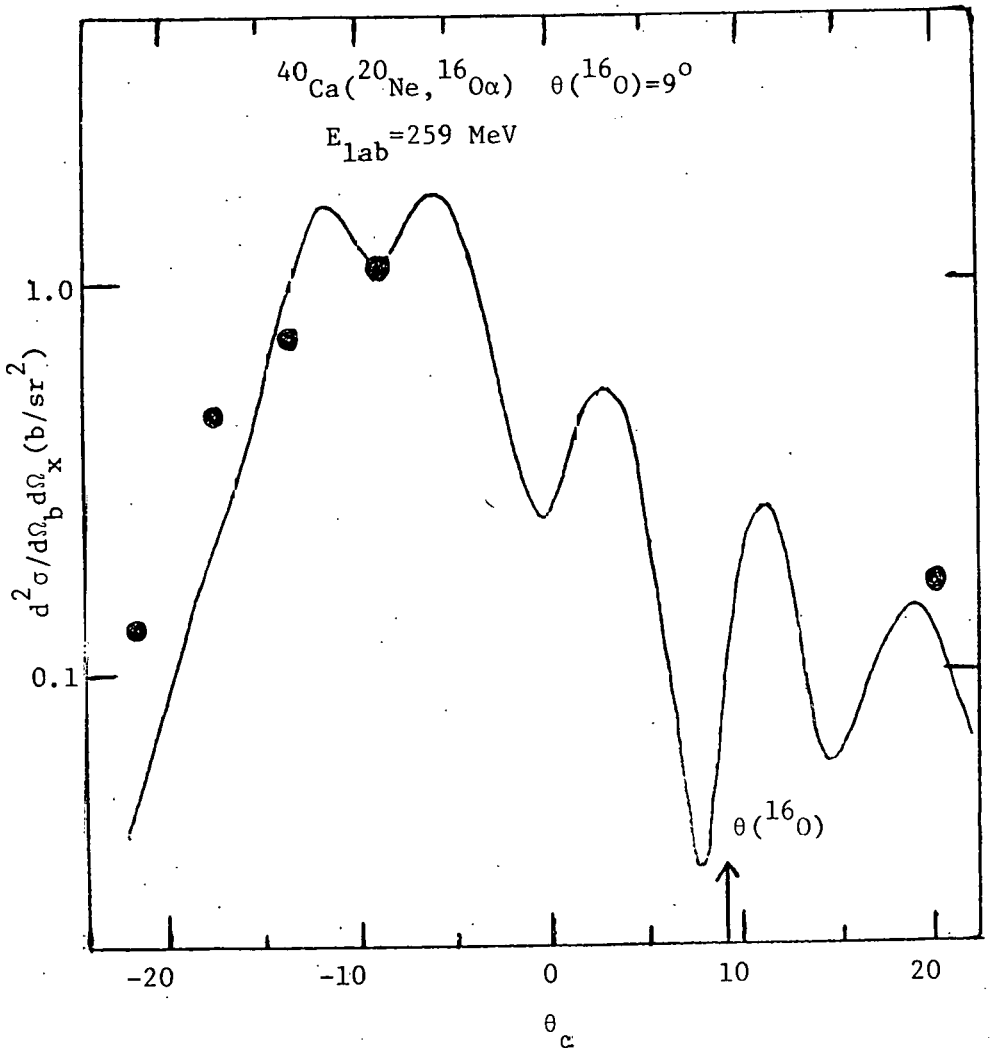
$^{40}Ca(^{20}Ne, ^{16}O\alpha)$ $\theta(^{16}O)=9^{o}$
E_{lab}=259 MeV
1.0
0.1
$d^2\sigma/d\Omega_b d\Omega_x$ (b/sr^2)
$\theta(^{16}O)$
-20
-10
0
10
20
θ_c

Fig. 14

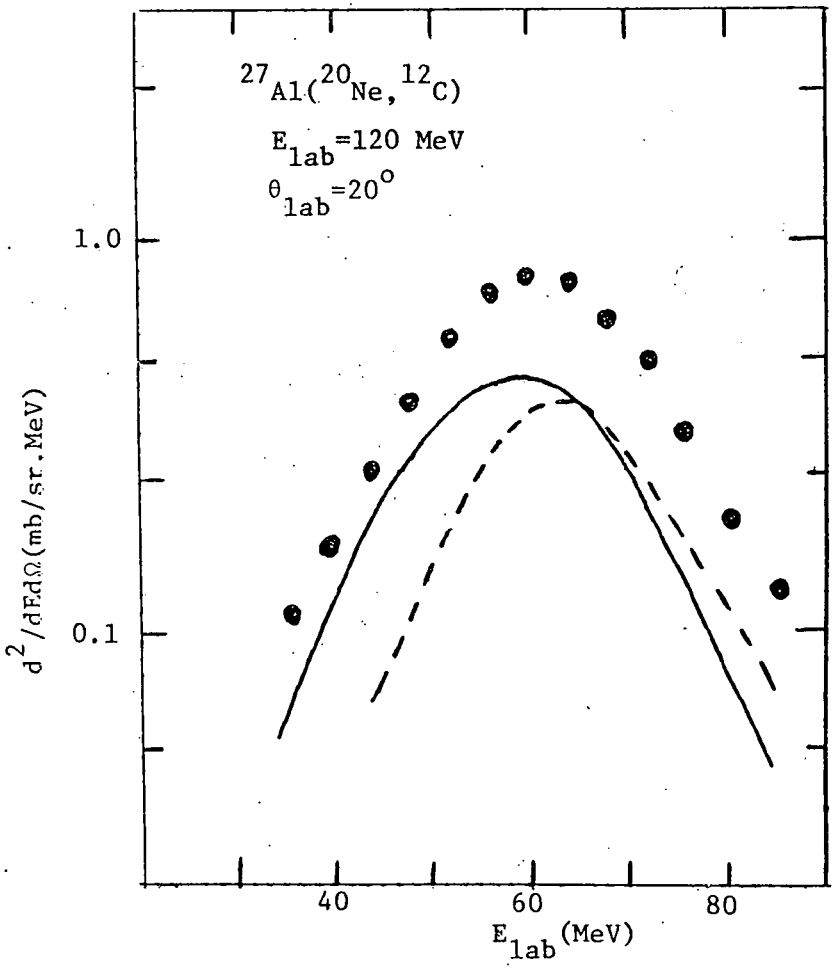
$^{27}Al(^{20}Ne, ^{12}C)$
E_{lab}=120 MeV
$\theta_{lab}=20^{o}$
1.0
0.1
$d^2/dEd\Omega$(mb/sr.MeV)
40
60
80
E_{lab}(MeV)

Fig. 15

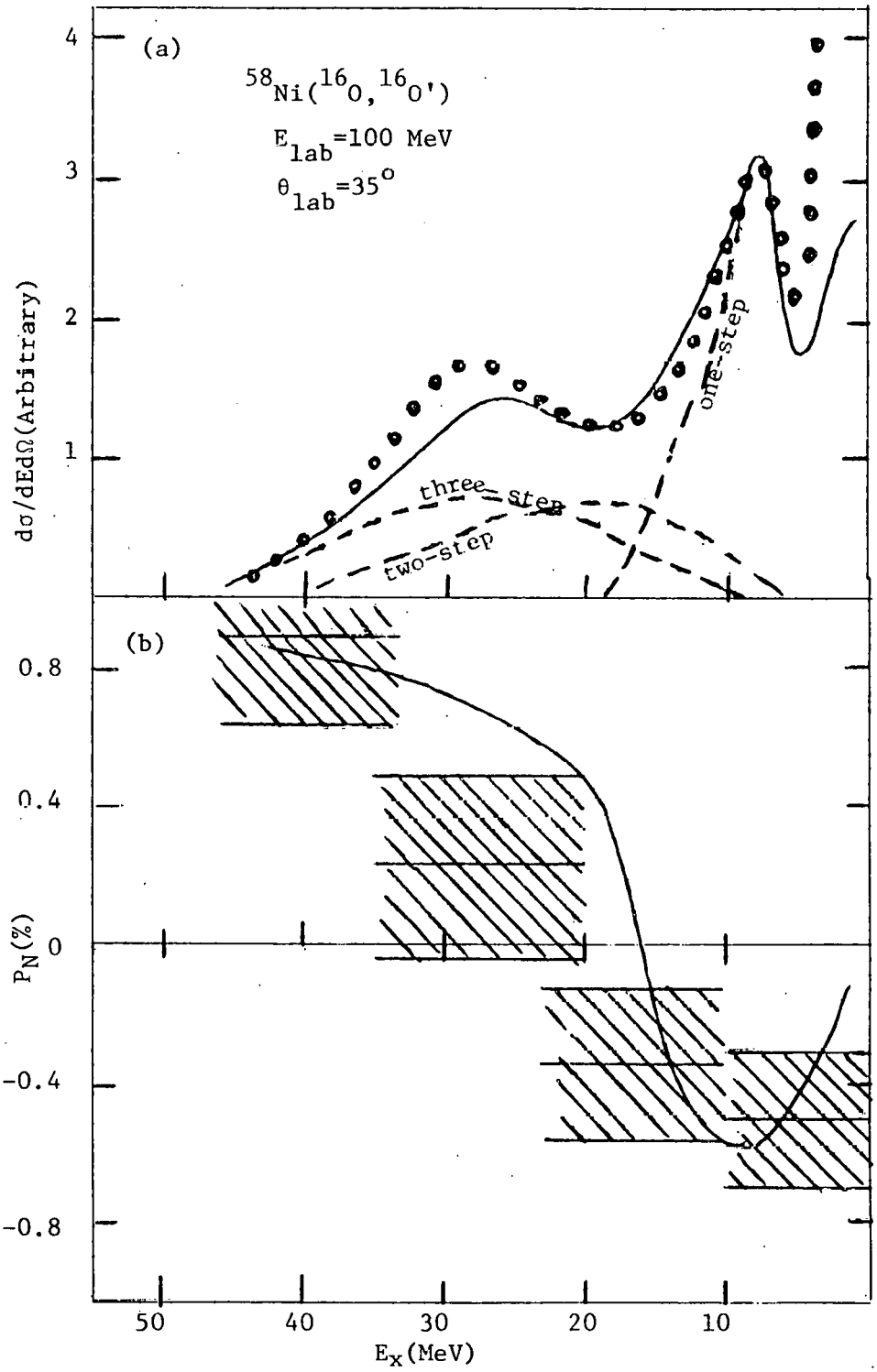
(a)
$^{58}Ni(^{16}O,^{16}O')$
E_{lab}=100 MeV
θ_{lab}=35°
dσ/dEdΩ(Arbitrary)
one-step
three-step
two-step
(b)
P_N(%)
E_x(MeV)

Fig. 16

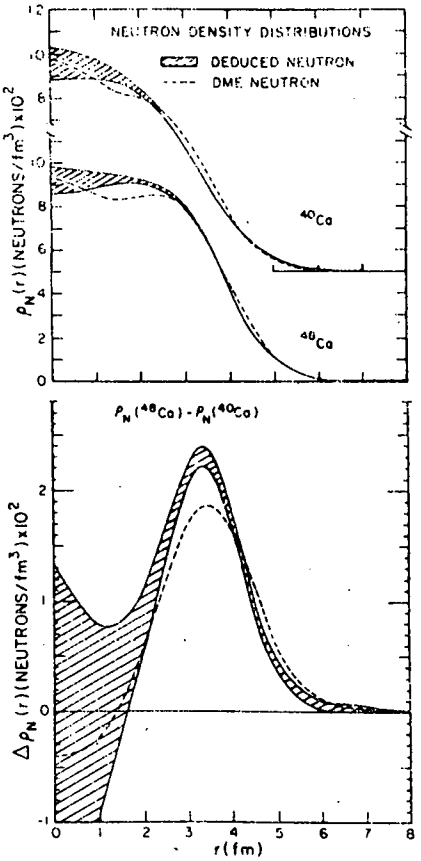

Fig. 17

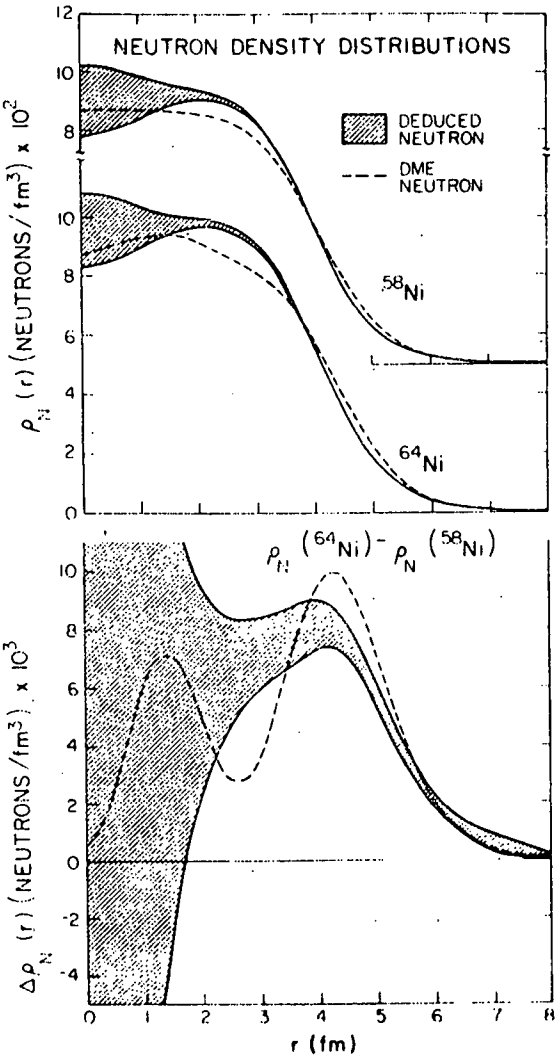

Fig. 18

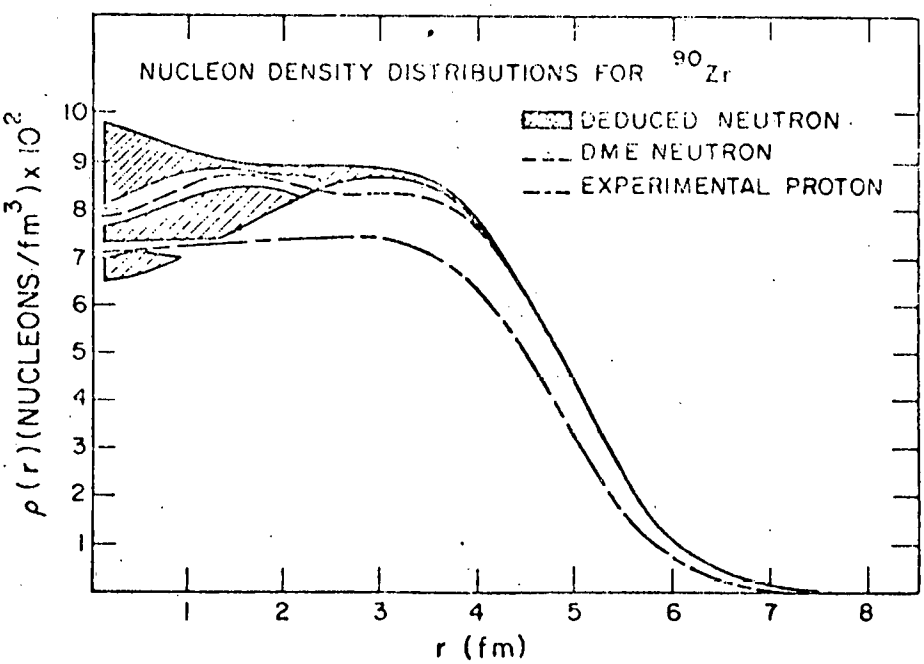

Fig. 19

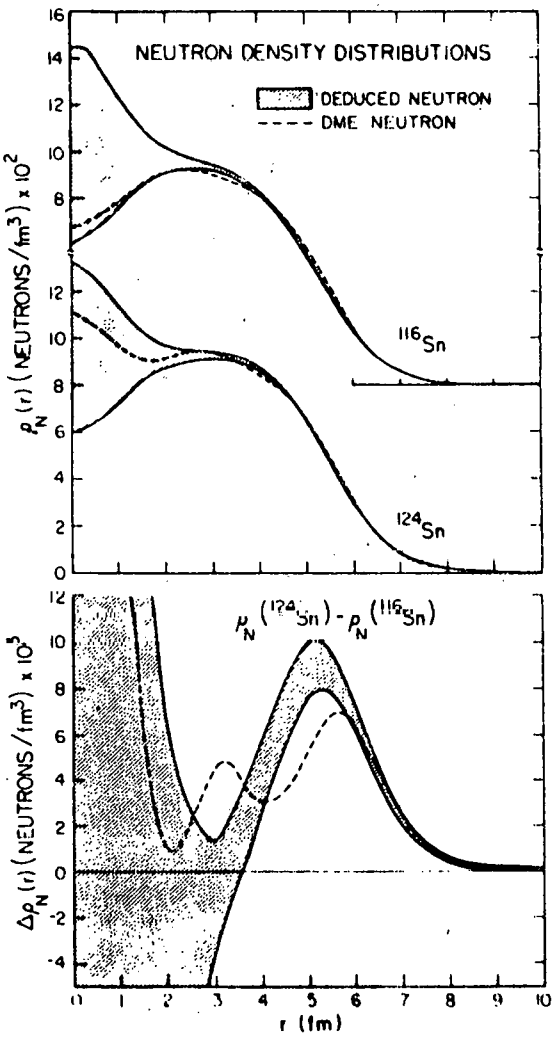
NEUTRON DENSITY DISTRIBUTIONS
DEDUCED NEUTRON
DME NEUTRON
$\rho_N(r)$ (NEUTRONS/fm^3) x 10^2
^{116}Sn
^{124}Sn
$\rho_N(^{124}Sn) - \rho_N(^{116}Sn)$
$\Delta\rho_N(r)$ (NEUTRONS/fm^3) x 10^3
r (fm)

Fig. 20

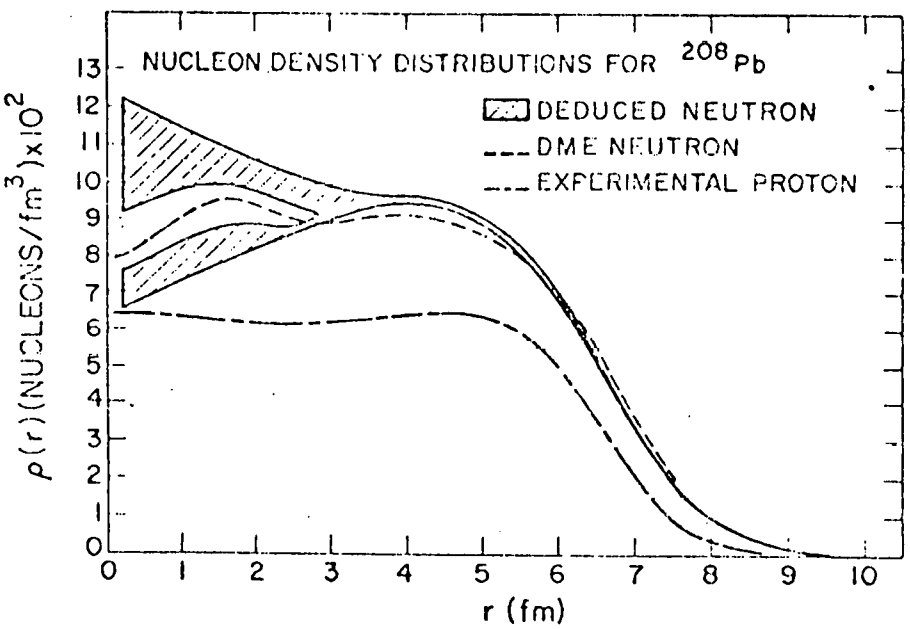
NUCLEON DENSITY DISTRIBUTIONS FOR ^{208}Pb
DEDUCED NEUTRON
DME NEUTRON
EXPERIMENTAL PROTON
$\rho(r)$ (NUCLEONS/fm^3) x 10^2
r (fm)

Fig. 21

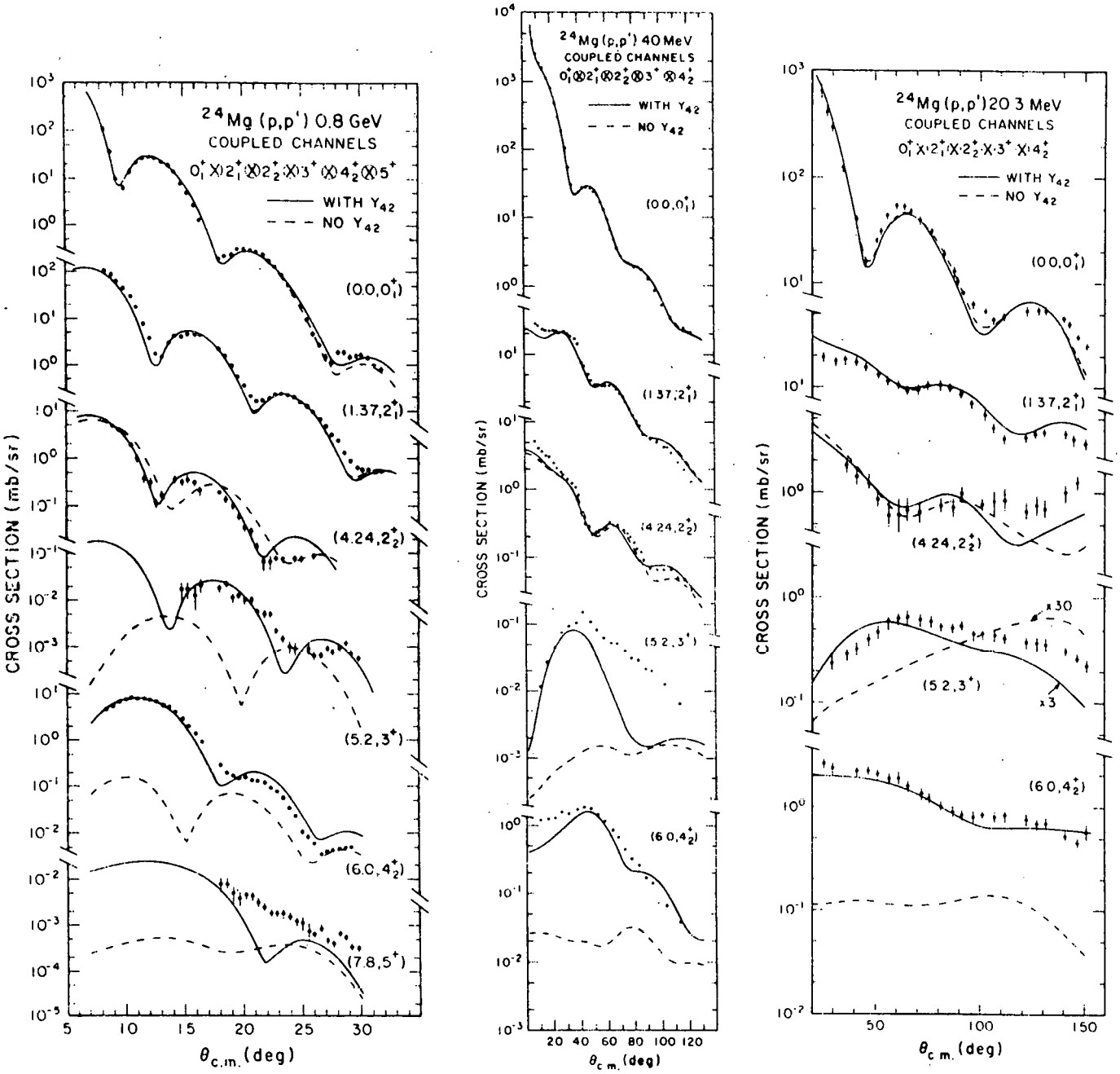
^{24}Mg (p,p') 0.8 GeV
COUPLED CHANNELS
$0_1^+ \otimes 2_1^+ \otimes 2_2^+ \otimes 3^+ \otimes 4_2^+ \otimes 5^+$
WITH Y_{42}
NO Y_{42}
$(0.0,0_1^+)$
$(1.37,2_1^+)$
$(4.24,2_2^+)$
$(5.2,3^+)$
$(6.0,4_2^+)$
$(7.8,5^+)$
CROSS SECTION (mb/sr)
$\theta_{c.m.}$ (deg)
^{24}Mg(p,p') 40 MeV
COUPLED CHANNELS
$0_1^+ \otimes 2_1^+ \otimes 2_2^+ \otimes 3^+ \otimes 4_2^+$
WITH Y_{42}
NO Y_{42}
$(0.0,0_1^+)$
$(1.37,2_1^+)$
$(4.24,2_2^+)$
$(5.2,3^+)$
$(6.0,4_2^+)$
CROSS SECTION (mb/sr)
$\theta_{c.m.}$ (deg)
^{24}Mg(p,p') 20.3 MeV
COUPLED CHANNELS
$0_1^+ \otimes 2_1^+ \otimes 2_2^+ \otimes 3^+ \otimes 4_2^+$
WITH Y_{42}
NO Y_{42}
$(0.0,0_1^+)$
$(1.37,2_1^+)$
$(4.24,2_2^+)$
x30
$(5.2,3^+)$
x3
$(6.0,4_2^+)$
CROSS SECTION (mb/sr)
$\theta_{c.m.}$ (deg)

Fig. 22

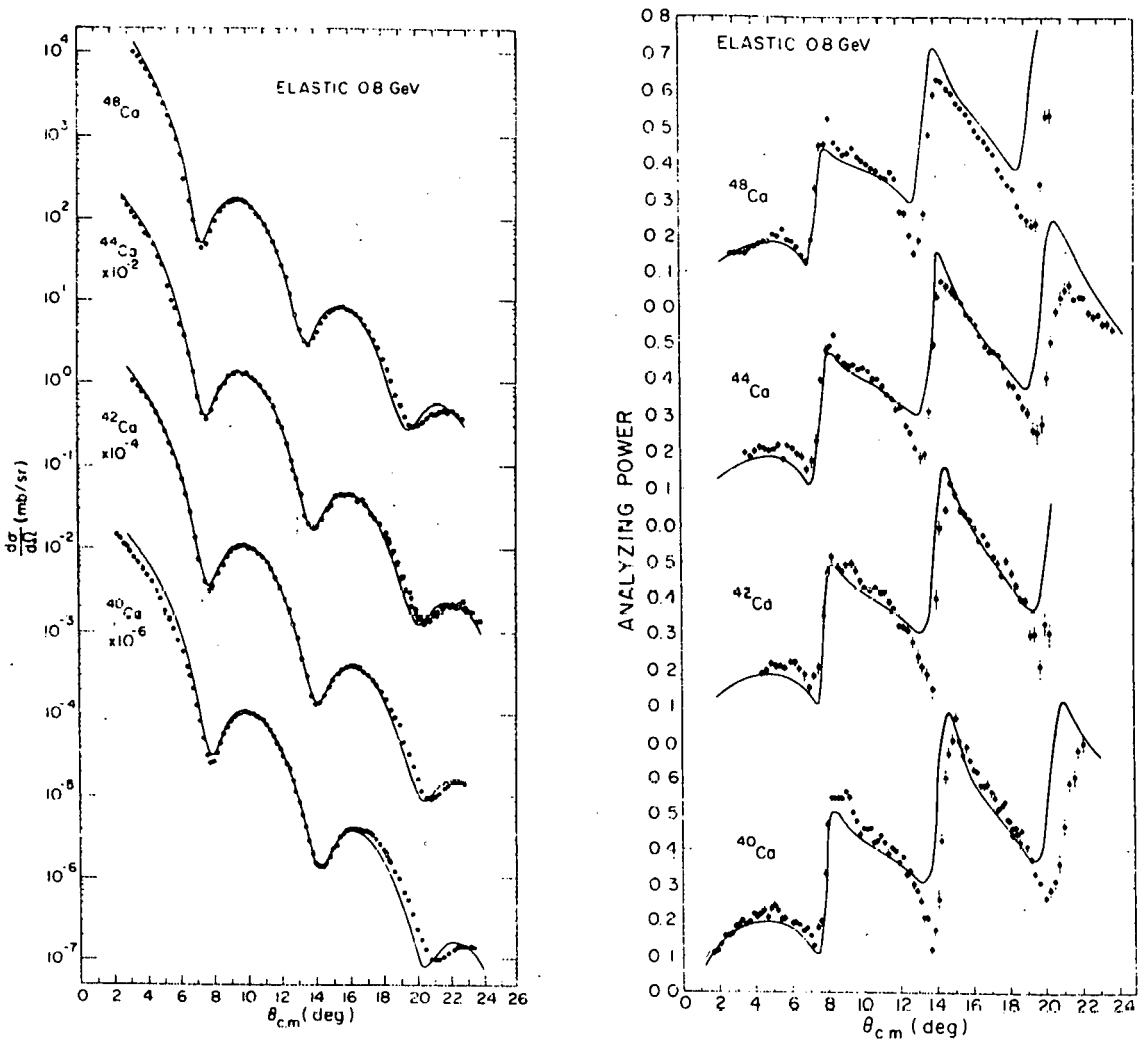
ELASTIC 0.8 GeV
^{48}Ca
^{44}Ca ×10^{-2}
^{42}Ca ×10^{-4}
^{40}Ca ×10^{-6}
$\frac{d\sigma}{d\Omega}$ (mb/sr)
$\theta_{c.m.}$ (deg)
ELASTIC 0.8 GeV
^{48}Ca
^{44}Ca
^{42}Ca
^{40}Ca
ANALYZING POWER
$\theta_{c.m.}$ (deg)

Fig. 23

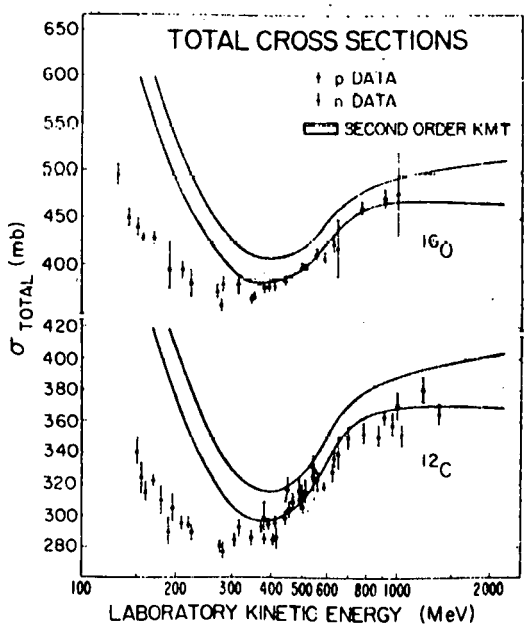
TOTAL CROSS SECTIONS
p DATA
n DATA
SECOND ORDER KMT
^{16}O
^{12}C
σ_{TOTAL} (mb)
LABORATORY KINETIC ENERGY (MeV)

Fig. 25

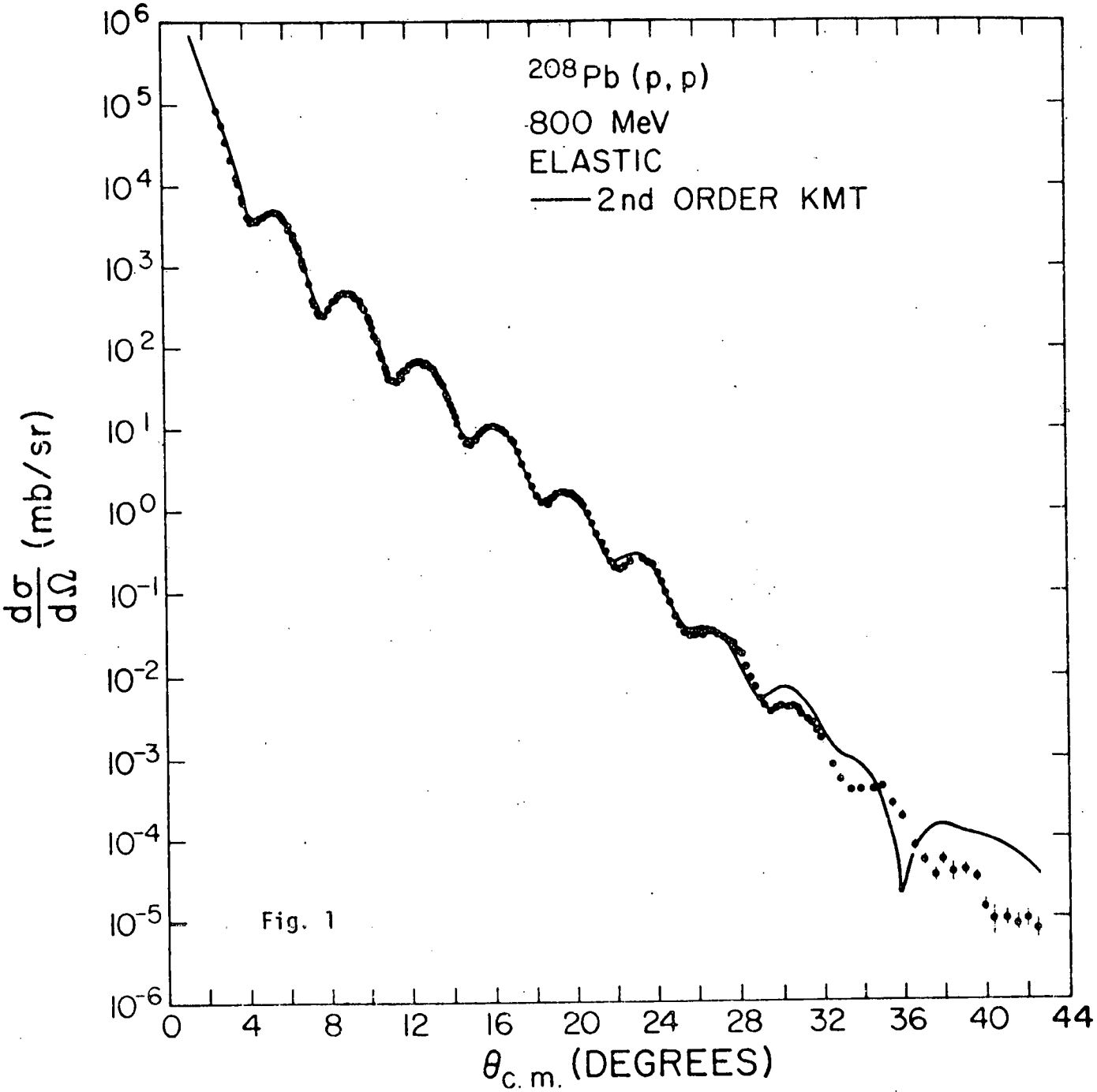
^{208}Pb (p, p)
800 MeV
ELASTIC
—— 2nd ORDER KMT
Fig. 1
$\frac{d\sigma}{d\Omega}$ (mb/sr)
$\theta_{c.m.}$ (DEGREES)
10^{6}
10^{5}
10^{4}
10^{3}
10^{2}
10^{1}
10^{0}
10^{-1}
10^{-2}
10^{-3}
10^{-4}
10^{-5}
10^{-6}
0
4
8
12
16
20
24
28
32
36
40
44

Fig. 24

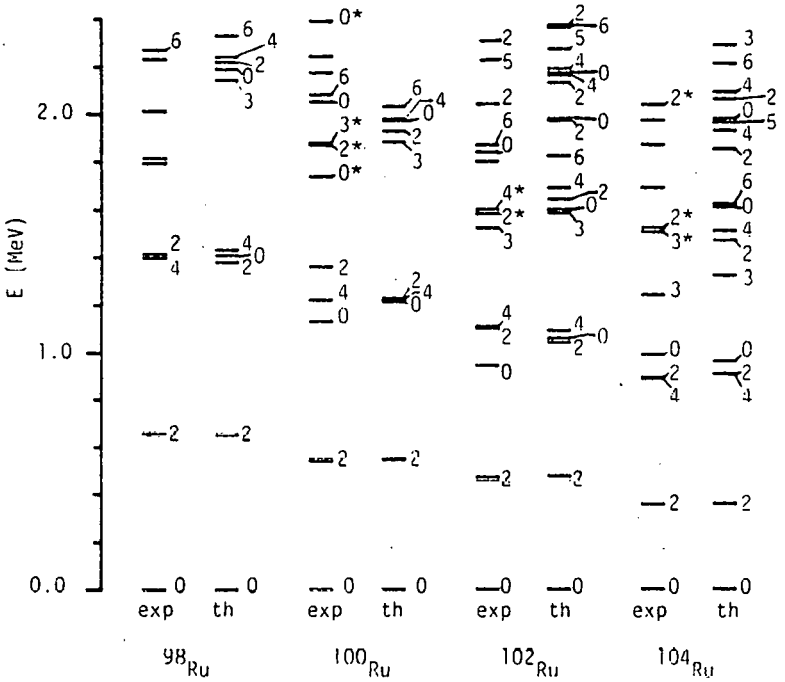
E (MeV)
2.0
1.0
0.0
exp
th
98Ru
100Ru
102Ru
104Ru

Fig. 26

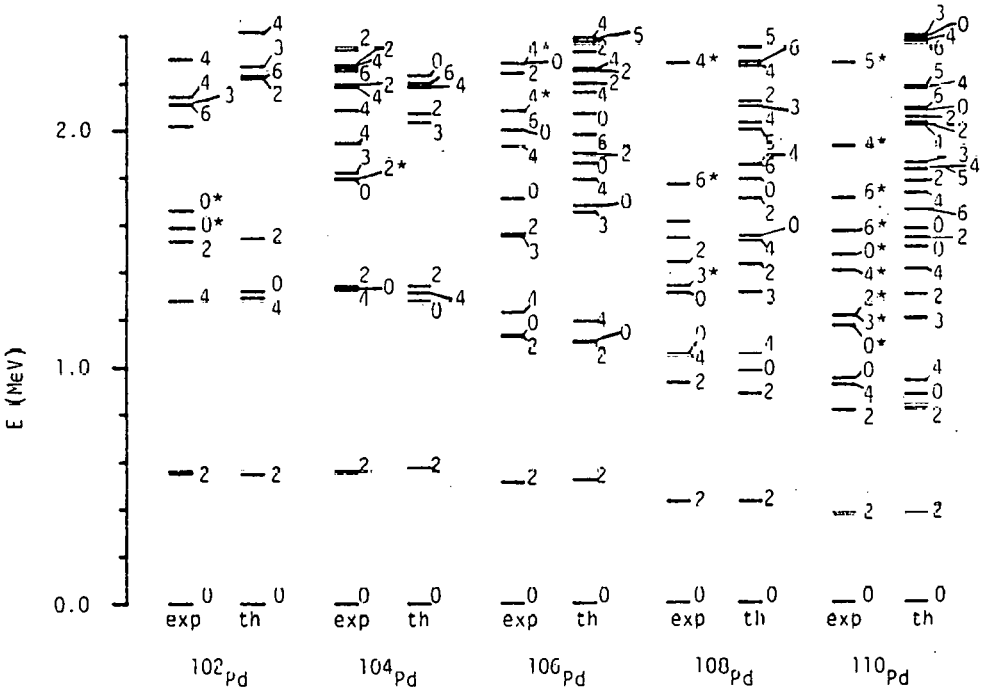
E (MeV)
2.0
1.0
0.0
exp
th
102Pd
104Pd
106Pd
108Pd
110Pd

Fig. 27

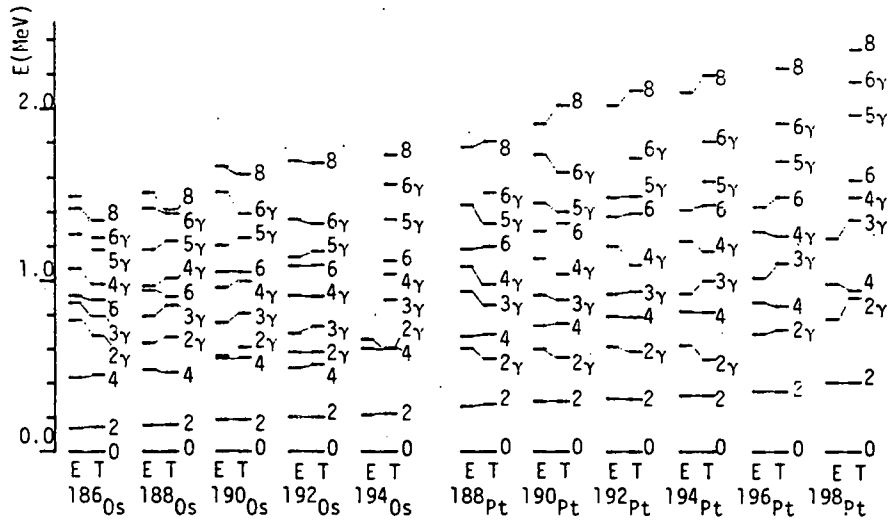

Fig. 28

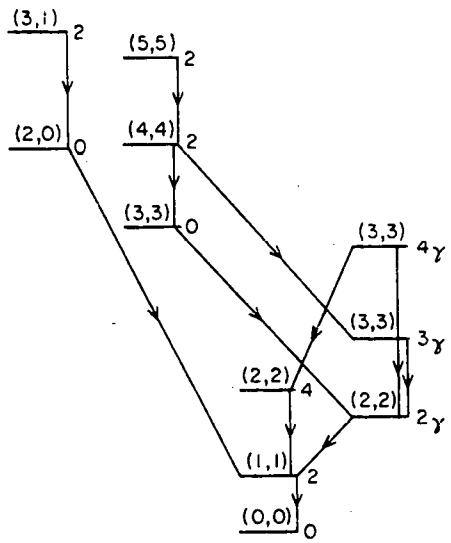

Fig. 29

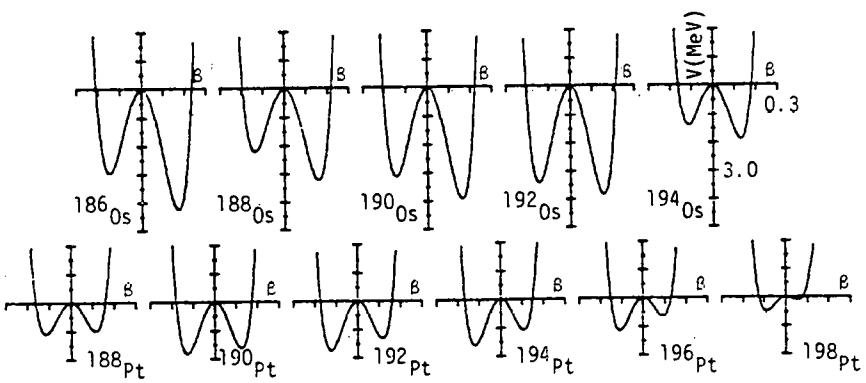

Fig. 30

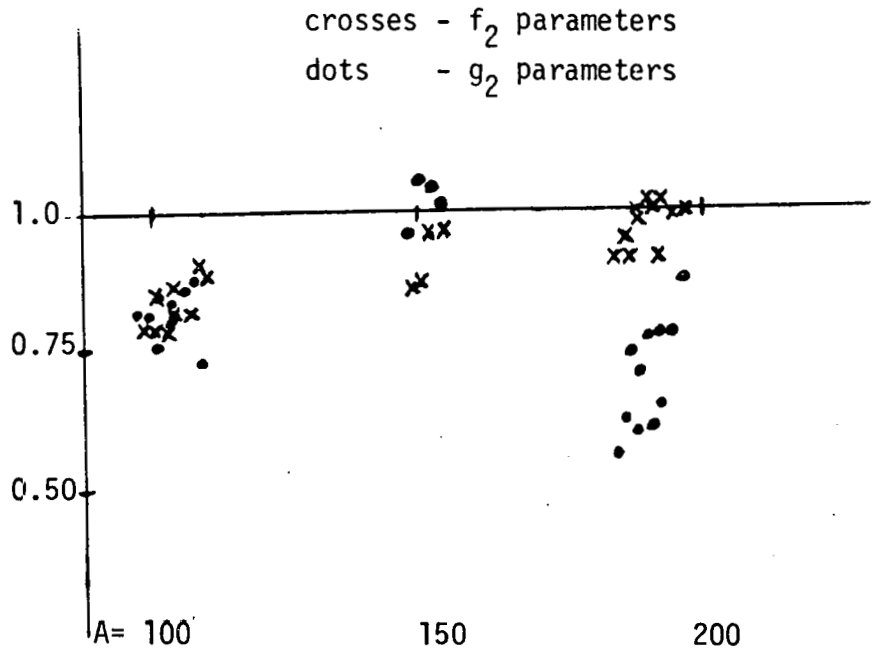
crosses - f_2 parameters
dots - g_2 parameters
1.0
0.75
0.50
A= 100
150
200

Fig. 31

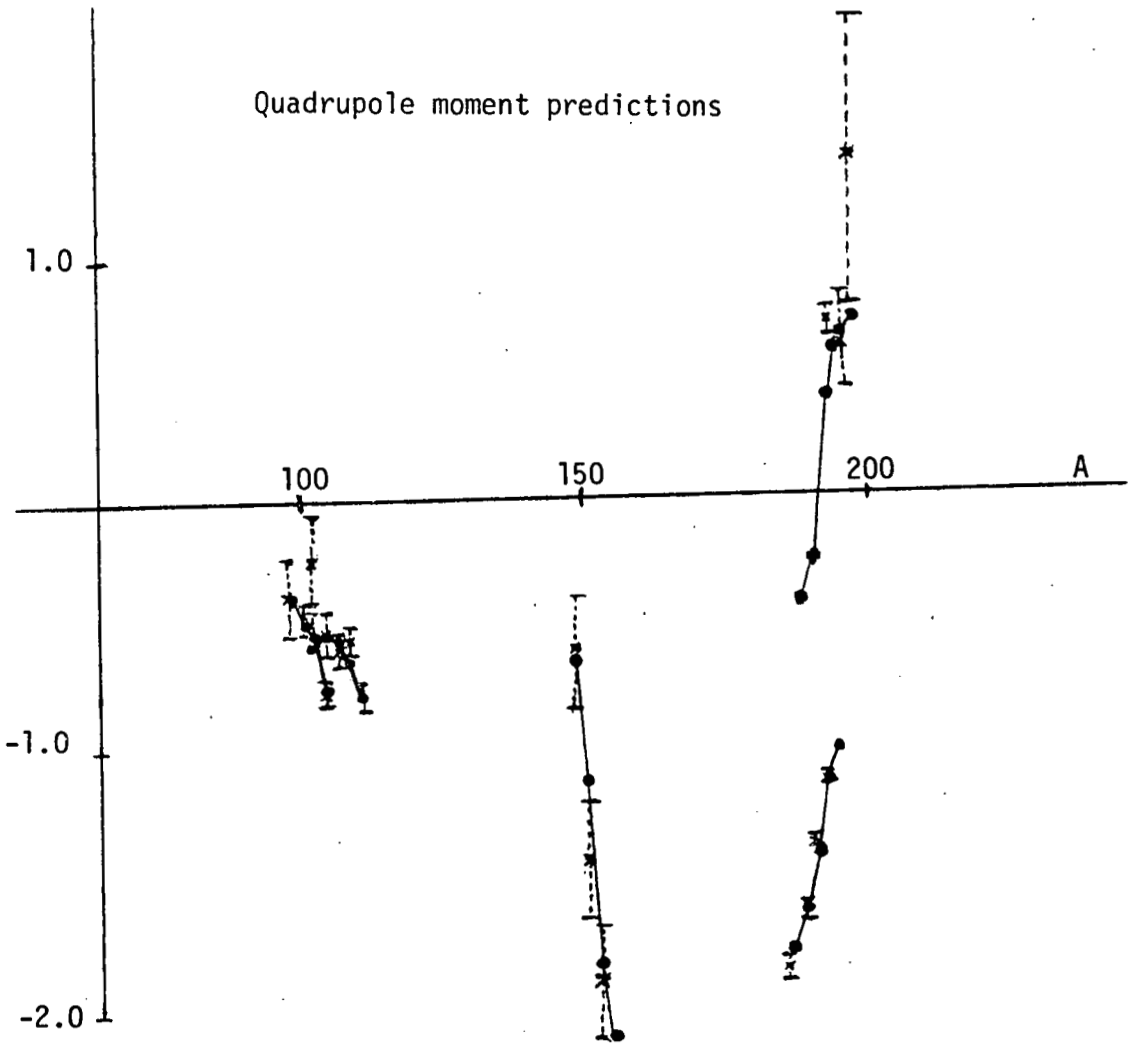
Quadrupole moment predictions
1.0
-1.0
-2.0
100
150
200
A

Fig. 32

PAIRING VIBRATION STATES (dotted lines)
First excited experimental 0^+ state (solid lines)

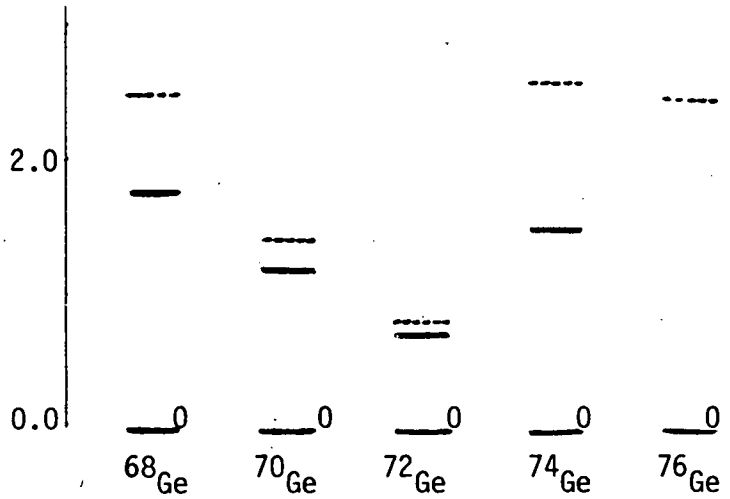

Fig. 33

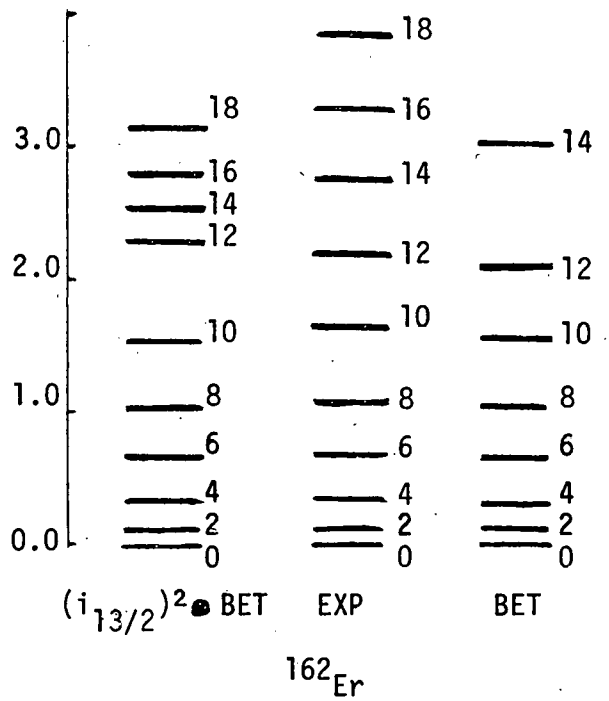

Fig. 34

II. B. COPY OF TITLE PAGES OF PUBLISHED PAPERS

2.G: 6.B

Nuclear Physics A321 (1979) 269 – 294; © *North-Holland Publishing Co., Amsterdam*

EXACT FINITE RANGE CALCULATIONS OF LIGHT-ION INDUCED TWO-NEUTRON TRANSFER REACTIONS

T. TAKEMASA †, T. TAMURA and T. UDAGAWA

Department of Physics ††, *University of Texas, Austin, Texas 78712*

Received 7 February 1979

Abstract: Exact finite-range (EFR) distorted-wave Born approximation calculations were performed for light-ion induced two-neutron transfer reactions, by using a technique to calculate the form factors rather fast. The use of this method made it possible to carry out calculations even when realistic light-ion wave functions and multi-configurational two-neutron wave functions were used and large transferred angular momenta were considered. It was found that, at lower bombarding energies, the predictions of the EFR and zero-range calculations agree very closely both in angular distributions and relative magnitudes of the cross sections, though they differ significantly in absolute magnitude. As the bombarding energy increases, the discrepancy between the predicted absolute magnitude becomes still larger, and noticeable differences are seen even in relative cross sections. For all the energies considered, the EFR calculations predicted the absolute magnitudes of the experimental cross sections to within a factor of several units.

1. Introduction

As is well known, two-nucleon transfer reactions offer a useful tool to extract information on certain important aspects of nuclear structure, and a great deal of work has been reported in the past. Historically, light-ion induced reactions were investigated first, and in most cases, analyses were made by using the distorted-wave Born approximation (DWBA) with a zero-range (ZR) approximation. The work with heavy ions then followed, where the use of a ZR approximation was evidently meaningless, and analyses consistently used exact finite-range (EFR) DWBA, although a no-recoil approximation was also used occasionally.

In spite of the fact that the majority of analyses of light-ion induced two-nucleon transfer reactions used ZR-DWBA, a limited number of EFR-DWBA calculations have in fact been reported [1-8]). However, most of these calculations [5-8]) were based on somewhat oversimplified forms for the wave function of light ions (such as t and α) and for the interaction that causes the transfer. Others [1-4]) used more realistic forms for the light-ion wave function and the interaction, but assumed a single configuration to describe the motion of the two nucleons in the target or residual nuclei, except for cases [3,4]) in which the transferred angular momentum

† On leave from Department of Physics, University of Saga, Saga 840, Japan.

†† Supported in part by the US Department of Energy.

Volume 87B, number 1,2 PHYSICS LETTERS 22 October 1979

A FULL FINITE-RANGE CCBA ANALYSIS OF THE ^{118}Sn(p, t) ^{116}Sn REACTION

T. TAKEMASA [1], T. TAMURA and T. UDAGAWA
Department of Physics [2], The University of Texas at Austin, Austin, TX 78712, USA

Received 2 August 1979

Exact finite-range coupled-channel Born approximation calculations, using a microscopic form factor, were performed for the ^{118}Sn(p, t) ^{116}Sn reaction. Good agreement with experiment was obtained, both in the shape of the angular distributions and the relative magnitudes of the cross sections. Corresponding results using a zero-range approximation were found to agree much more poorly with experiment.

A number of coupled-channel Born approximation (CCBA) calculations, performed for light-ion-induced two-neutron transfer reactions, showed that the effects of indirect transitions via inelastic processes are of importance for both spherical vibrational [1,2] and deformed nuclei [3,4]. However, all the CCBA calculations reported so far used the zero-range (ZR) approximation. This is due mainly to the long computational time required when full finite-range (FR) calculations are carried out in a straightforward manner. In fact, there does not exist any known proof justifying the use of the ZR approximation.

Recently we developed a method to construct rather fast FR form factors for use in distorted-wave Born approximation (DWBA) calculations, for (p, t) and/or (t, p) reactions [5]. The method utilizes an interpolation technique, which was originally developed for heavy-ion-induced transfer reactions [6]. This technique allowed us to speed up the calculations by a factor of 15–20, without loss of needed accuracy in the resultant cross section [5]. Because of this increased speed, it is now practical to perform exact finite-range (EFR) CCBA calculations. The purpose of the present paper is to report on the first result of such calculations, with the ^{118}Sn(p, t) ^{116}Sn reaction at E_p = 52 MeV [7] taken as an example. We show the significance of using the EFR-CCBA method by comparing its results with those obtained with the ZR-CCBA method.

As in ref. [5], the interaction responsible for causing the transfer was taken as the sum of two-body interactions between the incident proton and each of the transferred neutrons:

$$\mathcal{V} = V(r_{pn_1}) + V(r_{pn_2}) , \tag{1}$$

where

$$V(r) = P_0 V_0(r) + P_1 V_1(r) \tag{2}$$

and

$$\begin{aligned} V_{0(1)} &= \infty , && \text{if } r \leqslant r_C , \\ &= -V^0_{0(1)} \exp[-\kappa_{0(1)}(r - r_C)] , && \text{if } r > r_C . \end{aligned} \tag{3}$$

Here P_0 (P_1) is the spin-singlet (triplet) projection operator. This potential and the parameters involved are those of Tang and Herndon [8] (TH). Thus r_C = 0.45 fm, V^0_0 = 277.07 MeV, V^0_1 = 549.26 MeV, κ_0 = 2.211 fm^{-1}, and κ_1 = 2.735 fm^{-1}. The triton wave function used in our (p, t) calculation was obtained by a variational calculation, also discussed by TH. (In the following we shall simply refer to the "TH triton", meaning the combined use of this triton wave function and the potential of eqs. (1)–(3).)

Below we also present results obtained by assuming gaussian forms for both the triton wave function and the interaction potential. (We shall simply refer

[1] On leave from Department of Physics, Saga University, Saga 840, Japan.

[2] Supported in part by the US Atomic Energy Commission.

2.B: 2.G

Nuclear Physics **A315** (1979) 124 – 132;

STUDY OF THE ^{10}Be(d, p)^{11}Be REACTION AT 25 MeV †

B. ZWIEGLINSKI ††, W. BENENSON and R. G. H. ROBERTSON

Cyclotron Laboratory and Department of Physics, Michigan State University, East Lansing, Michigan 48824

and

W. R. COKER *

Department of Physics, University of Texas at Austin, Austin, Texas 78712

Received 18 July 1978
(Revised 25 September 1978)

Abstract: The distribution of the single-neutron strength up to an excitation energy E_x = 7.0 MeV in ^{11}Be was investigated with the ^{10}Be(d, p)^{11}Be reaction at E_d = 25 MeV. The $\frac{1}{2}^+$, g.s., $\frac{1}{2}^-$, 0.320 MeV and 1.785 MeV states are found to be excited with significant strength. The angular distribution for the 1.785 MeV state is typified by an orbital angular momentum transfer l_n = 2. This together with other available data indicate that its spin is $J^\pi = (\frac{5}{2})^+$. The spectroscopic factors for these three states are compared to the shell-model calculations of Teeters and Kurath and of Cohen and Kurath.

E NUCLEAR REACTIONS ^{10}Be(d, p), E = 25 MeV; measured $\sigma(\theta)$; deduced spectroscopic factors. Reactor-produced ^{10}Be target.

1. Introduction

Due to the work of Kurath and collaborators [1, 2]), shell-model wave functions are presently available for both positive and negative parity states in A = 11 and A = 13 nuclei. The wave functions for the negative parity states were obtained by Cohen and Kurath [1]) in 1965. An important step on the way to the wave functions for the positive parity states was the derivation [3]) of a particle-hole interaction which is capable of reproducing the A-dependence of the $2s_{\frac{1}{2}}$-$1d_{\frac{5}{2}}$ splitting in the $11 \leqq A \leqq 17$ nuclei. The ordering of the $1d_{\frac{5}{2}}$ and $2s_{\frac{1}{2}}$ orbits changes with decreasing mass in this mass range, with the $2s_{\frac{1}{2}}$ orbit lying lower in energy below mass number A = 15. This particle-hole interaction was subsequently used by Teeters and Kurath [2]) to calculate the wave functions for the positive parity states in the A = 11 and A = 13 nuclei. A full vector space compatible with the $(1s)^3(1p)^{4-3}$ and $(1s)^4(1p)^{4-5}(2s, 1d)$

† Work supported by the US National Science Foundation under Grant No. PHY 78-01684.
†† On leave from the Institute of Nuclear Research, Warsaw, Poland.
* Research supported in part by the US Department of Energy.

VOLUME 43, NUMBER 2 PHYSICAL REVIEW LETTERS 9 JULY 1979

Prevalence of Direct-Reaction Mechanism in a Deeply Inelastic Reaction, $^{197}Au(^{19}F,^{12}B)$

M. Ishihara,[a] T. Shimoda,[b] H. Fröhlich,[c] H. Kamitsubo,[a] and K. Nagatani
Cyclotron Institute, Texas A & M University, College Station, Texas 77843

and

T. Udagawa and T. Tamura
Department of Physics, University of Texas, Austin, Texas 78712
(Received 1 February 1979)

Continuum cross sections and spin polarizations of ^{12}B produced in the reaction $^{197}Au(^{19}F,^{12}B)$ induced by 186-MeV ^{19}F were measured. The observed data were reproduced very well in terms of a distorted-wave Born-approximation theory, indicating that this reaction transferring as many as seven nucleons proceeds as a direct process.

Recent measurement[1] of the spin polarization of the ejectile ^{12}B produced in the reaction $^{100}Mo(^{14}N,^{12}B)$ added a new dimension to the understanding of the mechanism of heavy-ion reactions leading to continuum excited states. The polarization (P) measured as a function of the energy (E_b) of ^{12}B revealed a unique feature characterized by a large positive P at the highest E_b, followed by a rapid decrease to negative values of P with decreasing E_b. It was recognized[2] that such behavior of P is completely opposite to the prediction made by a classical macroscopic model based on the frictional force.[3] A theoretical analysis[4] using an exact-finite-range distorted-wave Born approximation (EFR-DWBA) achieved a successful fit to the data and provided a quantitative explanation. Two ingredients inherent in the EFR-DWBA were crucial in reproducing the experimental observation: The transverse recoil effect yields large positive P values for high E_b; the l-window effect causes the decrease of P towards lower E_b. This theoretical finding suggests that such behavior of P may generally be considered as a "signature" of a one-step direct reaction. We recently studied a one-proton transfer reaction $^{232}Th(^{13}C,^{12}B)$ to corroborate this argument, and found that the observed P indeed exhibited the same behavior.[5]

The study was then extended in order to see whether the direct-reaction mechanism persists even in reactions involving much larger mass, charge, and energy transfers. The reaction $^{197}Au(^{19}F,^{12}B)$ at 186 MeV was chosen as an example of such a deeply inelastic reaction. Surprisingly enough, the same feature was found to prevail in this reaction. The discussion below is concerned with this unexpected result.

The experimental procedure was similar to that of the previous study[1]; several improvements, however, were made to cope with complexities involved in the ^{19}F-induced reaction. The spin polarization of ^{12}B is determined from the asymmetry of the β rays in the decay of $^{12}B(g.s.)$ to $^{12}C(g.s.)$, measuring the intensities in the directions of 0° and 180° with respect to the polarization axis [defined parallel to the $(\vec{k}_i \times \vec{k}_f)$ axis]. The 190-MeV $^{19}F^{5+}$ beam from the Texas A&M cyclotron was used to bombard a gold target of 5.6 mg/cm^2 thickness placed at 45° to the beam (the effective incident energy is estimated to be 186 MeV as a result of the energy loss in the target). The beam was pulsed with 40-ms duration and 130-ms repetition period; the β rays were counted during the beam-off intervals. The ^{12}B ejectiles scattered at the laboratory angle 25° were implanted into a platinum stopper foil which was placed in the vertical external magnetic field. An aluminum energy-degrading foil, whose thickness was varied, was inserted to select the ^{12}B energy bin. The β rays from the stopper foil were detected with a pair of threefold plastic counter telescopes placed above and below the stopper. To compensate for possible asymmetry in the counting efficiencies of the two telescopes, the spin orientation of the implanted ^{12}B was externally reversed in every second counting period using the NMR technique of the fast adiabatic method. For each thickness of the absorber the measurement was made both with a 15-μm and with a 5-μm platinum stopper. This, in turn, provided the correction for the depolarization effect due to the hyperfine interaction.

In the present reaction, the presence of a large number of background β emitters was noted in an independent measurement of charged-particle spectra using solid-state counter telescopes. Taking advantage of the large decay energy of ^{12}B, the low-energy threshold of β rays was set high, typically at 6 MeV, to eliminate a strong contribution from ^{20}F as well as other background. The

PHYSICAL REVIEW C VOLUME 20, NUMBER 5 NOVEMBER 1979

Breakup processes in heavy-ion induced reactions

T. Udagawa and T. Tamura
Department of Physics, University of Texas, Austin, Texas 78712

T. Shimoda,* H. Fröhlich,† M. Ishihara,‡ and K. Nagatani
Cyclotron Institute, Texas A & M University, College Station, Texas 77843

(Received 29 May 1979)

Cross sections for breakup of ^{20}Ne into ^{16}O and α during scattering from ^{40}Ca were calculated in terms of the distorted wave Born approximation. The inclusive ^{16}O cross section observed in the ^{40}Ca(^{20}Ne, ^{16}O) reaction was then found to be fitted very well by the sum of this breakup contribution and that of the α-transfer reaction calculated in our previous work.

[NUCLEAR REACTIONS ^{40}Ca(^{20}Ne,^{16}O) breakup reactions, calculated $d^2\sigma/d\Omega\, dE$; $E(^{20}\text{Ne}) = 149$–262 MeV, direct reaction mechanism for heavy-ion reaction.]

In a recent publication,[1] we reported on measurements of continuum cross sections of α-transfer (like) reactions with a ^{40}Ca target, induced by ^{20}Ne, ^{14}N, and ^{13}C ions with incident energies E_{lab}, respectively, equal to 262, 153, and 149 MeV. The continuum spectra were taken at several angles between $\theta_{lab} = 5^\circ$–20°, and the results were analyzed in terms of the distorted wave Born approximation (DWBA) assuming that the reaction proceeded as a one-step α-transfer process. It was found[1] that the calculation reproduced very well the experimental spectra at all angles for two of the three reactions, i.e., for (^{14}N, ^{10}B) and (^{13}C, ^{9}Be) reactions. On the other hand, for the (^{20}Ne, ^{16}O) reaction, it was found that, although we were able to fit very well the experimental spectra at $\theta_{lab} \geq 16^\circ$, the theoretical cross sections became progressively too small compared with experiment, as θ_{lab} was decreased. A very similar situation was again experienced in the analysis of more recent data taken at $E_{lab}(^{20}\text{Ne}) = 149$ MeV.

The purpose of the present article is to discuss ways this discrepancy can be removed, i.e., to explain the part of the experimental cross sections that were left *unexplained* within the framework of the DWBA calculations reported in Ref. 1. This unexplained part of the cross section has two distinct features, as can be seen in Fig. 1 of Ref. 1 [and by the dotted curves in Fig. 2(a) of the present work]. The first is that it is forward peaked, as we already remarked above. The second is that the cross section, seen as a function of $E_{lab}(^{16}\text{O})$, is peaked at 205 MeV, which is $\frac{4}{5}$ of $E_{lab}(^{20}\text{Ne})$, i.e., just the kinetic energy which the ^{16}O cluster had in the incident ^{20}Ne ion. These two features indicate that the excess cross section can be explained as the cross section associated with the breakup of the incident ^{20}Ne. We shall show below that such a supposition can indeed be proved correct.

To our knowledge not many calculations of the breakup cross section have been done for heavy-ion induced reactions. In the regime of light-ion induced reactions, however, it has been one of the classic problems, and a number of investigations have in fact been reported, see, e.g., a recent review by Baur and Trautmann.[2] Consider, as an example, the DWBA treatment of deuteron breakup, the amplitude being described in the post

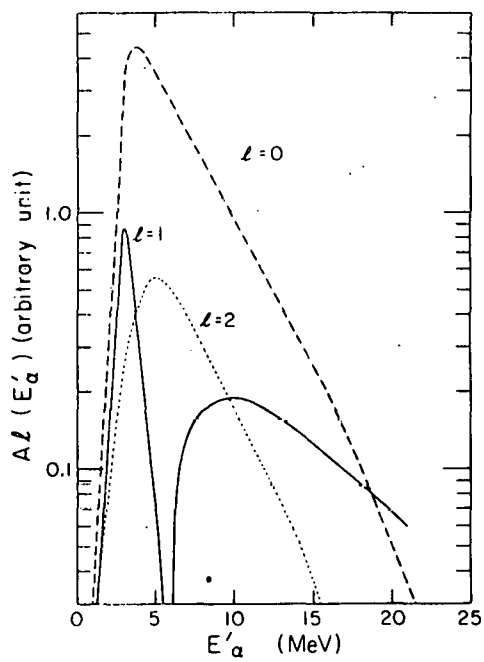

FIG. 1. Calculated $A_l(E'_\alpha)$ values for $l = 0$–2 as a function of E'_α.

VOLUME 42, NUMBER 23 PHYSICAL REVIEW LETTERS 4 JUNE 1979

Alpha-Transfer Reactions with Large Energy Transfers

H. Fröhlich,[a] T. Shimoda,[b] M. Ishihara,[c] and K. Nagatani
Cyclotron Institute, Texas A & M University, College Station, Texas 77843

and

T. Udagawa and T. Tamura
Department of Physics, University of Texas, Austin, Texas 78712

(Received 1 February 1979)

Alpha-transfer reactions (^{20}Ne, ^{16}O), (^{14}N, ^{10}B), and (^{13}C, ^{9}Be) on a ^{40}Ca target were studied at 262, 153, and 149 MeV, respectively. Analysis in terms of the direction-reaction theory reproduced the observed continuum spectra and angular distributions well, except for the cross section of the reaction (^{20}Ne, ^{16}O) at small angles, which is attributed to a projectile breakup process.

Heavy-ion reactions with bombarding energies well above the Coulomb barrier generally produce continuum spectra. One of the intriguing features in such reactions is the appearance of enhanced cross sections at ejectile energies considerably lower than the incident energy; that is, the process involves a large energy transfer. The surprising appearance of the deeply inelastic process has lead to various theoretical attempts introducing a variety of concepts, such as frictional forces, mass and energy transport, and so forth.[1]

Recently, however, a quantum mechanical treatment using the direct-reaction model, which has been routinely applied to analyses for discrete spectra, was extended to analyze data with continuum spectra.[2-4] If this method can demonstrate a wide range of applicability, especially for reactions of a deeply inelastic nature, it will provide a new theoretical approach for understanding the heavy-ion reaction. It should also be pointed out that the application of the direct-reaction theory, which is coupled to a microscopic description of the nuclear structure, may open up the possibility of using the heavy-ion reaction in the study of nuclear structure in the continuum region, such as the extraction of the spectroscopic density of multinucleon states with very high spins in high excitation regions of the residual nuclei. The choice of the present α-transfer reactions was made for specific reasons.

The projectiles ^{20}Ne, ^{14}N, and ^{13}C are known to have large α-transfer spectroscopic amplitudes. In addition, the angular momentum (L_α) of the cluster relative to the core in ^{20}Ne, ^{13}C, and ^{14}N is dominantly 0, 2, and 4, respectively. As discussed later, the difference in the L_α values results in a subtle difference in the spectral shape. Therefore, a simultaneous study of the α-transfer reactions with these projectiles on the same target should impose a stringent test on the theoretical analysis.

The experiments were carried out using 262-MeV ^{20}Ne^{6+}, 153-MeV ^{14}N^{4+}, and 149-MeV ^{13}C^{4+} beams from the Texas A&M cyclotron on a self-supporting natural calcium target of 1.0-mg/cm^2 thickness. Outgoing particles were detected using solid-state counter telescopes. Some of the energy spectra are shown in Fig. 1, and the angular distributions of the energy-integrated cross sections are displayed in Fig. 2. Several observations can be made from these spectra. Each shows a continuum spectrum and, within the statistics, no discrete peaks are observed. In the reactions (^{14}N, ^{10}B) and (^{13}C, ^{9}Be), the angular dependence of the spectral shapes is weak. On the other hand, at small angles the spectra of the reaction (^{20}Ne, ^{16}O) show an extra hump in the high-energy region; this disappears at large angles. This difference is more conspicuous in the angular distribution of the reaction (^{20}Ne, ^{16}O) which has a steeper slope in forward angles as compared with the other two reactions. Remarkably, the magnitude of the forward-angle cross section of the reaction (^{20}Ne, ^{16}O) is much larger than those of the other reactions.

Theoretical cross sections were calculated by using an exact-finite-range (EFR) distorted-wave Born-approximation (DWBA) method, assuming direct α-transfer processes leading to many overlapping continuum states. The details of the method have already been explained[2-4]; several salient points are noted below. The continuum cross section is given as a sum of products of the EFR-DWBA cross sections and the α-spectroscopic densities in the same residual nuclei of ^{44}Ti, where the sum is taken over the spins of the final states. In the EFR-DWBA calculation, the overlap integrals are expressed in an analytic form, which includes the quantum numbers and the Q

Volume 82B, number 3,4 PHYSICS LETTERS 9 April 1979

ANALYSIS OF CONTINUOUS SPECTRA OF THE REACTIONS (^{20}Ne, ^{16}O) AND (^{20}Ne, ^{12}C) IN TERMS OF MULTI-STEP DIRECT REACTION THEORY

T. UDAGAWA and T. TAMURA
Department of Physics[1], University of Texas, Austin, TX 78712, USA

and

B.T. KIM
DPh-N/BE, CEN Saclay, 91190 Gif-sur-Yvette, France

Received 12 September 1978

A multi-step direct reaction theory, which is completely quantum mechanical, is applied to analyze the deep inelastic cross sections of the (^{20}Ne, ^{16}O) and (^{20}Ne, ^{12}C) reactions. Possible extension of this method to more complicated cases is also discussed.

One of the most interesting subjects in heavy-ion induced reactions is to clarify the mechanism of the so-called deep inelastic collisions, i.e., processes in which a large amount of energy is transferred from relative to intrinsic degrees of freedom, often being accompanied by a large mass and charge transfer between the colliding partners [1]. Actually, however, similar processes do take place in light-ion induced reactions, and we showed recently that such processes can be explained nicely in terms of the multi-step direct reaction (MSDR) theory [2].

In the present article, we attempt to extend the application of the MSDR theory to heavy-ion induced reactions. We take as specific examples the (^{20}Ne, ^{16}O) and (^{20}Ne, ^{12}C) reactions, induced by 120 MeV ^{20}Ne impinging upon ^{27}Al [3]. We are interested in seeing whether we can fit the data by assuming that the (^{20}Ne, ^{16}O) reaction proceeds primarily as a one-step α-transfer reaction, while (^{20}Ne, ^{12}C) proceeds as a reaction in which two α-particles are transferred successively.

In the MSDR theory [2], the continuous spectra are described in terms of the ith Born cross sections $\sigma^{(i)}$ and of appropriate spectroscopic densities ρ. Thus the contribution from the one-step (a + A → b + B) process may be written as

$$d\sigma^{(1)}(E_b, \theta)/dE_b = \sum_{I_B(=l)} \sigma^{(1)}_{DW}(0^+ \to I_B E^*_B)\rho(I_B E^*_B). \quad (1)$$

(Note that, as in ref. [2], we assume that the target has spin 0^+. Throughout the present article we use the notation of ref. [4].) Both $\sigma^{(1)}_{DW}$ and ρ depend on the transferred angular momentum l (which equals the final state spin I_B) and on E^*_B, which is the excitation energy of the residual nucleus B. This E^*_B is related to the reaction Q-value, Q, by $E^*_B = Q_g - Q = Q_g - (E_b - E_a)$, Q_g being the Q-value for the ground state transition.

The corresponding two-step (A + a → C + c → B + b) contribution may be written as

$$d\sigma^{(2)}(E_b, \theta)/dE_b = \sum_{I_C(=l_1), I_B, l_2} \int dE^*_C \times \sigma^{(2)}_{DW}(0^+ \to I_C E^*_C \to (l_1 l_2) I_B E^*_B) \times \rho(l_1 E^*_C)\rho(l_2 E^*_B - E^*_C). \quad (2)$$

It is understood in $\sigma^{(2)}_{DW}$ that an angular momentum l_i is transferred in the ith step, and that $I_B = l_1 + l_2$. At the end of the first step, i.e., in the intermediate state,

[1] Work supported in part by the U.S. Department of Energy.

Summary talk

International Conference on
Dynamical Properties of Heavy-ion Reactions,
Johannesburg, South Africa, 1-3 August 1978

Taro Tamura

Taro Tamura
Department of Physics, University of Texas, Austin, Texas, USA

If I am to summarize this Conference in one word, I would say that it has been a great 'success', and I heartily congratulate Professor Sellschop and his colleagues of the Organizing Committee for their achievements. The Conference has attracted a large number of delegates from many countries, and the material presented during the past three days has been very dense and of high quality. I am sure that part of the attraction was supplied by the animals in the Kruger National Park, but their contribution cannot have been that significant. All of us have come to do good physics, and it has been done. I hope this summary turns out to be sufficiently good to keep up with the high standard of papers presented so far. I hope the glass of sherry I just had can help me to achieve this.

This Conference opened, very reasonably, with a paper by **Greiner**. He was supposed to give an 'overview of the field', but what he actually did was to talk exclusively of his own work. I am not complaining about this, however, because Greiner has worked in so many subjects of heavy-ion physics, that to talk exclusively of his own work is not too different from talking about the overview of this field.

Greiner talked about a number of subjects, starting with the application of the two-centre shell model calculation to predict fission asymmetry. He and his co-workers have been working on this subject in the past few years, and thus the idea is not necessarily new. They have succeeded recently, however, in overcoming a theoretical difficulty in applying this method to cases with very large mass asymmetry. As a consequence, they managed to produce a mass asymmetry curve which has in it four peaks, rather than two (or sometimes one), as had been the case earlier. Greiner then remarked that Epperson of Duke indeed found experimentally such a mass asymmetry curve with four peaks, although Wilhelmy commented that Epperson's result is not yet completely free from controversy among experimentalists in this field.

Concerning the mass asymmetry in fission, an extremely interesting contribution was made by **Wilhelmy**, who talked about spontaneous fission of very heavy actinides, in particular ^{258,259}Fm. The surprising discovery made was that, while lighter elements ^{254,256,257}Fm all favour asymmetric fission, this feature is abruptly changed by adding just one more neutron: the elements ^{258,259}Fm suddenly begin to favour symmetric fission. It is also remarkable that the symmetric peak in the fission of ^{258}Fm is extremely narrow. Wilhelmy further noted the fact that the average kinetic energy release (TKE) in the fission of ^{258,259}Fm is about 240 MeV, meaning an abrupt increase of TKE in going from lighter to heavier Fm elements. ^{254,256,257}Fm all had TKE of about 200 MeV.

Nix summarized beautifully the present status of the game of either finding in nature or creating in the laboratory the super-heavy elements (SHE). This is a story of the struggle of a number of people over the past twelve years, which has not yet been awarded by success. Perhaps because of this experimental failure, Nix's talk was largely theoretical.

Several groups of theoreticians who carried out extensive calculations have been involved, with the hope of coming up with suggestions to experimentalists as to where and how to look for SHE, and such efforts are still being made. As an outsider to this field, I was a little surprised to hear that so many theoretical uncertainties still exist, although it is clear that this is the case largely because the calculations have to be made by extrapolating to the SHE region knowledge well tested only for lighter elements.

In spite of the above theoretical discrepancies, however, it appears that everybody agrees with the presence of a sea of instability between the island of SHE and the actinide region, so that it is very unlikely that SHE were formed by the r process. Nix therefore stressed the use of heavy-ion reactions to create SHE. He suggested three possibilities; fusion-fission, compound processes and transfer reactions. The best experimental efforts made so far came up with the upper limit of 10^{-34} cm^2 for the cross section for creating SHE, if we talk about SHE that live longer than a day or so. Nix thus stressed the importance of looking for SHE of much shorter lifespan. In the extreme situation, the life-time may be as short as the nuclear transit time, which means that one might try to seek SHE created in the form of a resonance.

Concerning the possible presence of SHE in nature, **Molzahn** reported on efforts to understand the origin of some of the giant halos. His group located several big halos in Cordierite from Brazil, and measured α and fission activities. They observed no high-energy α-particles, nor spontaneous fission, casting doubt about the responsibility of the high-energy α-particles ($E \gtrsim 14$ MeV) suspected in early work of this field. Molzahn also talked about measuring fission in meteorite Allende, for which Flerov had reported the presence of unknown fission activity. Molzahn indeed observed fission-like events, by taking coincidence of fission fragments and associated neutrons. He wanted, however, to defer making a definite conclusion until a confirmation of fission is made by scanning the mica plates on which the samples were deposited. In general his tone sounded rather pessimistic about finding SHE in nature.

Boleu presented an interesting piece of theoretical information, discussing the energy surface, as a function of the deformation parameter ε, for nuclei way away from the stability line. In fact an example considered was ^{266}U (as well as ^{242}U). According to Boleu, this nucleus ^{266}U has three maxima in the energy surface, compared to two in ^{242}U. I am wondering whether he can predict a similar

MULTI-STEP DIRECT REACTION ANALYSIS OF DEEP INELASTIC SPECTRA IN NUCLEAR REACTIONS

T. Tamura and T. Udagawa

Department of Physics*, University of Texas

Austin, Texas, U.S.A. 78712

Abstract

Application of direct reaction theories in the past has been limited to reactions with discrete final states. In these lecture notes, we show that the applications can be extended to data with continuous spectra as well. Examples of analyses of data of reactions induced by both light- and heavy-ions are discussed. The latter application is limited so far to examples with comparatively light heavy-ions. The Scope of its extension to cases with heavier projectiles is also discussed.

Invited lecture delivered at the Post-Conference School - "Topical Themes in Heavy-ion Scattering", at the University of the Witwatersrand, Johannesburg, 9 - 11 August, 1978

* Supported in part by the U.S. Department of Energy.

Invited talk given at Workshop
held at Bad Honnet, Nov. 1978.

Multi-Step-Direct-Reaction Theory Applied to Continuum Spectra in Light- and Heavy-Ion Induced Reactions

Taro Tamura

Department of Physics+, University of Texas

Austin, Texas, U.S.A. 78712

It is my understanding that these proceedings are to be published as a collection of memoranda, largely intended for the use of the participants of the Symposium, rather than the use of the general public. I thus feel it appropriate to present in this note only the basic ideas of our work, and the results obtained. Most of the contents of the present note have been published[1-9]. This note will serve as a guide for the reader to see where to find more detail, if necessary.

Our group at Austin, including most notably Takeshi Udagawa, worked in the past, as did many other groups, on analyzing a number of reaction data leading to discrete final states, induced both by light and heavy ions. Either single-step (SS) or multi-step (MS) direct reaction (DR) theory was used, depending on the need. A conclusion we arrived at, through this experience, was that the DR theory works very well in general.

If the excitation energy E_x of the residual nucleus exceeds a critical value E_{crit}, which is a few MeV, the final states get very close together or begin to overlap, and the corresponding spectrum becomes continuous. However, in the reactions with continuous spectra of our interest, the incident energy is much higher than E_{crit}. Therefore, it is rather unlikely that the reaction mechanism changes abruptly, when E_x moves through E_{crit}. In other words, it seems more natural than not to expect that the MSDR theory (including SSDR theory as its limit), which works well in the discrete region, also works well in the continuum region. This is the point of view we take.

---

*Supported in part by the U.S. Department of Energy.

Computer Physics Communications 17 (1979) 351–355

COULOMB FUNCTIONS WITH COMPLEX ANGULAR MOMENTA

T. TAKEMASA * and T. TAMURA
*Department of Physics **, University of Texas, Austin, TX 78712, USA*

and

H.H. WOLTER
Sektion Physik Universität München, D-8046 Garching, Fed. Rep. Germany

Received 17 October 1978

PROGRAM SUMMARY

Title of program: CCOULM

Catalogue number: ABND

Program obtainable from: CPC Program Library, Queen's University of Belfast, N. Ireland (see application form in this issue)

Computer: CDC 6600; *Installation*: University of Texas Computer Center

Operating system: UT-2

Programming language used: FORTRAN IV

High speed storage required: 10816 words

Number of bits in a word: 60

Overlay structure: none

Number of magnetic tapes required: none

Other peripherals used: card reader, line printer

Number of cards in combined program and test deck: 400

Card punching code: CDC

Keywords: general purpose, nuclear, atomic, Schrödinger, scattering, reactions, Regge, complex angular momentum, wave function, Coulomb, complex Coulomb, potential, asymptotic expansion, phase shift, logarithm of complex gamma function

Nature of physical problem
The subroutine CCOULM calculates regular and irregular Coulomb functions and their derivatives associated with complex angular momenta. This program may thus be used, for example, in locating Regge poles that appear in atomic and nuclear scattering problems [1].

Method of solution
The calculation utilizes the asymptotic expansion method of Fröberg [2]. When the asymptotic expansion does not give a satisfactory result at a desired ρ, a larger value is chosen for ρ and the differential equation is solved inward for the irregular solution. Then the method of Wills [3] is used to obtain the regular solution. The complex Coulomb phase shift is obtained by using a subroutine which calculates the logarithm of the gamma function for complex argument.

Restrictions on the complexity of the problem
Subroutine CCOULM can be used for real values ρ and η and for complex (as well as real) angular momentum l that satisfy the condition $\eta^2 << \rho$ and $|l|^2 << \rho$. Even when this condition is not fulfilled, the program may be used with somewhat reduced accuracy.

Typical running time
The evaluation of regular and irregular Coulomb wave functions and their derivatives for a given value of l takes about 0.3 s of the CDC 6600 computer.

References
[1] T. Tamura and H.H. Wolter, Phys. Rev. C6 (1972) 1976; T. Takemasa and T. Tamura, ibid., C18 (1978) 282.
[2] C.E. Fröberg, Rev. Mod. Phys. 27 (1955) 399.
[3] J.G. Wills, J. Comput. Phys. 8 (1971) 162.

* On leave from Department of Physics, University of Saga, Saga 840, Japan.
** Supported in part by the U.S. Department of Energy.

Computer Physics Communications 18 (1979) 163–169

EXACT FINITE RANGE DWBA FORM FACTOR FOR HEAVY-ION INDUCED NUCLEAR REACTIONS

T. TAMURA, T. UDAGAWA and K.E. WOOD
*Department of Physics *, University of Texas, Austin, TX 78712, USA*

and

H. AMAKAWA
Cyclotron Laboratory, the Institute of Physical and Chemical Research, Wako-shi, Saitama, 351 Japan

Received 17 March 1979

ADAPTATION SUMMARY

Title of adaptation: SATURN-2-FOR-EFR-DWBA

Adaptation number: 0001

Program obtainable from: CPC Program Library, Queen's University of Belfast, N. Ireland (see application form in this issue)

Reference to original program:
Cat. No.: ABPA; *Title*: SATURN-1-FOR-EFR-DWBA;
Ref. in CPC: 8 (1974) 349

Authors of original program: T. Tamura and K.S. Low

High speed store required: 39 872 words

Other peripherals used: card reader, line printer

Number of cards required to effect adaptation (including directive cards): 869

Card punching code: CDC

Method of solution
Calculation of the form factor involves a four-fold integral, though it can normally be reduced to a sum of single-fold integrals. When the original program is used for cases with large angular momentum transfer the sum results in a severe cancellation between summands, making the results inaccurate. The present program uses a new coordinate system in performing the above integral and makes it possible to avoid the difficulty.

* Supported in part by the U.S. Department of Energy.

PHYSICAL REVIEW C VOLUME 19, NUMBER 5 MAY 1979

Dissipation in time-dependent Hartree-Fock calculations

Kit-Keung Kan* and Taro Tamura
Department of Physics, University of Texas, Austin, Texas 78712
(Received 6 October 1978; revised manuscript received 5 January 1979)

Dissipation is studied in a one-dimensional time-dependent Hartree-Fock system which simulates the capture of a slow neutron by a nucleus. It is shown that this time-dependent Hartree-Fock system is unable to approach thermodynamic equilibrium and that the time of damping of a collective vibration, induced by the capture, is much longer than the relaxation time of realistic nuclear collective motion. The dissipation in this time-dependent Hartree-Fock system is further compared with predictions of various one-body dissipation theories.

[NUCLEAR REACTIONS time-dependent Hartree-Fock calculation, slow neutron capture, one-body dissipation.]

Many calculations for heavy-ion collision which employ the time-dependent Hartree-Fock (TDHF) theory have been performed since the pioneering work of Bonche, Koonin, and Negele.[1] In spite of many interesting results obtained by such large-scale numerical calculations,[2] the validity of this approximation remains, to a large extent, an open question. Therefore, at this stage a theoretical consideration or a numerical calculation which may shed some light on the question of the validity or the limitation of the TDHF theory could be useful. With this in mind, we report in the present article on a TDHF calculation performed for a relatively simple problem, i.e., the capture of a slow neutron by a nucleus. We concentrate our interest on the dissipation aspect of this system.

If we neglect the coupling of the nucleus with the radiation field, the excess energy of the captured neutron will gradually be shared with other nucleons through particle collisions, and the system will gradually tend to thermodynamic equilibrium and become a compound nucleus. The relaxation time for this equilibrium may be given as $\tau_{CN} = l/v_F$, where CN stands for compound nucleus, l is the mean free path of the captured neutron inside the nucleus, and v_F is the Fermi velocity. Using[3] $l = 5.2$ fm and $v_F = 0.27\,c$ we obtain $\tau_{CN} \simeq 20$ fm$/c \simeq 0.7 \times 10^{-22}$ s. This relaxation time may be taken as a standard measure against which the dissipation time derived by a TDHF calculation can be compared.

Once the dissipation in TDHF is known, one is naturally led to another question: How does this dissipation compare with the prediction of the one-body dissipation theories?[4,5] Since TDHF is a one-body system, a satisfactory one-body dissipation theory ought to reproduce the TDHF result. Hence, by extracting the dissipation from our TDHF calculation, we may test the validity of the TDHF approximation itself and, at the same time, test the theories of one-body dissipation. This is what we intend to do in the present article.

In describing by TDHF the capture of a slow neutron by a nucleus of A nucleons, we make the following assumptions: (a) Before capture, nucleus A is represented by a static Hartree-Fock (HF) state of the A-particle system; (b) the state of A is not affected when the neutron is brought near to it; and (c) the neutron is captured in a barely bound orbital of the static HF potential of A. [One may think of, e.g., direct capture of a neutron via a (d,p) reaction.] The system after the neutron is captured is then approximated by a TDHF system whose initial determinant consists of the $A+1$ orbitals in the static HF potential of the A-particle system.

Immediately after the instant of capture, the TDHF potential is determined by $A+1$ orbitals and will differ from the original static HF potential. This abrupt change of the potential, in the spirit of TDHF is a one-body approximation to the interaction of the captured neutron with the other nucleons in the nucleus. Because of this change in the potential, the orbitals are no longer eigenstates, and the corresponding energies of the particles can vary among themselves. We then ask whether the energy distribution of this system can approach that of a Fermi gas of finite temperature and, if it can, over what time scale?

In order to obtain the energy distribution of the system, we project the TDHF single-particle states onto a set of stationary states. For convenience, we choose the original static HF single-

PHYSICAL REVIEW C VOLUME 18, NUMBER 6 DECEMBER 1978

Uncertainties in neutron densities determined from analysis of 0.8 GeV polarized proton scattering from nuclei

L. Ray
Theoretical Division, Los Alamos Scientific Laboratory, University of California, Los Alamos, New Mexico 87545

W. Rory Coker
Department of Physics, University of Texas, Austin, Texas 78712

G.W. Hoffmann
Department of Physics, University of Texas, Austin, Texas 78712 and Los Alamos Scientific Laboratory, University of California, Los Alamos, New Mexico 87545

(Received 11 July 1978)

The first order, spin-dependent microscopic proton-nucleus optical potential of Kerman, McManus, and Thaler is used to analyze 800 MeV polarized proton elastic differential cross section and analyzing power data for target nuclei ^{58}Ni, ^{90}Zr, ^{116,124}Sn, and ^{208}Pb. Approximately model-independent target neutron density distributions are constructed in order to investigate the uncertainty in the deduced neutron densities resulting from the statistical error and the finite range of momentum transfer in the experimental angular distributions. Numerous other experimental and theoretical sources of error and uncertainty are considered to obtain a realistic estimate of the total error in the deduced neutron densities and their root-mean-square radii. The typical error in the root-mean-square radii is found to be ±0.07 fm. Impressive qualitative agreement is found between the deduced neutron matter densities and the corresponding densities predicted by Hartree-Fock calculations.

[NUCLEAR REACTIONS Proton-nucleus scattering, $E = 0.8$ GeV; targets ^{58}Ni, ^{90}Zr, ^{116,124}Sn, ^{208}Pb; analyzing power; spin-dependent Kerman, McManus, and Thaler optical potential; model-independent densities; error analysis; neutron radii.]

I. INTRODUCTION

The nuclear radius and the shape of the nuclear matter density distribution have received continued study throughout the history of nuclear physics. References 1–21 are some of the more recent works on these topics. A major goal of much of this work has been to obtain empirical matter densities unambiguously enough to permit meaningful comparisons with predictions of the shell model[22] or various self-consistent-field models[23–26] of nuclei.

Experiments with electrons and muons have provided data from which the nuclear charge density has been reliably determined for stable nuclei throughout the table of nuclides.[1–2] Generally, there is good qualitative agreement between the experimental charge densities and those predicted by Hartree-Fock calculations.[1]

Unambiguous neutron density distributions are much harder to obtain. Experimental data from which one can attempt to deduce these densities necessarily involve the hadron-nucleus interaction; thus, scattering experiments with beams of protons, ^{4}He, and pions are used to provide the data for theoretical interpretation. Unfortunately, a model-independent description of the interaction and reaction mechanism is lacking.[13–15,17,27] Also, a correct relativistically invariant equation of motion is not available.[1,27–29] Because of these uncertainties, the neutron distributions deduced using different projectiles and/or different methods of analysis are sometimes found to substantially disagree.[12,15,16] Varma and Zamick offer a brief critique of this situation.[12]

The purpose of this paper is to present a thorough investigation of the sources of uncertainty in the deduced neutron densities found from analysis of 0.8 GeV polarized proton elastic differential cross section and analyzing power data for target nuclei ^{58}Ni, ^{90}Zr, ^{116,124}Sn, and ^{208}Pb. Experimental errors, theoretical models, and assumptions, as well as various systematic errors are considered. This work offers a more detailed explana-

VOLUME 42, NUMBER 6 PHYSICAL REVIEW LETTERS 5 FEBRUARY 1979

Effects of Spin-Orbit Deformation in Inelastic Scattering at 0.8 GeV

R. P. Liljestrand,[a] G. S. Blanpied,[b] W. R. Coker, and C. Harvey
University of Texas, Austin, Texas 78712

and

G. W. Hoffmann
University of Texas, Austin, Texas 78712, and Los Alamos Scientific Laboratory, Los Alamos, New Mexcio 87545

and

L. Ray
Los Alamos Scientific Laboratory, Los Alamos, New Mexico 87545

and

C. Glashausser
Rutgers University, New Brunswick, New Jersey 08903

and

G. S. Adams, T. S. Bauer, G. Igo, G. Pauletta, and C. A. Whitten, Jr.
University of California, Los Angeles, California 90024

and

M. A. Oothoudt[c]
University of Minnesota, Minneapolis, Minnesota 55455

and

B. E. Wood
University of Oregon, Eugene, Oregon 97403

and

H. Nann
Northwestern University, Evanston, Illinois 60201

(Received 10 October 1978)

New differential cross section and analyzing-power data for 800-MeV p_{pol}+ ^{12}C, ^{116,124}Sn inelastic scattering to the first 2^+ states are presented. A distorted-wave Born-approximation analysis which utilizes collective form factors and includes deformation of the spin-orbit potential is shown to provide a reasonable description of the analyzing-power data.

Distorted-wave Born-approximation (DWBA)[1] analyses of some of the available medium-energy (~ 1 GeV) proton-nucleus inelastic differential cross-section data were found generally to give good overall agreement for both shapes and magnitudes of the cross sections, using *spin-independent* collective form factors and deformation lengths consistent with averages of results of many low-energy determinations.[2-4] A recent investigation[5] of the sensitivity of the calculations to a spin-orbit contribution to the macroscopic collective form factor suggested considerable sensitivity of the predicted analyzing powers to deformation of the spin-orbit potential, but unfortunately, no inelastic analyzing-power data were available for comparison with the predic-

Volume 81B, number 2 PHYSICS LETTERS 12 February 1979

ELASTIC DIFFERENTIAL CROSS SECTIONS AND ANALYZING POWERS FOR $\vec{p}$ + ^{40,42,44,48}Ca AT 0.8 GeV

G. IGO, G.S. ADAMS, T.S. BAUER, G. PAULETTA, C.A. WHITTEN Jr. and A. WREIKAT
University of California, Los Angeles, CA 90024, USA

G.W. HOFFMANN
University of Texas, Austin, TX 78712, USA
and Los Alamos Scientific Laboratory, Los Alamos, NM 87545, USA

G.S. BLANPIED [1], W.R. COKER, C. HARVEY and R.P. LILJESTRAND [2]
University of Texas, Austin, TX 78712, USA

L. RAY, J.E. SPENCER [4] and H.A. THIESSEN
Los Alamos Scientific Laboratory, Los Alamos, NM 87545, USA

C. GLASHAUSSER
Rutgers University, New Brunswick, NJ 08903, USA

N.M. HINTZ and M.A. OOTHOUDT [3]
University of Minnesota, Minneapolis, MN 55455, USA

H. NANN and K.K. SETH
Northwestern University, Evanston, IL 60201, USA

B.E. WOOD and D.K. McDANIELS
University of Oregon, Eugene, OR 97403, USA

and

M. GAZZALY
University of Pennsylvania, Philadelphia, PA 19174, USA

Received 10 October 1978

Differential cross sections and analyzing powers for the elastic scattering of 800 MeV polarized protons from ^{40,42,44,48}Ca are reported. A first-order, spin-dependent KMT optical potential analysis is presented from which the rms radii of the neutron densities are deduced. A comparison of these results with other determinations and with various theoretical predictions is given.

[1] Present address: New Mexico State University, Las Cruces, NM 88001, USA.
[2] Present address: TRIUMF, University of British Columbia, Vancouver, B.C., Canada.
[3] Present address: Los Alamos Scientific Laboratory, Los Alamos, NM 87545, USA.
[4] Present address: Stanford University, Stanford, CA 94305, USA.

PHYSICAL REVIEW C VOLUME 20, NUMBER 4 OCTOBER 1979

Coupled-channels analysis of proton inelastic scattering to the γ-vibrational band in ^{24}Mg

L. Ray
Theoretical Division, Los Alamos Scientific Laboratory, Los Alamos, New Mexico 87545

G. S. Blanpied
Department of Physics, New Mexico State University, Las Cruces, New Mexico 88003

W. R. Coker
Department of Physics, University of Texas at Austin, Austin, Texas 78712

(Received 22 May 1979)

Results are presented of coupled-channels analyses of proton inelastic scattering data for the nucleus ^{24}Mg, in which the 2_2^+, 4.24 MeV, 3^+, 5.2 MeV, 4_2^+, 6.01 MeV, and 5^+(?), 7.8 MeV states of the γ-vibrational band are excited, at incident proton energies of 20.3, 40, and 800 MeV. Previous coupled-channels analyses of proton and α particle inelastic scattering data for these states in ^{24}Mg have completely failed to account for the shapes and magnitudes of the 3^+, 4_2^+, and 5^+ inelastic cross sections. In the present analysis, the inclusion of an additional nuclear vibrational multipole which permits a direct transition from the ground state to the 4_2^+, 6.01 MeV state is shown to provide a tremendous improvement in the theoretical description of the inelastic cross sections of all the members of the γ-vibrational band, at each of the three incident proton energies considered. The same nuclear structure parameters are used at all three incident energies, along with phenomenological optical potentials specific to each energy. The new results for the 3^+, 5.2 MeV state also shed light on the energy dependence of the direct spin-flip mechanism in proton inelastic scattering.

[NUCLEAR REACTIONS ^{24}Mg (p,p'), E_p=20.3, 40, and 800 MeV; coupled-channels analysis; deformed-vibrational model; coupling parameters.]

I. INTRODUCTION

Vibrational states in deformed nuclei have attracted considerable attention from nuclear physicists for many years, with a number of studies of various kinds having been made in the s-d shell and in the rare earth and actinide regions.[1-13] In the even-even deformed nuclei, for instance, the first several excited states can be classified as belonging either to the ground state rotational band, or to the β- and γ-vibrational band sequences.[1,14] Generally, these excited states have been investigated through the inelastic scattering of either protons[2-7] or α particles[8-11] from the nuclei of interest. In the majority of these investigations, an effort was made to describe the inelastic scattering data in terms of macroscopic collective models of deformed nuclei[14] and a coupled-channels reaction theory formalism, as developed, for example, by Tamura.[15]

For the specific case of ^{24}Mg, a number of analyses have been made of inelastic scattering data, employing the collective rotational model and the coupled-channels formalism.[2-8,10] While these analyses have met with considerable success, there have also been significant failures. Calculated angular distributions for the 2^+, 1.37 MeV and the 4^+, 4.12 MeV members of the ground state rotational band, as well as the 2_2^+, 4.24 MeV "bandhead" of the γ-vibrational band in ^{24}Mg, agree quite well in shape and magnitude with the measured cross sections and confirm the applicability of the simple rotational model to this nucleus. On the other hand, very drastic disagreement between predictions and data is found for the 8.12 MeV 6^+ state, assumed a member of the ground state rotational band, as well as for the 5.2 MeV 3^+, the 6.01 MeV 4_2^+, and the 7.8 MeV 5^+ states, assumed to be members of the γ-vibrational band.[2-8,10] In this paper we will be particularly concerned with these latter discrepancies and their extirpation. The 7.8 MeV state is not definitely known to be a 5^+ (Ref. 16) but, following Blanpied *et al.*,[2] it will be assumed to be in what follows.

The nature of the failure of previous coupled-channels predictions[2-8,10] for the angular distributions of the 3^+, 4_2^+, and 5^+ members of the γ-vibrational band of ^{24}Mg can be summarized as follows: Magnitude predictions are too small by one or two orders of magnitude, and the predicted shapes bear little resemblance to the data, often having slopes of the wrong algebraic sign. The drastic failure to predict the observed strength of the inelastic cross sections is common to both proton and α particle inelastic scattering[8,10] and is not affected by inclusion or exclusion of spin-flip

PHYSICAL REVIEW C VOLUME 20, NUMBER 1 JULY 1979

Sixth-order boson expansion calculations applied to samarium isotopes

T. Tamura and K. Weeks
Department of Physics, University of Texas, Austin, Texas 78712

T. Kishimoto*
Cyclotron Institute, Texas A&M University, College Station, Texas 77843
(Received 26 October 1978)

In previous publications we reported on calculations based on the boson expansion method, and showed that good overall fits can be obtained to levels of a number of collective nuclei chosen over a wide range of the periodic table. In the present paper we concentrate on Sm isotopes and obtain much improved results, the fits to experiment being very good in all cases. In achieving this, the calculations are made by first removing a few errors committed in the previous work and also by including all terms up to sixth order in the Hamiltonian. In addition to calculating energy levels, $B(E2)$ values, and quadrupole moments as in our previous work, we also calculated isomer shifts and spectroscopic amplitudes for two-nucleon transfer reactions.

[NUCLEAR STRUCTURE ^{148,150,152,154}Sm microscopic calculation of energy levels, $B(E2)$'s, static quadrupole moments, isomer shifts, two-nucleon transfer spectroscopic amplitudes, boson expansion.]

I. INTRODUCTION

In the past few years, two of us (T.K. and T.T.) have been engaged in describing nuclear collective motions in terms of a boson expansion technique. A paper[1] which dealt with the formulation (here called I) was published some time ago. The second paper (here called II) which dealt with additional formulation, as well as numerical calculations, was published recently.[2] (References to a number of earlier publications made by other authors can be found in these two papers.) In this second paper, about ten nuclei were chosen over a wide range of the periodic table, and it was shown that our calculations successfully reproduced important characteristic features of all the nuclei considered.

These calculations were nevertheless made to serve primarily as a general survey of the applicability of our boson-expansion method. Therefore, little effort was expended to obtain further improved fits to data for individual nuclei or isotopes. Encouraged by the success achieved in II, we have since been engaged in performing improved calculations, and to report on the results obtained so far for Sm isotopes is the purpose of the present paper. The Sm isotopes were chosen because of the experimental fact that a transition from spherical to rotational character takes place in going from ^{148}Sm to ^{154}Sm. Because of this, the Sm isotopes have been used as an example by a number of authors in the past to test various theories of nuclear collective motions.[3-5]

In Sec. II we, very briefly, summarize the formulation given in I and II and used in the present calculations. The results of the new calculations are given in Sec. III. As will be remarked in Sec. II, a few errors were committed in I and II which have now been corrected. Also the calculation was restricted in II to fourth order, but it has now been extended fully to sixth order. It will be evident from Sec. III that these modifications allow us to get much better agreement of the obtained results with experiment than was possible in II. It will also be seen in Secs. II and III that the present work has been extended beyond that of I and II, in that it now includes calculations of isomer shifts and of spectroscopic amplitudes for two-nucleon transfer reactions. The results obtained for these quantities also agree rather well with experiment. Discussion of the present work is given in Sec. IV.

II. BRIEF SUMMARY OF FORMULATION

The Hamiltonian that we take as our starting point is given as a sum of a single-particle Hamiltonian, a particle-hole type quadrupole-quadrupole interaction, and a pairing interaction of both monopole and quadrupole types.[1,2] Taking first the single-particle Hamiltonian and the monopole-type pairing interaction, the Bogoliubov transformation is made, so that the original, shell-model type single-particle system is replaced by a system of

II. C. COPY OF TITLE PAGES OF SUBMITTED PAPERS

BREAK-UP OF STRONGLY ABSORPTIVE PROJECTILES

-- Application to (h,dp) Reaction --

T. Udagawa and T. Tamura

Department of Physics, University of Texas

Austin, Texas 78712, U.S.A.

ABSTRACT

The well known DWBA formula for break-up processes was first simplified by introducing several approximations, all of which are believed justified for strongly-absorptive high-energy projectiles. This made the theory very transparent and the ensuing numerical calculations rather easy to perform. This new formula, which was applied earlier with success to the break-up of ^{20}Ne, is applied in the present work to that of ^{3}He, again with success.

[NUCLEAR REACTION Distorted-Wave Born approximation; Break-up reaction of strongly absorptive projectiles; $^{51}V(^{3}He,dp)$ reaction, calculated $d^{3}\sigma/dEd\Omega d\Omega$; $E(^{3}He)$=90 MeV.]

PARAMETRIZATION OF EFR-DWBA OVERLAP INTEGRAL FOR REACTIONS INDUCED BY HEAVY IONS

T. Udagawa, T. Tamura and D. Price

Department of Physics, University of Texas, Austin, Texas 78712

ABSTRACT

In a few recent publications, which utilized exact-finite-range distorted wave Born approximation, we successfully fit continuum spectra observed in a variety of heavy-ion induced reactions. In making it feasible to carry out numerical calculations involved, we found the use of properly parametrized transition amplitudes was very powerful and almost indispensable. In the present article, the method of this parametrization is explained in detail.

[NUCLEAR REACTIONS Distorted-wave Born approximation; exact-finite-range form factors; parametrization of overlap integrals; recoil effects; heavy-ion reactions; continuum spectra.]

DIRECT REACTION ANALYSES OF LIGHT HEAVY ION INDUCED DEEP INELASTIC REACTIONS

T. Udagawa and T. Tamura
Department of Physics, University of Texas
Austin, Texas 78712

We first discuss the basic concept, based on which the multi-step direct reaction (MSDR) theory became applicable to describe the continuum spectra in nuclear reactions. We then show that, in applying the MSDR theory to heavy-ion reactions in particular, an important technical development was made. It was to parametrize, i.e., to express in terms of an analytic function, the overlap integrals appearing in the DWBA theory, the building block of the MSDR theory. We show how this function looks like, and how closely it reproduces the values of the original overlap integrals. It will further be shown that, in many circumstances, the above functional form allows one to express analytically even the final forms of cross sections and other related quantities, like polarization. Results of calculations, made by using thus constructed theoretical framework, will then be presented. We first discuss the one-step transfer processes, with a particular emphasis of describing the polarization of ^{12}B, that comes out as an ejectile. Transfer of alpha-particles is then discussed, considering at the same time its competition with the break-up processes. Reasons for why some projectile breaks up so easily, while the others do not, will be explained in a very transparent manner. We finally consider processes in which higher-step processes seem to be playing a significant role. A notable example is the very deep inelastic scattering of ^{16}O by ^{58}Ni. It will be shown that the spectrum of ^{16}O and the polarization of $^{58}Ni^{*}$ are explained very consistently this way.

I. INTRODUCTION

It is already a decade since the deep-inelastic phenomena were first discovered in heavy-ion induced reactions. A huge amount of experimental data have been accumulated

COMPLEX ANGULAR MOMENTUM METHODS FOR ELASTIC SCATTERING WITH AN OPTICAL POTENTIAL

T. Takemasa and T. Tamura

Department of Physics, University of Texas

Austin, Texas 78712, U.S.A.

and

H. H. Wolter

Sektion Physik, Universitaet Muenchen

D-8046 Garching, W.-Germany

BOSON EXPANSION DESCRIPTION OF COLLECTIVE STATES IN Ru AND Pd ISOTOPES

K. Weeks and T. Tamura

Department of Physics

University of Texas, Austin, Texas 78712

ABSTRACT

We have applied the boson expansion method to describe the low lying positive parity states of even-even Ru and Pd isotopes. Energy levels, B(E2)'s, branching ratios, and magnetic dipole and electric quadrupole moments have been calculated and are in good agreement with experiment. In particular, the lowering of the 3_1^+ state energy in this mass region can be understood with our method. This is in contrast to some of the parameterized theories such as IBA which fail in this respect.

[NUCLEAR STRUCTURE $^{98\text{-}104}$Ru, $^{102\text{-}110}$Pd, energy levels, B(E2)'s, branching ratios, magnetic moments, static quadrupole moments, Boson Expansion.]

Description of Collective States in ^{190}Os and ^{196}Pt in terms of the Boson Expansion Theory

K. J. Weeks and T. Tamura

Department of Physics, University of Texas, Austin, Texas 78712

ABSTRACT

It is shown that the boson expansion theory can describe very well various features of nuclei in the Os-Pt region. In particular it fits the sign and magnitude of the static quadrupole moment of the 2_1^+ state, where the O(6) theory encounters difficulties.

BOSON EXPANSION DESCRIPTION OF COLLECTIVE STATES IN OSMIUM AND PLATINUM ISOTOPES

K. J. Weeks and T. Tamura

Department of Physics, University of Texas, Austin, Texas 78712

Abstract

The boson expansion theory, based on which successful explanations were made earlier of collective properties of Ru, Pd, Sm and other isotopes, is applied here to the Os and Pt isotopes. These nuclei are characterized by the fact that their energy spectra and the E2 transitions embody in themselves a very strong γ-unstable nature, yet making the quadrupole moment $Q(2_1^+)$ have very large values, being negative in Os and positive in Pt isotopes. It is shown that all these properties are explained by the boson expansion theory in a very natural manner.

[NUCLESR STRUCTURE $^{186-194}$Os, $^{188-198}$Pt, energy levels, B(E2)'s, branching ratios, magnetic moments, static quadrupole moments, boson expansion theory.]

FINITE AND INFINITE BOSON EXPANSIONS

F.J.W. Hahne* and T. Tamura

Department of Physics, University of Texas

Austin, Texas 78712

ABSTRACT

A comparison between the finite Dyson-type and the infinite Holstein-Primakoff-type boson expansion is presented, considering both particle-hole and pairing type excitations. The significance of truncating to the truely collective branches is emphasized, and the convergence of the Holstein-Primakoff expansion is discussed. It is shown that in both expansions there is no need to construct physical basis states. Complete equivalence between the two types of expansion is exhibited by treating these excitations within models which are schematic but not totally unrealistic.

REMARKS ON THE USE OF THE BOSON EXPANSION THEORY FOR THE DESCRIPTION OF COLLECTIVE NUCLEI

K. J. Weeks and T. Tamura

Department of Physics, University of Texas, Austin, Texas 78712

Abstract

A clear understanding of how to construct the boson expansion of a collective fermion pair operator is given. The criteria for the applicability of the procedure is also discussed. Following this prescription, the Pauli-principle violation is made negligible for the low lying states of collective nuclei.

[NUCLEAR STRUCTURE Boson expansion; Criteria for truncation and convergence; collective motions.]

II. D. ABSTRACTS OF TALKS PRESENTED AT MEETINGS

APS New York Meeting January 1979

EB2 Coincidence Measurement of Direct Break-up for the Reaction of $^{40}Ca(^{20}Ne,^{16}O)$ at E_{lab} = 260 MeV. E. TAKADA, T. SHIMODA, T. YAMAYA, N. TAKAHASHI, and K. NAGATANI, Texas A&M U.*, T. UDAGAWA and T. TAMURA, U. Texas**--We have been studying α-transfer-like heavy-ion reactions to the continuum and could explain successfully the data by one-step α-transfer calculation, while in $(^{20}Ne,^{16}O)$ reaction the anomalous energy spectra were observed at forward angles.[1] The speculation of the direct projectile breakup was made for this anomaly.[2] To ascertain this feature, ^{16}O-α correlation measurement has been done. Results obtained are: (1) energy correlations show strong enhancement along the locus of three-body Q value = 0. (2) angular correlation shows strongly forward peaking to the beam axis. These results support the projectile breakup interpretaion for continuum spectra.[3] As for smaller yields in large negative Q value region, they are attributed to the sequential α-decay from highly excited residual nuclei in the transfer reaction. For this region analysis is now in progress.

1)Phys. Rev. Lett. 42, 1518 (1979).
2)T. Shimoda et al., Bull. Am. Phys. Soc. 24, 14 (1979).
3)T. Udagwa et al., this meeting.
* Supported in part by the National Science Foundation.
**Supported in part by the U.S. Department of Energy.

APS Knoxville Meeting October 1979

AF 12

Anomalous Energy Spectra in the Alpha Transfer Reaction $(^{20}Ne,^{16}O)$. T. SHIMODA, H. FRÖHLICH, M. ISHIHARA, and K. NAGATANI,* Texas A&M U. and T. UDAGAWA and T. TAMURA,** U. of Texas--We have studied[1] the alpha transfer reactions $(^{20}Ne,^{16}O)$, $(^{14}N,^{10}B)$ and $(^{13}C,^{9}Be)$ on ^{40}Ca. The continuum energy spectra observed were analyzed using the exact finite-range DWBA with the α-spectroscopic strength function extending to very high excitation region in the residual ^{44}Ti. The shapes and angular distributions of all these reactions were simultaneously reproduced by the theory as direct alpha transfers. However, in the reaction $(^{20}Ne,^{16}O)$, an anomally was observed as an additional broad peak at the highest energy region. The angular distribution of that component shows also an anomalously steep peaking towards very forward angles. It is speculated that such an anomally is due to somewhat different mechanism reflecting a direct breakup process. Various experimental and theoretical attempts are being made to clarify the anomally.

[1]H. Fröhlich et al., Bull. Am. Phys. Soc. 23, 941 (1978).
*Supported in part by the National Science Foundation.
**Supported in part by the U, S. Department of Energy.

AF 13

Systematic Study of Spin-Polarization in Heavy-Ion Transfer Reactions. M. ISHIHARA, T. SHIMODA, H. FRÖHLICH and K. NAGATANI*, Texas A&M U., T. UDAGAWA and T. TAMURA†, U. of Texas--Using the measurements of the β-asymmetry of ^{12}B, we have investigated[1] the spin polarization in the reactions $^{232}Th(^{13}C,^{12}B)$, $^{222}Th(^{14}N,^{12}B)$ and $^{197}Au(^{19}F,^{12}B)$ at incident energies of about 10 MeV/nucleon. The spin polarizations demonstrate quite similar patterns; at the highest energy ends the polarization shows large positive values (in Madison convention), then it decreases rapidly towards low energy regions crossing the null polarizations at around the energies of the optimum Q-values. Analyses were made using a full quantum mechanical treatment in terms of the DWBA[2] model, which well explained the polarizations together with the cross sections in the highest energy regions. However, the theoretical fits deviates from the experimental results in the low energy regions. Detailed study to extend the understanding is explored.

*Supported in part by the National Science Foundation.
†Supported in part by U. S. Department of Energy.
[1]M. Ishihara et al., Bull. Am. Phys. Soc. 23, 941 (1978).
[2]T. Udagawa and T. Tamura, Bull. Am. Phys. Soc. 23, 947 (1978).

Background of (p,p') Spectra in the QGR Energy Region

T. Udagawa and T. Tamura, University of Texas

It is well known that, when the QGR is excited by an inelastic scattering of hadrons, the resonant part of the spectrum is seen as a small bump superimposed upon a huge background. Because an arbitrariness is involved in subtracting this background, the cross section exciting QGR can be extracted only to within an error of, say, 20-30%. Thus, although it was shown[1], for the (p,p') case, that the magnitude and the shape of this bump can be accounted for, if in addition to the ℓ=2 (QGR) contribution, those of ℓ=0, 1 and 4 are taken into account, it is desirable to have a better understanding of the origin of the background. This may be achieved if one knows how to explain the continuum spectra, which certainly extends into regions way beyond the QGR energy. Such was, in fact, attempted[2,3] with fair but not complete success, in that the predicted cross sections, considering up to two-step processes[3], were somewhat too small compared with experiment, and also that the theory failed to explain a sharp rise of the differential cross section at very small angles.[4] A possible way to remove (part of) these difficulties may be to take into account the contributions of (p,2p) and (p,pn) type processes. Most simply these processes may be treated as pick-up processes to form a di-proton or an unbound deuteron. Zero-range DWBA calculations made so far show that a sharp forward peak does emerge this way. The obtained magnitude is, however, too small by a factor of about two. It is our belief that the use of an exact-finite-range DWBA method would remove this last difficulty, and such work is underway.

1. F.E.Bertrand and D.C.Kocker, Phys. Rev. C 13, 2241 (1976).
2. G.F.Bertsch and S.F.Tsai, Phys. Rep. 18C, 125 (1975).
3. T.Tamura et al., Phys. Lett. 66B, 109(1977);78B,189(1978).
4. F.E.Bertrand and R.W.Peelle, Phys. Rev. C 8, 1045 (1973).

POLARIZATION OF ^{12}B PRODUCED AND HIGH SPIN STATES POPULATED IN DEEPLY INELASTIC HEAVY-ION REACTIONS

M. Ishihara, T. Shimoda, H. Frölich, H. Kamitsubo and K. Naganani

Cyclotron Institute*, Texas A&M University, College Station, Texas 77843

T. Udagawa and T. Tamura

Department of Physics**, University of Texas, Austin, Texas 77812

ABSTRACT

The polarization P was measured of ^{12}B produced in deeply inelastic heavy-ion reactions such as $^{232}Th(^{13}C, ^{12}B)$, $^{100}Mo(^{14}N, ^{12}B)$ and $^{197}Au(^{19}F, ^{12}B)$. In all these reactions, the measured P exhibited a common feature, seen as a function of the kinetic energy E_b of ^{12}B; it is large and positive at the highest energy E_b, and is followed by a rapid decrease to negative values with decreasing E_b. We found that this behaviour is well explained in terms of a simple direct reaction mechanism. Two important ingredients inherent to the EFR-DWBA theory, i.e. the transverse recoil and the ℓ-window are playing the crucial role, in that the former produces large positive values of P for higher E_b, while the latter causes the decrease of P towards lower E_b. The presence of the ℓ-window further suggests a preferential population of very high spin states in the residual nucleus, and we can extract the (relative) probability of populating these states.

*Supported in part by the National Science Foundation.

**Supported in part by the U.S. Department of Energy.

PHYSICAL INTERPRETATION OF CORRELATION SPECTRA $^{40}Ca(^{20}Ne,^{16}O\alpha)$: INELASTIC EXCITATION OF ^{20}Ne INTO THE CONTINUUM

E. Takada, N. Takahashi, T. Shimoda, T. Yamaya, and K. Nagatani*

Cyclotron Institute, Texas A&M University. College Station, Texas 77843

The shapes of the ^{16}O energy spectra and angular correlation, which are obtained from our correlation measurement in the reaction $^{40}Ca(^{20}Ne,^{16}O\alpha)$ at 259 MeV incident energy,[1] are well reproduced by the DWBA calculations based on the direct breakup process.[2] This process is interpreted as the inelastic scattering of ^{20}Ne into the continuum. The results of the theoretical calculations include the following features: 1) Spectroscopic strength for the inelastic excitation of ^{20}Ne has a sharp peak around excitation energy $E_x(Ne) \sim 9$ MeV and, predominantly, at $\ell = 0$. 2) Angular distribution of $^{20}Ne^*$ peaks at forward angles.

Thus, it is instructive to inspect the two-dimensional spectra in relation to $E_x(Ne)$ and the scattering angle of ^{20}Ne θ_{Ne}, which are known from the relative energy between the observed ^{16}O and α particles, and from their center-of-mass motion, respectively. Fig. 1 gives a schematic diagram of the two-dimensional spectra and shows the loci along the Q-values (from the α threshold of ^{20}Ne), $E_x(Ne)$ and θ_{Ne}. It is anticipated that the resulting spectra should demonstrate strong cross section at the optimum condition of these three parameters: $Q = 0$, $E_x(Ne) \sim 9$, and forward θ_{Ne}. Fig. 2a shows the locus of θ_{Ne} and $E_x(Ne)$ for $Q = 0$, which explicitly indicates the kinematic condition for this angular configuration. Figs. 2b and 2c show the observed spectra projected onto $E_x(Ne)$- and θ_{Ne}-axis, respectively. In Fig. 2b one can see the sharp increase of cross sections as $E_x(Ne)$ decreases and is cut off by kinematics. For a given $E_x(Ne)$, the kinematical condition provides two angles (one forward and another backward with respect to the $\theta_{Ne} = 5.6°$, indicated by the dashed line in Fig. 2a). Figure 2c clearly shows a dominant contribution from the forward θ_{Ne} side. These features are also seen in the other angular configurations.

As for the excitation of the target ^{40}Ca, the Q-value will directly show $E_x(Ca)$, provided ^{16}O and α particles are in their ground states. In Fig. 1 of Ref. 1, the yield is concentrated to small-Q region, confirming that the process mainly corresponds to direct breakup, without exciting ^{40}Ca.

These observed features consistently agree with the prediction of the DWBA calculation for the projectile breakup process.

FOOTNOTE AND REFERENCES

*Supported in part by the National Science Foundation.

1. E. Takada, T. Shimoda, T. Yamaya, N. Takahashi, K. Nagatani, T. Udagawa, and T. Tamura, contribution to this symposium.

2. T. Udagawa, T. Tamura, T. Shimoda, H. Fröhlich, M. Ishihara, and K. Nagatani, to be published in Phys. Rev. C.

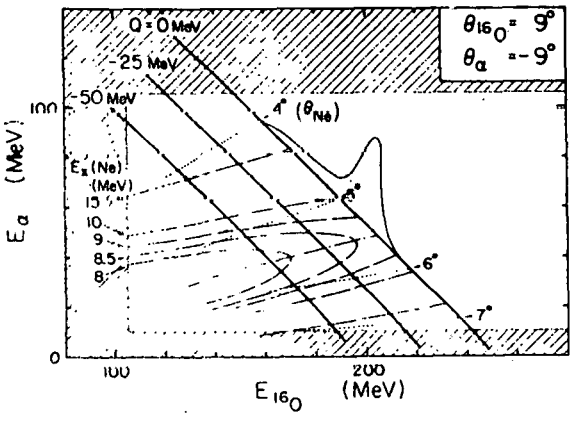

Fig. 1 Schematic two-dimensional spectrum with loci along the Q-values (thick solid lines), $E_x(Ne)$ (dashed lines), and θ_{Ne} (dotted lines). Dash-dotted line indicates minimum $E_x(Ne)$ points for various Q-values. Hatched area is region cut off by detectors. A schematic spectrum is sketched on $Q = 0$.

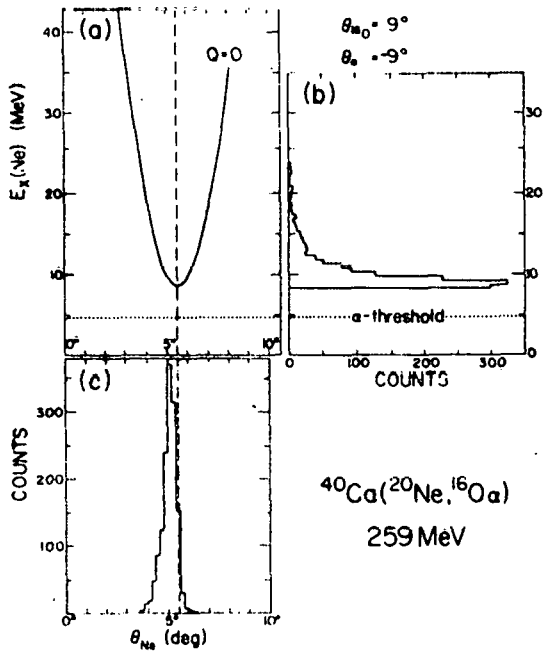

Fig. 2 (a) θ_{Ne}-$E_x(Ne)$ diagram for the $Q = 0$ locus in Fig. 1. (b) Yields projected on $E_x(Ne)$ axis. (c) Yields projected on θ_{Ne} axis.

Intern. Symposium on Cont. Spectra of Heavy Ion Reac. San Antonio Dec. 1979

CORRELATION MEASUREMENTS IN $^{40}Ca(^{20}Ne,^{16}O\alpha)^{40}Ca$ REACTION

E. Takada, T. Shimoda, T. Yamaya, N. Takahashi, and K. Nagatani*

Cyclotron Institute, Texas A&M University, College Station, Texas 77843

and

T. Udagawa and T. Tamura**

Physics Department, University of Texas, Austin, Texas 78712

Alpha-transfer reactions, such as $(^{14}N,^{10}B)$ and $(^{13}C,^{9}Be)$, leading to continuum regions have recently been studied.[1] The experimental results were well explained by a theoretical model based on the direct transfer scheme. In the $(^{20}Ne,^{16}O)$ reaction, however, an extra component of high energy ^{16}O was observed in very forward angles, and the existence of the direct projectile breakup process was suggested. In fact, a theoretical analysis of a direct breakup following the inelastic excitation of ^{20}Ne explains the extra component observed in such inclusive energy spectra of ^{16}O.[2]

In order to substantiate these observations and understand the mechanism more conclusively, we performed correlation measurements of ^{16}O-α in the reaction $^{40}Ca(^{20}Ne,^{16}O\alpha)$ at 259 MeV bombarding energy. Two solid-state detector telescopes were used to obtain ^{16}O-α coincidence spectra. In Fig. 1, an example of two dimensional spectra with the ^{16}O counter at 9° and the α counter at -9° (negative angle indicates opposite side of the beam axis) is shown. As seen, the yields are concentrated along the Q = 0 line (Q measures the Q-value from the α-threshold in ^{20}Ne), which corresponds to the transition without exciting ^{40}Ca, thus implying the direct ^{20}Ne breakup process presently considered. The energy spectra projected to the ^{16}O-energy axis at various angular configurations are shown in Fig. 2. In addition, the ^{16}O single spectra are displayed on the top for comparison. As expected,[2] the strong peak observed at the high energy region of the ^{16}O single spectra do indeed correspond to the peak seen in the coincidence spectra which is attributed to the breakup process. The spectral shapes and their cross sections, that is all the observed results, are quantitatively reproduced by the theoretical analysis, which will be discussed.

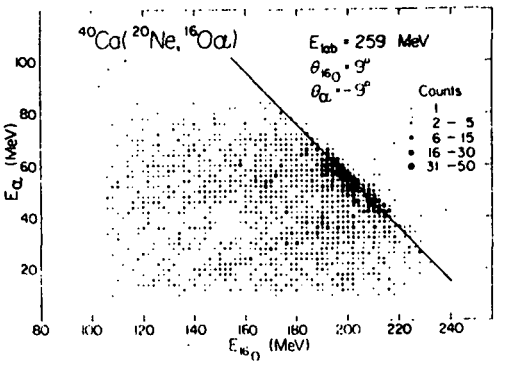

Fig. 1 Two-dimensional spectra in laboratory system. Solid line indicates Q = 0 locus.

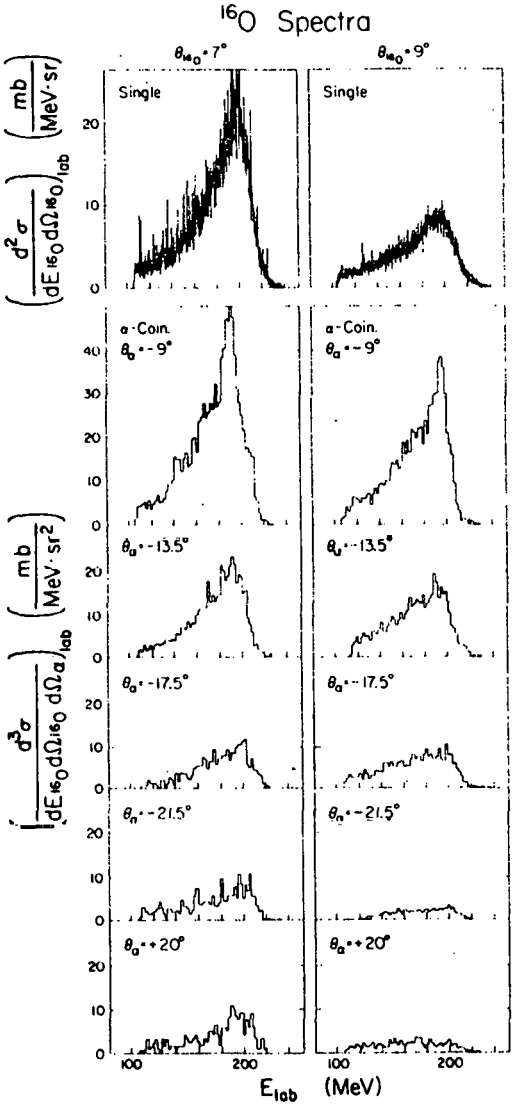

Fig. 2 α-coincidence and single (inclusive) spectra of of ^{16}O taken at various angular configurations.

FOOTNOTES AND REFERENCES

*Supported in part by the National Science Foundation.

**Supported in part by the U. S. Department of Energy.

1. H. Fröhlich, T. Shimoda, M. Ishihara, K. Nagatani, T. Udagawa, and T. Tamura, Phys. Rev. Lett. 42, 1518 (1979).

2. T. Udagawa, T. Tamura, T. Shimoda, H. Fröhlich, M. Ishihara, and K. Nagatani, to be published in Phys. Rev. C.

III. PERSONNEL OF GROUP

Faculty

Dr. W. Roy Coker, Assoc. Prof.

Dr. Taro Tamura, Prof.

Dr. Takeshi Udagawa, Assoc. Prof.

Post- Doctoral Appointments

Dr. H. Amakawa (From September 1, 1979)

Dr. A. Cunsolo (October and November, 1979)

Dr. F. J. W. Hahne (Till April, 1979)

Dr. H. Lenske (From September 1, 1979)

Dr. T. Takemasa (Till August 31, 1979)

Dr. K. J. Weeks

Pre-Doctoral Appointments

Y.- J. Chang

V. G. Pedrocchi

D. R. Price

K. E. K. Woods